Technische Universität München

Lehrstuhl für Bodenkunde

Organic matter protection through interactions with Fe and Al (hydro) oxides in soil

Thiago Massao Inagaki

Vollständiger Abdruck der von der Fakultät Wissenschaftszentrum Weihenstephan für Ernährung, Landnutzung und Umwelt der Technischen Universität München zur Erlangung des akademischen Grades eines

Doktors der Naturwissenschaften (Dr. rer. nat.)

genehmigten Dissertation.

Vorsitzender: Prof. Dr. Jörg Völkel

Prüfer der Dissertation: Prof. Dr. Ingrid Kögel-Knabner

Prof. Johannes Lehmann

Die Dissertation wurde am 30. Januar 2020 bei der Technischen Universität München eingereicht und durch die Fakultät Wissenschaftszentrum Weihenstephan für Ernährungam 4. März 2020 angenommen.

Table of Contents

LIST OF FIGURES

LIST OF TABLES

Summary

Organo-mineral interactions stand out as an important mechanism for soil organic carbon (SOC) stabilization in ecosystems. However, it is not yet clear how these interactions are affected by different climate conditions, neither if they are always the predominant mechanism for SOC protection. In this context, Andosols stand out through their enhanced capacity of carbon storage, mainly through mineral associations, making them ideal soils to study these mechanisms. Several analyses at the macro- and microscale are available to help answering those questions. However, particular characteristics of these soils such as high microaggregate stability hamper many soil analyses (e.g., soil organic matter fractionation), making them difficult to investigate. In addition, while microscale analyses cannot represent all processes occurring in a soil profile due to their small scale, bulk soil analyses cannot represent the scale at which many SOC stabilization mechanisms occur (i.e., μm to nm).

Funded by the Institute for Advanced Study from the Technical University of Munich through the Hans Fischer Senior Fellowship, this thesis aimed to answer the above-mentioned questions by investigating organo-mineral interactions throughout a climate gradient. We have used samples from 11 soil profiles throughout a climate gradient in the Kohala region in Hawaii. The climate gradient is composed of Andosols under pastureland and forest vegetation and it encompasses precipitation rates varying from approximately 1800 to 2300 mm $year^{-1}$. The objectives of this thesis were approached through three main projects:

1. **Investigating soil organic matter fractionation methods in Andosols.** Soil organic matter fractionation in Andosols is critical to perform, especially due to the high stability of microaggregates. Therefore, the first goals of this project were to investigate soil fractionation procedures including the use of NaCl to promote aggregate dispersion and the best approach to analyze the clay fraction through spectromicroscopic techniques. These analyses revealed important observations regarding the performance of the soil organic matter fractionation in Andosols, especially at the microscale.
2. **Assessing changes in organo-mineral associations across a climate gradient.** Aware of the best fractionation approaches, we aimed at investigating the influence of a climate gradient on subsoil organo-mineral associations. By using a combined

approach at the bulk soil scale (e.g., SOC contents and Fe and Al extractions) and microscale (e.g., Nanoscale secondary ion mass spectrometry – NanoSIMS), we were able to discern the relative role of Fe and Al in promoting SOC stabilization under contrasting climate conditions.

3. **Evaluating the influence of microscale spatial distribution on organic matter stabilization.** Motivated by observations of the unusually high SOC contents in the middle part of the climate gradient (i.e., ~2100 mm year^{-1}), we aimed at understanding the mechanisms responsible for such high SOC accrual. Choosing a soil profile with the highest SOC and mineral contents (Fe and Al), we conducted a microcosm experiment with ^{13}C and ^{15}N labeled microbially derived organic matter. We were able to unravel important how the distribution of these OM forms affect their stabilization and mineralization rates.

Study 1 revealed re-aggregation effects on the < 2 μm clay fraction after freeze-drying procedure, which caused the formation of assemblages larger than 20 μm. Such artifact precludes certain spectromicroscopic analysis (e.g., NanoSIMS), but it was easily avoided by sampling aliquots from soil suspension after ultrasonication procedure. We also observed that Na saturation through the addition of 1 M NaCl solution caused did not affect the distribution of SOC among fractions (less than 2% in SOC amount of < 2 μm clay) compared with the dispersion when water alone was used.

The findings of study 2 revealed that SOC associations with Fe and Al shifted across a climate gradient. At a lower precipitation level (~1800 mm year-1) the clay fraction < 2 μm displayed higher organic matter associations with Fe and Al together, while at a higher precipitation level (~2300 mm year^{-1}) the organic matter was mostly unassociated or only associated with Al. These observations could not be ascertained from bulk soil analyses alone. Our combined approach at the bulk soil and microscale demonstrated to be of fundamental importance to evaluate the impact of climate differences on organo-mineral associations.

The findings of study 3 revealed that microscale spatial distribution of microbially derived dissolved organic matter (DOM) could significantly reduce mineralization rates by 17% and increase sequestration in subsoil by 10% compared to point source DOM added in easily dissolvable pellets. Through fine-scale microspatial analysis in the interior of aggregates we could see that aggregate occlusion may be a more important mechanism for point source

inputs whether mineral associations is more relevant for distributed sources of OM but. Here we demonstrate the importance microscale spatial distribution, a yet unrecognized factor in SOC stabilization.

Overall, this dissertation innovates by discerning the relative roles of Fe and Al in promoting organo-mineral associations in contrasting climate conditions. It provides important recommendations for avoiding clay re-aggregations at the microscale during soil organic matter fractionation in Andosols. It also demonstrates the yet under recognized influence of microscale spatial distribution on organic matter mineralization and stabilization in soils.

Zusammenfassung

Organisch-mineralische Wechselwirkungen sind ein wichtiger Mechanismus für die Stabilisierung von organischem Kohlenstoff (organic carbon, OC) im Boden in Ökosystemen. Es ist jedoch noch nicht klar, wie diese Wechselwirkungen von unterschiedlichen Klimabedingungen beeinflusst werden, und auch nicht, ob diese immer der vorherrschende Mechanismus für den Schutz von OC sind. Andosole zeichnen sich durch eine sehr hohe Kohlenstoffspeicherkapazität aus, hauptsächlich bedingt durch Mineralverbände, und eignen sich daher ideal für die Untersuchung dieser Mechanismen. Zur Beantwortung dieser Fragen stehen verschiedene Analysen auf Makro- und Mikroskala zur Verfügung. Besondere Eigenschaften dieser Böden, wie eine hohe Stabilität der Mikroaggregate, behindern jedoch viele Bodenanalysen (z. B. Fraktionierung organischer Substanzen im Boden), was ihre Untersuchung schwierig macht. Während Analysen auf der Mikroskala aufgrund ihres geringen Maßstabs nicht alle in einem Bodenprofil auftretenden Prozesse darstellen können, können Gesamtbodenanalysen (Analysen auf der Makroskala) nicht den Maßstab darstellen, in dem viele OC-Stabilisierungsmechanismen auftreten (µm bis nm).

Diese vom Institute for Advanced Study der Technischen Universität München im Rahmen des Hans-Fischer-Senior Fellowship geförderte Dissertation zielte darauf ab, die oben genannten Fragen zu beantworten, indem organo-mineralische Wechselwirkungen entlang eines Klimagradienten untersucht wurden. Wir haben Proben von 11 Bodenprofilen entlang eines Klimagradienten in der Kohala-Region auf Hawaii verwendet. Das Klimagefälle umfasst Niederschlagsraten zwischen etwa 1800 und 2300 mm pro Jahr und beinhaltet Andosole unter Weideland- und Waldvegetation. Die Ziele dieser Arbeit wurden durch drei Hauptprojekte erreicht:

1. Untersuchung von Fraktionierungsmethoden für organische Bodensubstanzen in Andosolen. Die Fraktionierung organischer Bodensubstanzen in Andosolen ist schwierig durchzuführen, insbesondere aufgrund der hohen Stabilität von Mikroaggregaten. Daher bestand das erste Ziel dieses Projekts in der Untersuchung von Bodenfraktionierungsverfahren, einschließlich der Verwendung von NaCl zur Förderung der Aggregatdispersion und der besten Methode zur Analyse der Tonfraktion durch spektromikroskopische Techniken. Diese Analysen führten zu

wichtigen Beobachtungen hinsichtlich des Fraktionierungserfolgs organischer Substanzen im Boden in Andosolen, insbesondere im Mikromaßstab.

2. Beurteilung von Veränderungen in organisch-mineralischen Assoziationen entlang eines Klimagradienten. In Kenntnis der besten Fraktionierungsansätze hatten wir das Ziel, den Einfluss eines Klimagradienten auf die organo-mineralischen Assoziationen im Unterboden zu untersuchen. Durch die Verwendung eines kombinierten Ansatzes auf der Ebene (der Makroskala - des Gesamtboden) (z. B. OC-Gehalte und Fe- und Al-Extraktionen) und auf der Mikroskala (z. B. Nanoscale Secondary Ion Mass Spectrometry - NanoSIMS), konnten wir die Rolle von Eisen (Fe) und Aluminium (Al) bei der Stabilisierung von organischem Kohlenstoff in Böden (soil organic carbon, SOC) unter kontrastierend klimatischen Bedingungen identifizieren.
3. Bewertung des Einflusses der räumlichen Verteilung im Mikromaßstab auf die Stabilisierung der organischen Substanz. Motiviert durch die Beobachtung von ungewöhnlich hohen SOC-Gehalten im mittleren Teil des Klimagradienten (~ 2100 mm Jahr^{-1}), wollten wir die Mechanismen verstehen, die für eine solche hohe SOC-Anhäufung verantwortlich sind. Wir wählten ein Bodenprofil mit dem höchsten SOC- und Mineralgehalt (Fe und Al) und führten ein Mikrokosmenexperiment mit ^{13}C- und ^{15}N-markierten, mikrobiell abgeleiteten organischen Substanzen (organic matter, OM) durch. Wir konnten herausfinden, wie sich die Verteilung dieser OM-Formen auf ihre Stabilisierungs- und Mineralisierungsraten auswirkt.

Studie 1 ergab Re-Aggregationseffekte in der < 2 µm-Tonfraktion nach dem Gefriertrocknungsverfahren, die zur Bildung von artifizielle Aggregate von mehr als 20 µm führten. Ein solches Artefakt schließt eine bestimmte spektromikroskopische Analyse (z. B. NanoSIMS) aus, kann jedoch leicht vermieden werden, indem Aliquote aus der Bodensuspension nach dem Ultraschallverfahren entnommen werden. Wir beobachteten auch, dass die durch die Zugabe von 1 M NaCl-Lösung verursachte Na-Sättigung die Verteilung des SOC auf die Fraktionen (weniger als 2% in der SOC-Menge von <2 & µm Ton) nicht beeinflusste, im Gegensatz zur Dispersion mit reinem Wasser

Die Ergebnisse von Studie 2 zeigten, dass sich die OC-Assoziationen mit Fe und Al entlang des Klimagradienten verschoben haben. Bei einem niedrigeren Niederschlagsniveau

(~ 1800 mm Jahr^{-1}) zeigte die Tonfraktion < 2 µm höhere Assoziationen von organischem Material mit Fe und Al, während bei einem höheren Niederschlagsniveau (~ 2300 mm Jahr^{-1}) das organische Material größtenteils nicht assoziiert oder nur mit Al verbunden war. Diese Beobachtungen konnten nicht allein durch Bodenuntersuchungen auf der Makroskala ermittelt werden. Unser kombinierter Ansatz auf der Ebene der Makroskala und der Mikroskala hat sich als von grundlegender Bedeutung erwiesen, um die Auswirkungen von Klimadifferenzen auf organisch-mineralische Assoziationen zu bewerten.

Die Ergebnisse von Studie 3 zeigten, dass die mikroskalige räumliche Verteilung von mikrobiell abgeleiteten gelösten organischen Substanzen (dissolved organic matter, DOM) die Mineralisierungsraten um 17% und die Sequestrierung im Unterboden um 10% im Vergleich zu Punktquellen-DOM, die in leicht auflösbaren Pellets zugesetzt wurden, signifikant reduzieren könnte. Durch mikroskalige räumliche Analyse des Aggregatinneren konnten wir feststellen, dass die der Einschluss in Aggregate ein wichtiger Mechanismus für die Aufnahme von Punktquellen-DOM sein kann, unabhängig davon, ob Mineralassoziationen für räumlich verteilte OM-Quellen relevanter sind. Hier zeigen wir die Bedeutung der räumlichen Verteilung im Mikromaßstab, einem noch nicht erkannten Faktor für die OC-Stabilisierung.

Insgesamt ist diese Dissertation innovativ, da sie die Rolle von Fe und Al bei der Förderung von organisch-mineralischen Assoziationen unter kontrastierenden Klimabedingungen untersucht. Sie enthält wichtige Empfehlungen zur Vermeidung von Rückaggregationen von Ton auf der Mikroskala während der Fraktionierung organischer Substanzen im Boden in Andosolen. Sie zeigt auch den bislang wenig bekannten Einfluss der räumlichen Verteilung im Mikromaßstab auf die Mineralisierung und Stabilisierung von organischen Substanzen in Böden.

Acknowledgments

I express my gratitude to my supervisors Prof. Dr. Dr. h.c. Ingrid Kögel-Knabner and Prof. Dr. Johannes Lehmann for their guidance at each stage of this thesis. I thank for giving me the opportunity to work on this research project and for their contribution to my development as a scientist.

I am grateful to the Institute for Advanced Study (IAS) of the Technical University of Munich (TUM) for providing funding for the development of this study through the Hans-Fisher Senior Fellowship, awarded to Prof. Johannes Lehmann. I acknowledge the Technical University of Munich, the TUM Graduate School and the Graduate Center Weihenstephan for providing the framework for the development of my doctoral program.

I thank Dr. Carsten W. Mueller for his support in soil analyses (especially NanoSIMS), experiment designing, scientific discussions and career advices. Steffen A. Schweizer for his support with NanoSIMS image processing and scientific discussions. I express my gratitude to Dr. Angela R. Possinger for her support with XANES measurements and several other analyses conducted during my period at Cornell University. Prof. Dr. Louis Derry and Dr. Katherine E. Grant for providing me the soil samples for the development of this project and their support with the overall research.

I would like to thank all the employees of the TUM Chair of Soil Science that helped during my PhD. I am especially grateful to the technicians Maria Greiner and Bärbel Deischl for their support with the laboratory analysis. Dr. Carmen Höschen, Gertraud Harrington and Johann Lugmeier for their support with the NanoSIMS measurements. Dr. Werner Häusler for his support with XRD analyses and Franz Buegger for his support with IRMS measurements. I am also grateful to Akio Enders and Kelly Hanley for their support with several analyses during my period at Cornell University.

I thank my family: Pedro, Edna and Jaqueline for supporting me with everything, and all my colleagues that I met during my PhD time for being nice friends.

List of publications and contributions

First authored research articles

Study 1

Inagaki, T. M., Mueller, C. W., Lehmann, J., & Kögel-Knabner, I. (2019). Andosol clay re-aggregation observed at the microscale during physical organic matter fractionation. Journal of Plant Nutrition and Soil Science, 182(2), 145-148.

Contributions: I participated in the experiment designing, carried out the fractionation and microscopy analyses, performed data evaluation and wrote the manuscript.

Summary:

Soil organic matter (SOM) fractionation is an important tool used to investigate the distribution and composition of differently stabilized C pools. However, separating fine fractions especially from allophanic Andosols by physical fractionation was shown to be critical because the dispersion of such soils is hampered by the high stability of microaggregates. Therefore, we aimed at evaluating the influence of NaCl saturation prior to ultrasonic dispersion in a Allophanic Andosol. Two different approaches were employed to avoid clay flocculation at the microscale and analyzed using scanning electron microscopy (SEM), including the standard method of using freeze-dried samples and taking a liquid aliquot from the clay suspension during the final step of fractionation. We have determined that NaCl addition displayed little influence on clay dispersion (less than 2% in SOC amount). Direct effects of freeze-drying on Andosol clay fractions at the microscale were also observed, which caused the formation of assemblages larger than 20 mm. The presence of strong binding effects of the poorly crystalline mineral phases in Andosols is likely the primary reason for this effect. Therefore, in future studies, we recommend reserving a small liquid aliquot from soil suspensions after sonication to proceed with microscopy analyzes.

Study 2

Inagaki, T. M., Possinger, A. R., Grant, K. E., Schweizer, S. A., Mueller, C. W., Derry, L. A., Lehmann J., Kögel-Knabner, I. (2020). Subsoil organo-mineral associations under contrasting climate conditions. Geochimica et Cosmochimica Acta, 270, 244-263.

Contributions: I participated in the experiment design, carried out the laboratory analyses with support of co-authors, analyzed the data and wrote the manuscript.

Summary:

Organo mineral associations intermediated by Fe and Al are considered one of the most important mechanisms for soil organic carbon (SOC) stabilization in ecosystems. However, this stabilization mechanism can be profoundly affected by climate differences, but the magnitude of this influence whether as a direct effect or an indirect consequence due to changes in soil mineralogy is not yet fully known. In this study, we evaluated a series of subsoil samples throughout a climate gradient (1800–2400 mm precipitation $year^{-1}$ and 15–24º C) on Kohala Mountain, Hawaii to understand the impact of climate differences on organic matter protection. We have used a combined approach of analyses at the bulk soil and microscale using NanoSIMS. At the bulk soil scale, we have observed a concurrent decline of subsoil Fe, Al (i.e., dithionite citrate and ammonium oxalate extractions) and SOC above a precipitation level of 2000 to 2200 mm $year^{-1}$. This decline demonstrated to be influenced by changes in Fe to more reduced forms (evaluated by Fe K-edge XANES) and declines in carboxyl-C (evaluated by CP-MAS ^{13}C NMR). We could discern the relative role of Fe and Al in promoting organo-mineral associations in contrasting climate conditions (e.g., ~1800 and ~2300 mm $year^{-1}$) using NanoSIMS. While Fe contributed to approximately 40% of the microscale organo-mineral associations in the lower precipitation site (assessed by co-localizations with OM segments), this contribution at the higher rainfall regime was only 5%. In contrast, the contribution of Al was approximately the same in both rainfall levels (approximately 30%).The normalized CN:C ratio was higher when associated with Fe and Al especially in the high precipitation level, which demonstrates the importance of Fe and Al in stabilizing N-rich organic matter. Here we demonstrate that spatial relationships between Fe and Al with SOC at the microscale display a shift towards Al-dominated SOC associations at higher precipitation that could not be ascertained from bulk measurements alone. Thus, they are of great importance to understand the impact of climate differences on SOC protection.

Study 3

Inagaki, T. M., Possinger, A. R., Grant, K. E., Schweizer, S. A., Mueller, C. W., Derry, L. A., Kögel-Knabner, I., Lehmann J. (2020). Microscale distribution increases microbially derived C stabilization in soils. (*to be submitted to Nature Geosciences*).

Contributions: I participated in the experiment design, carried out the laboratory analyses with support of co-authors, analyzed the data, and wrote the manuscript.

Summary

Organic matter (OM) association with minerals and occlusion in aggregates are thought to be the dominant mechanisms of C sequestration in soil, while the effect of spatial distribution of OM on its own is unclear. Here we use ^{13}C- and ^{15}N-labeled OM to assess the influence of the microscale spatial distribution of microbially-derived dissolved organic matter (DOM) and plant litter on SOC stabilization. We demonstrate that greater spatial distribution of DOM in a mineral-rich subsoil reduced SOC mineralization by 17% and increased the formation of mineral-associated OC by 10% compared to a point-source DOM added as easily dissolvable pellets. The stabilization of microbially-derived DOM or plant litter in C-rich topsoil largely occurred without the influence of clay minerals, especially for distributed DOM. Fine-scale spatial analysis in the interior of sectioned macroaggregates from top- and subsoil demonstrated that the distributed DOM promoted less aggregate occlusion than the point-source DOM. This demonstrates that aggregate occlusion may not be a major mechanism for stabilization of distributed DOM in soils. Here we demonstrate that the greater microscale spatial distribution of microbially-derived DOM significantly decreases SOC mineralization and increases sequestration rates.

Contributions in joint experiments

i) Possinger A. R., Bailey S. W., **Inagaki T.M.**, Kögel-Knabner I., Dynes J. J., Arthur Z. A., Lehmann J. Organo-mineral interactions and soil carbon mineralizability with variable saturation cycle frequency. (under review in Georderma)

ii) Shabtai I., Das S., **Inagaki T.M.**, Kögel-Knabner I., Lehmann J. Elucidating the Shifting Controls on Organic Carbon Stabilization Across a Soil Moisture Gradient. (in preparation to submission).

iii) Webster T. M., Wilhelm R. C., Lynch L., Inagaki T. M., Schweizer S. A., Mueller C. W., Tfaly M., Kukkadapu R., Woolf D., Kögel-Knaber I., Buckley D. H., Lehmann J. Stabilization of soluble and insoluble organic carbon in soils with contrasting mineralogy along a precipitation gradient. (in preparation to submission)

Contributions

i) I helped to perform and analyze the data from ^{13}C NMR spectroscopy and NanoSIMS, revised and commented the manuscript.

ii) I performed ^{13}C NMR analyses and helped with data interpretation.

iii) I performed NanoSIMS analyses and helped with data interpretation

Dissertation at a glance

1 Study I
Testing methods for soil organic matter fractionation in Andosols

Andosol clay re-aggregation observed at the microscale during physical organic matter fractionation.

Aim: Evaluating the influence of NaCl saturation prior to ultrasonic dispersion in an allophanic Andosol and testing two preparation approaches (freeze drying vs. liquid suspension) for microscopy analysis.

Results:
- We have determined that NaCl addition displayed little influence on clay dispersion
- At the microscale, we observed the re-aggregation of the clay fraction caused by freeze-drying. This issue was avoided by analyzing aliquots of soil suspension.

2 Study II
Climate differences on organo-mineral associations

Subsoil organo-mineral associations under contrasting climate conditions

Aim: Understanding how different climate conditions impact subsoil organo-mineral associations at the macro- and microscales.

Results:
- Fe contributed more to mineral associations at lower precipitation rates while Al was more important in higher rainfall regimes.
- Changes in Fe speciation to more reduced forms and lower levels of carboxylic-C diminished the Fe-C associations in higher precipitation.
- The differential roles of Fe and Al could not be discerned from bulk soil measurements alone.

3 Study III
Microscale distribution as a driver for SOC stabilization

Microscale distribution increases microbially derived C stabilization in soils

Aim: Understanding the influence of microscale spatial distribution of microbially derived dissolved organic matter (DOM) in stabilization of the C-richest samples of the climate gradient.

Results:
- Greater spatial distribution of DOM reduced SOC mineralization and increased the formation of mineral-associated OC compared to a point source DOM added as easily dissolvable pellets.
- This yet unrecognized influence could be of great importance for SOC models especially regarding belowground inputs.

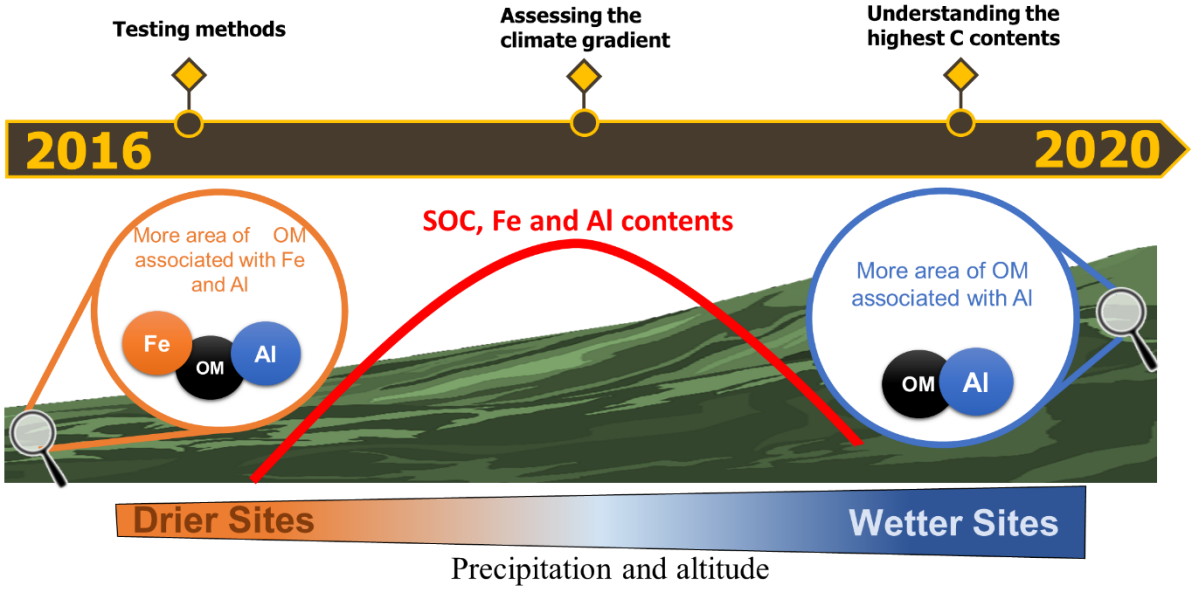

Introduction

1.1 Organo-mineral interactions affected by climate differences

Soils have the potential to store more organic carbon (SOC) than the global vegetation and atmosphere together (Lehmann and Kleber, 2015). Understanding C stabilization mechanisms in soils thus becomes increasingly important in our current climate change scenario. This capability is recognized to be primarily a function of so-called organo mineral interactions (Kögel-Knabner et al., 2008). Soil mineralogy changes throughout the process of soil development (e.g., variation of Fe and Al contents), mainly influenced by climate factors, such as precipitation and temperature variations. These changes have an important influence on organo-mineral associations (Harden, 1982) and are therefore known to play an important role in SOC stocks, especially in subsoil depths (Torn et al., 1997).

Climate differences, especially in precipitation, may play a fundamental role in SOC stabilization, since soil moisture stands out as one of five major factors affecting interactions between organic matter and minerals in soil (Kleber et al., 2015). Higher levels of moisture may promote biological activities, acting as a solvent for various reactions in the microbiota, which may increase organo-mineral associations. (Hong et al., 2013). At the microscale, the formation of anaerobic microsites under higher moisture levels are recognized to promote SOC stabilization (Keiluweit et al., 2017). On the other hand, reducing conditions promoted by higher precipitation regimes are also known to decrease SOC stabilization mainly by decoupling associations with Fe in soil (Huang and Hall, 2017). Therefore, it is not yet clear how climate differences can affect mineral interactions in soil, especially at the microscale. In addition, studies evaluating different environmental conditions often cover large areas including different soil types and ecosystems (O'Gorman, 2015; Trenberth, 2011). Therefore, there are still relatively few studies evaluating the impact of climate changes on organo-mineral associations within soils of similar mineralogy.

1.2 The use of Andosols to investigate organo-mineral interactions and the issues regarding organic matter fractionation

Volcanic-ash soils, classified as Andosols (IUSS Working Group, 2015), are considered an optimal soil to investigate organo-mineral associations, because they hold higher amounts of SOC and short-range-order (SRO) minerals compared to other type of soils (Dahlgren et al.,

2004). Allophane and imogolite stand out as major SROs found in Andosols. They are nano-sized minerals with hollow spherule and tube structures with extensive variable-charged surfaces (Filimonova et al., 2016; Kitagawa, 1971; Nanzyo et al., 1993). These structures can work as strong binding agents for aggregate formation and SOC stabilization. Besides it, complexes between Fe and Al ions with SOC via covalent bonding are abundant in Andosols (Asano and Wagai, 2014). However, detailed information about the assemblage of these structures to form aggregates in soil is still poorly understood.

In addition, separating fine fractions from allophanic Andosols by physical fractionation was demonstrated to pose experimental challenges because the dispersion of such soils is hampered by the strong stability of microaggregates (< 63 mm), which is derived from powerful interactions between organic matter, Al oxides and Fe oxides (Asano and Wagai, 2014). To obtain clay size particles < 2 μm during fractionation of Andosols, ultrasonic dispersion levels of up to 1600 J ml^{-1} are required (Silva et al., 2015).

In addition, clay flocculation after soil dispersion is a common artifact reported in studies that focused on the fractionation of Andosols (Asano and Wagai, 2014; Asano et al., 2018; Wagai et al., 2018). Therefore, suggestions such as performing the procedure within a single day has been recommended to avoid biases in SOM distribution between fractions (Asano and Wagai, 2014). However, this fact becomes even more important when we aim to analyze the soil fractions through spectromicroscopy techniques (e.g., nanoscale secondary ion mass spectrometry–NanoSIMS) due to the formation of sample topography (Mueller et al., 2013a). We still lack studies that evaluate the implications of these effects on results at the microscale, and methodological procedures to avoid such artifacts.

1.3 The relative role of Fe and Al in promoting organo-mineral associations in soils

Among the different soil minerals, Fe and Al oxides stand out as two major components of organo-mineral associations in soils (Adhikari and Yang, 2015; Matus et al., 2006; Souza et al., 2017). However, both minerals are often mentioned together as stabilization agents. Efforts to differentiate their role have been made especially through correlations in the bulk soil. Comparisons of the relative role of Fe and Al in promoting SOC storage vary according to the region and soil type (Wiesmeier et al., 2019). Overall in Andosols, Al seems to be the main driver as demonstrated by Matus et al. (2006), who concluded that Al extracted by acid ammonium acetate was the principal factor controlling SOC stocks in a series of volcanic soils

in Chile. On the other hand, Eusterhues et al. (2005) concluded that Fe oxides were the most relevant mineral phases for the formation of organo-mineral associations in subsoil layers of an acidic forest Cambisol. Therefore, the relative role of both elements in promoting SOC stabilization is not yet fully understood.

For this purpose, extraction techniques using different reagents, such as dithionite citrate bicarbonate and ammonium oxalate, are commonly used as proxies for Fe and Al oxides in the soil (Mehra and Jackson, 1958; Schwertmann, 1964). The use of chemical extraction methods is widespread because they are inexpensive and do not demand special laboratory infra-structure (Rennert, 2019). Although the use of extractable reactive metals has been recognized as a good indicator of SOC accrual (Asano and Wagai, 2014; Beare et al., 2014; McNally et al., 2017), this metric may not represent the scale at which organo-mineral association processes occur (i.e., micro to nanoscale). Because soils show a high spatial heterogeneity (Lehmann et al., 2008), processes occurring at small scales are of extreme importance to explain the mechanisms for SOC accrual in ecosystems. In this sense, evidence from microenvironments regarding the role of Fe and Al oxides in promoting organo-mineral associations is still relatively rare.

1.4 Microbially-derived organic matter and the importance of its spatial distribution

The storage of SOC is mainly determined by a balance between metabolic activities and C inputs (mainly through plant biomass) (Janzen, 2015). Therefore, investigating microbial activities in soil is of high importance, since they serve as a basis to understand SOC dynamics (Schimel and Schaeffer, 2012). The microorganisms play a role in not only reducing SOC stocks by mineralization, but also increasing them through the formation of microbial biomass and necromass at later decomposition stages (Liang et al., 2017). It is now recognized that the organo-mineral associations in soils exert a great influence of microorganisms, emphasizing that most persistent SOC has already passed microbial biomass at some point (Benner, 2011; Cotrufo et al., 2013; von Lützow et al., 2006). Recent studies have demonstrated that microbial necromass can make up more than half of SOC (Liang et al., 2019). However, the ways that microbial necromass is retained in soil in comparison to plant debris are not yet fully understood.

The inputs of organic matter, either aboveground as belowground, can vary widely especially in chemical parameters, such as proportions of components including cellulose,

holocellulose, lignin, lipids and polymers (Cotrufo et al., 2013). For instance, these inputs can have different spatial distribution ranging from being a point source (e.g., particulate organic matter and root exudates) (Baumert et al., 2018) to being evenly distributed (e.g., leachates of dissolved organic matter) (Marin-Spiotta et al., 2011) and it is unknown what effect spatial distribution of OM sources has on SOC stabilization.

Interactions of these OM inputs with minerals and microorganisms occur at small scales, as soils are recognized by their high spatial complexity at the nano and micrometer scales (Lehmann et al., 2008; Steffens et al., 2017). It is recognized that substrate availability to microorganisms plays a key role in SOC turnover (Blagodatsky and Richter, 1998). The search of soil microorganisms for food is characterized by a series of methods such as random walks (Van Haastert and Bosgraaf, 2009) or shortest possible routes (Reynolds et al., 2010). Therefore co-occurrence of substrate and microbes at the same location is considered an important pre-requisite for SOC microbial decomposition (Dungait et al., 2012). Point-source distribution of microbially-derived OM inputs could potentially favor microbial specialization on specific substrates, due to the higher concentration of a specific food source (Dechesne et al., 2007). This fact could justify, for example, the higher microbial activity enhanced by root exudates (Baumert et al., 2018). On the other hand, associations with minerals and aggregates may be reduced when large amounts of OM are present due to C saturation (Six et al., 2002). However, it remains unknown whether microscale spatial distribution of OM in general can significantly affect their mineralization and stabilization in soil. It is also not fully understood whether the effects of the spatial distribution are more influenced by mineral interactions or characteristics intrinsic to microbial ecology.

Objectives and hypothesis

Aiming at answering these questions, this thesis focused in the following goals and hypotheses:

1. Improving the methods for soil organic matter fractionation in Andosols, especially regarding the preparation of these fractions for spectromicroscopy analyses. We hypothesized that separating samples for microscopy images immediately after the soil dispersion in aliquots could avoid problems with clay re-aggregation.

2. Discerning the relative roles of Fe and Al oxides in promoting organo-mineral associations under contrasting climate conditions. We hypothesized that they would perform differentiated roles on organo-mineral associations influenced mainly by reduction conditions.

3. Understand the effect of a climate gradient (~1800 - ~2300 mm $year^{-1}$) affect soil mineralogy and consequent changes to organo-mineral associations at the macro- and microscales. We hypothesized that changes in Fe and organic matter composition driven by climate differences would be important factors for subsoil organo-mineral associations in the gradient.

4. Assessing the spatial influence of microscale spatial distribution on microbially derived organic matter inputs. We hypothesized that distributed organic matter inputs are stabilized to a greater extent than point source ones due to higher organo-mineral associations.

Materials and methods

2.1 Experimental area and soil sampling

The study was carried out in the Kohala region (20°4'14.16"N, 155°43'21.94"E) of northern Hawaii in a rainfall gradient varying from approximately 1800 to 2400 mm $year^{-1}$, with annual temperatures ranges of 15 to 24ºC, depending on elevation (Giambelluca et al., 2013). The vegetation canopy at the sites changes with elevation. The native vegetation constituted of mixed ohi'a (*Metrosideros polymorpha* Gaudich.) and koai'a (*Acacia koaia* Hillebr.) in the lower part of the transect, grading to a o'hia and mixed fern vegetation at higher parts of the transect (hapu'u - *Cybotium spp.*- and uluhe – *Dicronopteris linearis* Burm.). In the 20th century, the mid elevation forest (up to 1400 m at this site) was largely cleared and replaced by kikuyu pasture grasses (*Pennisetum clandestinum* Hochst.).

We used eleven sites in this study along the climate gradient, six collected from grassland and five from forest vegetation (*Metrosideros polymorpha)*. Soil profiles were excavated by hand and sampled by genetic horizon until approximately 1 m depth. Since the main objective of this study was to evaluate subsoil organic carbon stabilization, we focused

mainly on 23 samples from 0.4–0.9 m B subsoil horizons across the rainfall gradient. We also included 23 samples from the respective 0.2 m A topsoil horizons to evaluate the influence of aboveground biomass and vegetation change on topsoil layers. A detailed description of the sampling locations are displayed in Figure 1 and Table 1.

The soil is characterized as an Andosol derived from alkalic lavas of the 350 ka Pololu basalt that likely also received ash deposition from the younger (150 ka) Hawi basalt series (Wolfe and Morris, 1996). The soils were sieved (4-mm mesh). In order to maintain field-moist conditions, we kept the samples in boxes with ice bags while they were transported to the laboratory and stored in climate-controlled rooms at 4ºC. All bulk soil analyses were performed in duplicate and the results were corrected by the respective moisture level of each sample.

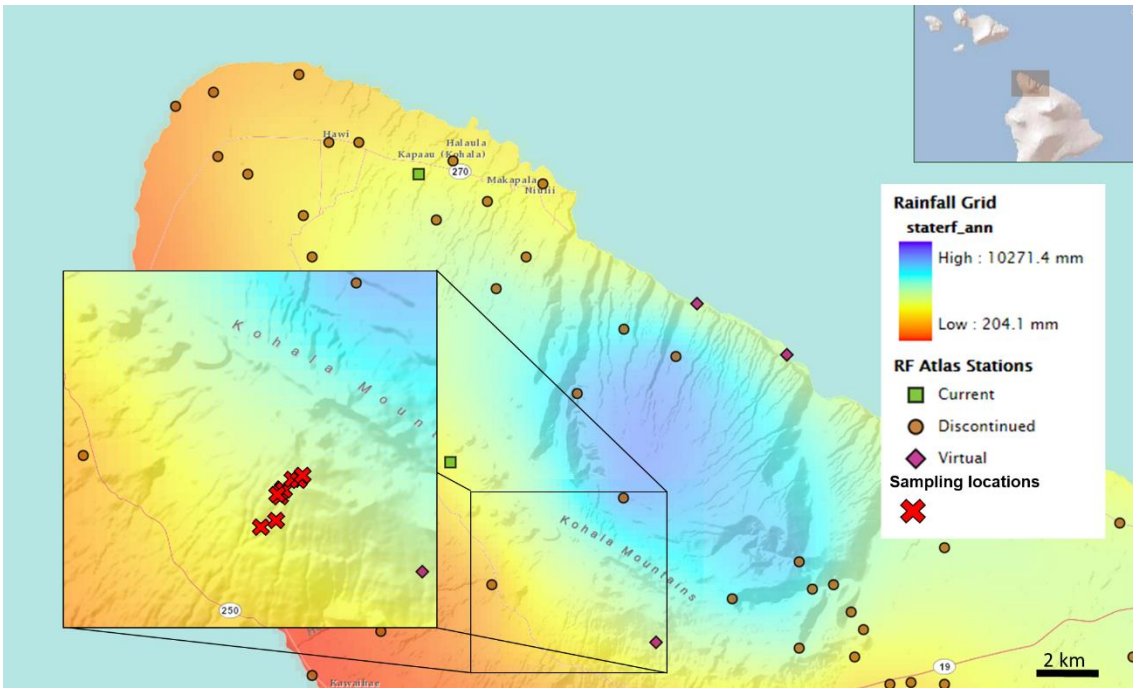

Figure 1: Locations of the sampling areas along the precipitation gradient at the Pololu lava flow, Kohala Hawaii. Source: Giambelluca et al. (2013).

Table 1: Soil samples collected in distinct elevation levels at top and subsoil depths throughout the precipitation gradient at the Pololu lava flow, Kohala Hawaii.

Altitude (m)	Vegetation	Precipitation (mm year^{-1})*	Coordinates		Depths (m)
1176	Grassland	1800	20°3'35.10"N	155°43'56.82"E	0.0–0.05 0.05–0.25 0.5–0.7 0.7–0.9
1251	Grassland	1900	20°3'44.68"N	155°43'45.55"E	0.0–0.15 0.15–0.25 0.5–0.9 0.7–0.9
1416	Grassland	1900	20°3'48.54"N	155°43'35.30"E	0.0–0.15 0.15–0.25 0.5–0.7 0.7–0.9
1361	Grassland	2000	20°4'13.33"N	155°43'30.83"E	0.0–0.05 0.05–0.25 0.5–0.7 0.6–0.7
1388	Grassland	2000	20°4'4.98"N	155°43'33.24"E	0.0–0.10 0.10–0.16 0.4–0.6 0.6–0.8
1409	Grassland	2100	20°4'8.04"N	155°43'31.65"E	0.0–0.12 0.12–0.20 0.5–0.7 0.6–0.8
1429	Forest	2100	20°4'8.36"N	155°43'28.02"E	0.0-0.03 0.03-0.10 0.4–0.6 0.6–0.8
1440	Forest	2100	20°4'5.54"N	155°43'33.24"E	0.0–0.05 0.05–0.15 0.4–0.5 0.5–0.7
1460	Forest	2200	20°4'14.16"N	155°43'21.94"E	0.0–-0.13 0.13–-0.17 0.4–0.6 0.6–0.7
1478	Forest	2300	20°4'17.40"N	155°43'18.48"E	0.0–-0.08 0.08–-0.15 0.4–0.6 0.6–0.7
1554	Forest	2400	20°4'25.93"N	155°43'13.84"E	0.0–0.10 0.10–0.17 0.4–0.6 0.6–0.7

* Precipitation values were obtained through interpolation between elevation and the different isoheytes in the Hawaii Rainfall atlas (Giambelluca et al. 2013). Source: Inagaki et al. (2020)

The following topics describe analyses made on samples throughout the climate gradient. Quantitative analyses such as total CN content and extractions of Fe and Al oxides were performed in all 11 sampled profiles, while qualitative analyses such as Fe and SOC composition were performed in selected strategic positions. In Fig. 2 we summarize the main analyses performed in the project.

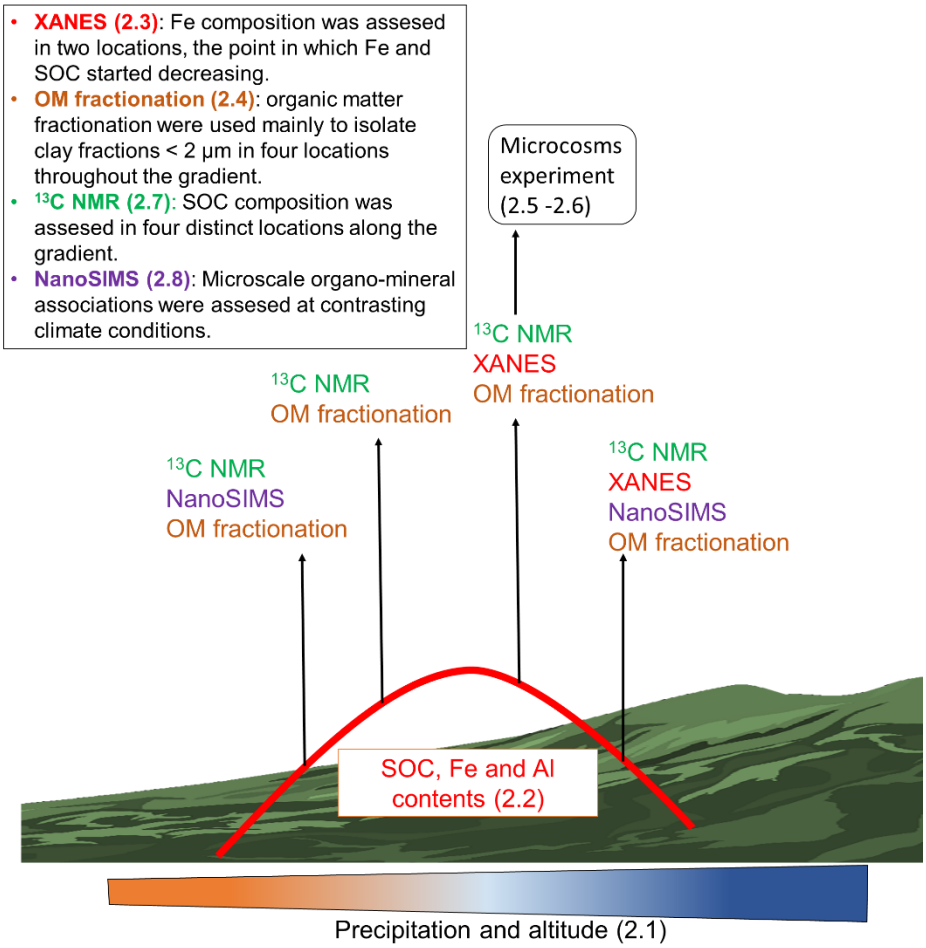

Figure 2: Summary of the main analyses performed in the thesis. The numbers between parentheses indicate the section number in which each analysis is described. The box in the upper left side of the figure explains the main goals of each analysis. The microcosms experiment (Study 3) of this thesis was performed in samples of higher SOC, Fe and Al contents.

2.2 Soil mineralogy and organic matter distribution along the climate gradient

Soil organic carbon contents were measured by dry combustion (CHNSO Elemental Analyzer, Hekatech, Wegberg – Germany). Due to the high rainfall regime and soil pH < 7,

($CaCl_2$), no pre-treatment for carbonate removal was necessary. Pre-tests conducted with 1 M HCl solution also demonstrated no reaction in the samples.

We determined what we call "reactive metals" in this study, which refers to Fe and Al extractable from soil by selective dissolution techniques of acid ammonium oxalate and citrate-dithionite. These reactive phases include monomeric metal cations related to organic ligands, short-range order minerals such as allophane- and imogolite-type minerals, amorphous metal phases, and minor fractions of crystalline Fe oxides, hydroxides and oxyhydroxides (Levard et al., 2012; Parfitt and Childs, 1988; Thompson et al., 2011; Wagai et al., 2018).

I performed extractions of Fe and Al in parallel with dithionite-citrate following the method of Mehra and Jackson (1958) and with NH_4 oxalate at pH 3 according to the method described by Schwertmann (1964). Soil pH was measured in 0.01 M $CaCl_2$ solution (1 : 2.5 soil : solution ratio) using a pH meter (Orion Star A111, ThermoFisher Scientific, Waltham – MA, USA) and exchangeable Ca, Mg, and K were extracted using the NH_4OAc method at pH 7 (Lavkulich, 1981). All the extracted elements were measured by inductively coupled plasma optical emission spectroscopy (ICP-OES) (Vista-Pro CCD simultaneous, Varian, Darmstadt - Germany). In addition, the composition of the fine clay fraction (< 2 μm) was assessed by X-ray diffraction (PW 1830, Phillips, Amsterdam - Netherlands; X-ray source: Co K alpha).

2.3 Fe speciation by Iron K-edge X-ray Absorption Near Edge Structure (XANES) spectroscopy

To assess the presence of reducing conditions at higher precipitation levels, we performed Fe K-edge XANES measurements at the Cornell High Energy Synchrotron Source (CHESS) F3 beamline on two bulk subsoil samples of approximately 2200 and 2300 mm precipitation $year^{-1}$, respectively. Data were collected for the Fe K-edge in fluorescence mode, with a spot size of approximately 0.5 × 4 mm. The Fe K-edge (E_0) was set to 7.112 keV (Prietzel et al., 2007), and scans were collected for the pre-edge region (6.912–7.092 keV) with 0.005 keV step size and 1 s dwell time. For the near-edge (7.092–7.142 eV) region we used a 0.001 keV step size and 2 s dwell time. Multiple scans were collected for each sample; specifically, we collected 2–3 scans for Fe standards and 5 scans for soil samples. Elemental Fe foil was used to collect simultaneous Fe K-edge alignment measurements for each scan.

Fe-organic complex standards (previously published in Bhattacharyya et al. (2018)) included Fe (III) EDTA, Fe (III) citrate, and Fe (II) citrate. Commercially obtained mineral

standards include elemental Fe^0 (energy calibration), goethite, and fayalite. Additionally, Fe^{2+}-substituted nontronite and ferrihydrite were prepared for this experiment following standard protocols. Briefly, structural Fe^{3+} in nontronite was reduced using the dithionite method described by Stucki et al. (1984). Fe^{2+}-substituted nontronite was stored in an anaerobic environment in ultrapure water suspension prior to XAS analysis. Ferrihydrite ($Fe^{3+}{}_2O_3 \bullet 0.5H_2O$) was prepared by titration of Fe (III) nitrate (0.005 M) by addition of base (0.05 M KOH) to pH 7 and purification by dialysis (1000D MWCO) and subsequent rinsing and re-suspension in water until XANES analysis (modified from Schwertmann and Cornell (2008)). Samples were prepared for XANES measurements by deposition of ~2.5 g material on polyimide tape (1-mil) thickness. Reduced Fe samples were prepared and stored anaerobically prior to analysis.

Additionally, the relative contribution of Fe^{2+} to the total Fe XANES spectrum was described using the first derivative of normalized μ(E). In the first derivative μ(E) spectrum, the area of the peak assigned to the 1s-4s transition (~7120 eV) can be used to estimate relative Fe^{2+} (Berry et al., 2003). The ~7120 eV peak area relative to total area was determined by fitting four Gaussian functions at 7112, 7120, 7124, and 7128 eV to the first derivative μ(E) over the range > 7100 and < 7140 eV using the Levenberg-Marquadt algorithm in Fityk v 0.9.8. (Wojder, 2010), with the function at 7120.0 eV fixed and the remaining functions constrained by ±3*sin(~0) eV. Peak full-width half-maximum was constrained to 2 ±1*sin(~0) eV and peak height was unconstrained. The fitted area of the 7120 eV peak was divided by the sum of all four-peak areas to determine relative contribution to the total XANES spectrum.

2.4 Soil organic matter fractionation

In order to obtain a pure clay-sized fraction that was free of particulate organic matter, we performed soil organic matter fractionation. The fractionation was used in the three main projects. In the **Study 1:** *Andosol clay re-aggregation observed at the microscale during physical organic matter fractionation*, we compared the soil dispersion in deionized water with and without NaCl saturation (performed by making the soil dispersion in 1M NaCl solution). In the **Study 2**: *Subsoil organo-mineral associations under contrasting climate conditions,* we have used the approach without NaCl saturation, based in the main conclusions of Study 1. In the **Study 3:** *Microscale distribution increases microbially derived C stabilization in soils*; we have used a dense solution of sodium polytungstate (SPT), due to the topsoil samples rich in particulate organic

matter. In this third study, fractions of free and occluded particulate organic matter (fPOM and oPOM) were fused into what we call the "light fraction" (density <1.8 g cm-3) and mineral fractions of 20-2 and < 2 μm were merged, fused into what we call the "heavy fraction" (density> 1.8 g cm-3). Besides the solution used in the process (e.g., H_2O, 1 M NaCl or SPT 1.8 g cm^{-3}), the remaining procedures were the same for all the fractionations performed in this dissertation. Below, the method is briefly described.

The procedure was adapted from the soil organic matter fractionation method described by Golchin et al. (1994), using 4-mm sieved soils under field-moist conditions. First, we gently saturated the soil by adding deionized water yielding a suspension of 1 : 2.5 soil : water volume. For the dispersion of macroaggregates and larger microaggregates, we utilized ultrasonic dispersion (SonopulsHD2200, Bandelin, Berlin - Germany) with an energy input of 1500 J ml^{-1}. This energy level is considered sufficient for providing dispersion of the highly stable Andosol microaggregates without causing damage to the primary mineral structure (Silva et al., 2015). After centrifuging the suspension (8000 g for 40 min), the floating particulate organic matter was removed from the supernatant using a vacuum pump.

Later, the soil mineral fraction (i.e., free of particulate organic matter) was sieved with a 20-μm sized mesh in order to separate sand and coarse silt-sized fractions. The mineral fraction was then subjected to sedimentation to separate the medium silt and clay-sized fractions of 20-2 μm and < 2 μm, respectively. The < 2 μm clay-sized fraction was subsequently freeze-dried and used for imaging and ^{13}C NMR spectroscopy (Figure 3).

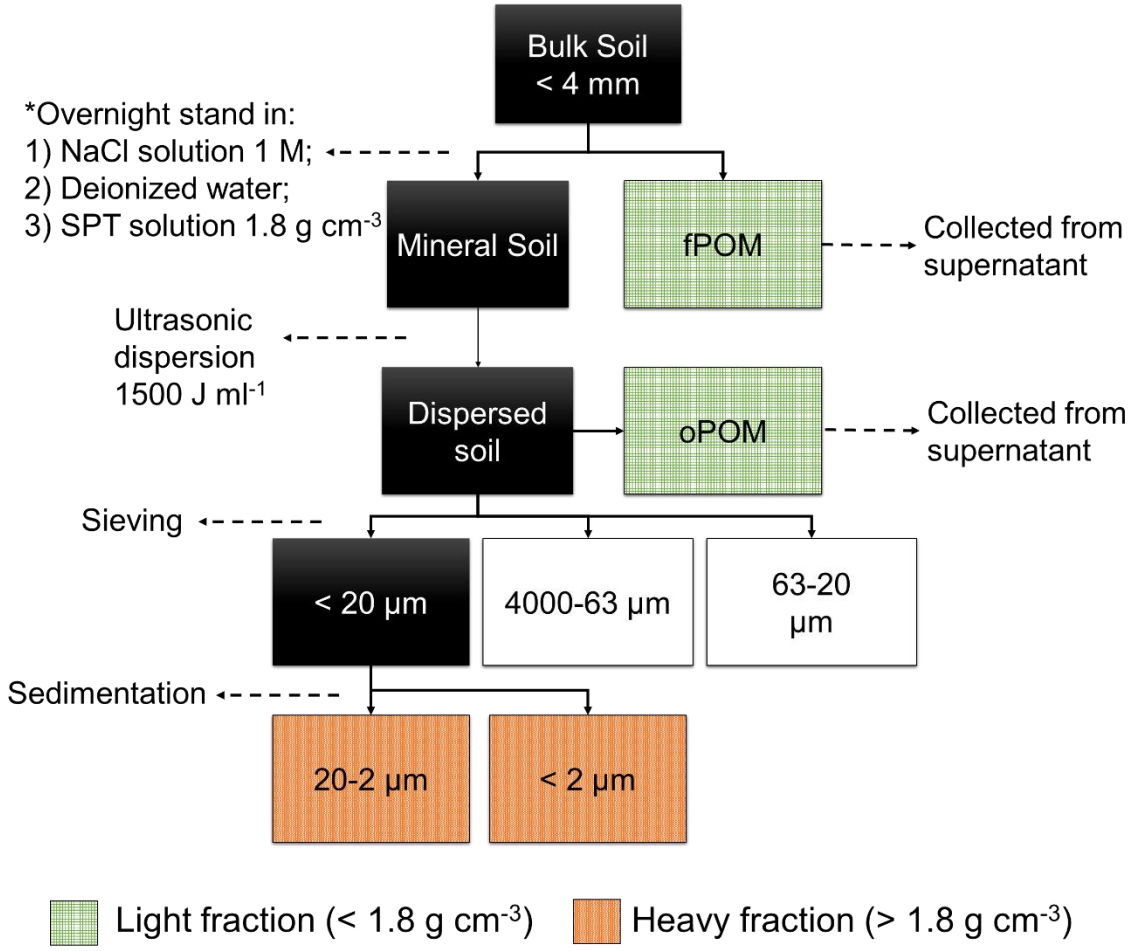

Figure 3: Schematic figure of the soil organic matter fractionation procedure. White boxes represent the different fractions separated by the procedure (i.e., light particulate organic matter – fPOM; occluded particulate organic matter – oPOM; mineral fractions of 4000-64 µm, 63-20 µm, 20-2 µm and < 2 µm). *NaCl and H_2O were used in the Study 1 and 2, while sodium polytungstate (SPT) was used in the Study 3. Dashed arrows and observations represent the procedures performed for conducting each step. Green boxes represent the "light fraction" (fPOM + oPOM) and the orange boxes represent the "heavy fraction" (20-2 + < 2 µm) used in the Study 3.

2.5 Incubation experiment design and organic matter inputs (Study 3)

In the study 3, we have selected the soil profile at 2200 mm year -1 (Table 1), which presented the highest C and mineral contents (e.g., extracted Fe and Al). We have used topsoil (0 – 0.2 m) and subsoil (0.8 – 0.9 m) depths of this soil profile as the base for the incubation experiment to test the effect of microscale spatial distribution.

The incubation experiment consisted in a completely randomized design with three replicates. We used soil samples from two depths: 0 – 0.2 m and 0.8 – 0.9 m (Figure 4). For each depth, we added ^{13}C and ^{15}N labelled amendments as follow: 1) control: incubated soil without amendment; 2) plant debris (willow leaves - *Salix viminalis x S.miyabeana*); dissolved organic

matter (DOM) in two different forms: 3) point source (1 – 2 mm size pellets); and 4) distributed (colloidal particles filtered at 0.7 µm). A summary figure of the experimental design is presented in Figure 4.

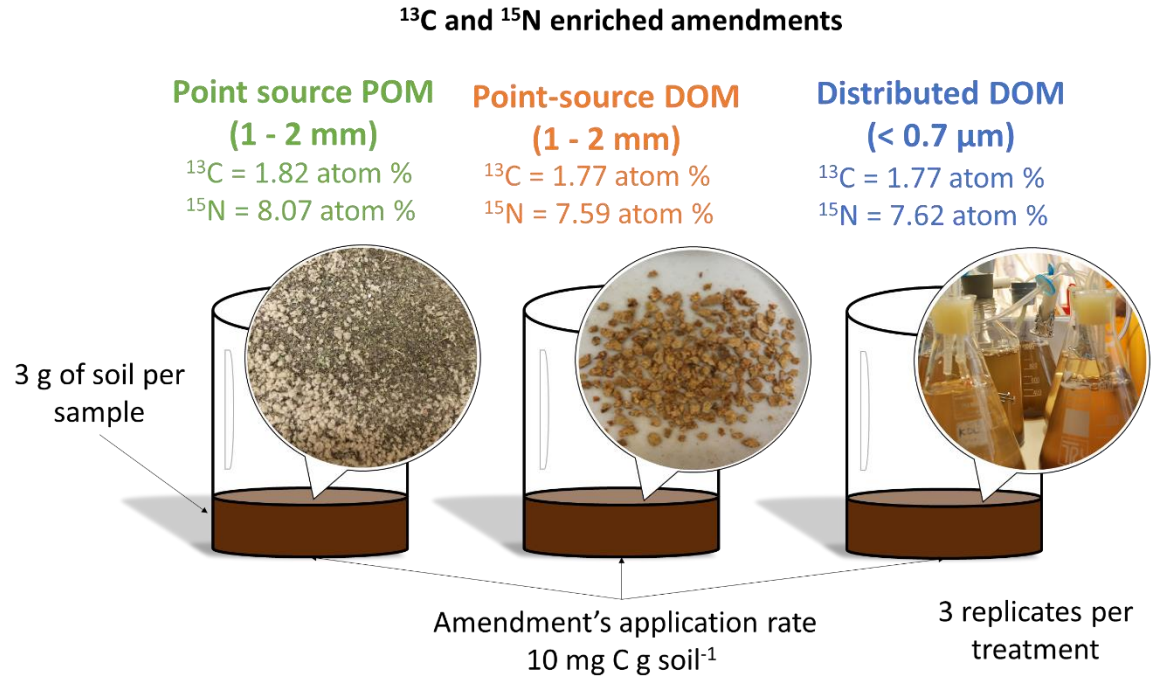

Figure 4: Summary Figure of the incubation experiment. The three units represent the C inputs used in the incubation as follow: 1 – Point source particulate organic matter (POM); 2 – Point source dissolvable organic matter (DOC); and 3 – Distributed DOC. The DOC was extracted from the POM material by shaking it in water during 72h at 32ºC. After this period, the material was filtered with a 0.7 µm filter and freeze-dried. The point source DOC treatment was pelleted in 1-2mm size pellets and the distributed DOC treatment was re-dissolved in water.

The ^{13}C and ^{15}N labelled DOM was extracted from shrub willow leaves enriched with $^{13}CO_2$ (the same used in the experiment as amendment). A detailed description of the plant cultivation can be found in DeCiucies et al. (2018). Briefly, the willow leaves were sieved with a 2 mm sieve and shaken in deionized water (leaves/water proportion of 1:10) during 72h at 32ºC with an orbital shaker at 100 rpm. After the shaking period, the suspension was filtered with a Whatman glass microfiber filter of 0.7 µm. The solution that passed through the filter was then freeze-dried.

For producing the point source DOM form, we have pressed the freeze-dried DOC using a hydraulic press to form solid pieces. Then, I have cracked the compressed material into 1 – 2 mm pieces and used them for the incubation. For the dissolved form, I simply

dissolved the freeze-dried DOM into deionized water and used them as amendments for the incubation. I have also incubated the willow leaves used for producing the DOM as a reference. The ^{13}C enrichment levels of the amendments were 1.82, 1.77 and 1.77 atom percentage for the treatments leaves, point source DOM and distributed DOM, respectively. The ^{15}N enrichment levels were 8.07, 7.59 and 7.62 atom percentage for the leaves, point source DOC and distributed DOM, respectively. For the incubation, I standardized the amendments inputs to 10 mg C g $soil^{-1}$. All the soil + amendment samples were maintained at 50% of their water hold capacity.

2.6 Input-derived C-CO_2 emissions (Study 3)

The samples were added to 60 ml Qorpak bottles with 3 g of soil + amendment mixture. The Qorpak bottle was placed in a 1 L Mason jar containing 30 ml of water to maintain 100% humidity. All the samples were incubated during 50 days. I have used a Picarro CO_2 stable isotope analyzer (G2201-I, Santa Clara, CA, USA) to monitor continuously the incubation and measure the CO_2 emissions. The headspace gas of each jar was sampled for 6 min during each sampling period, and in sequence purged with CO_2-free air.

I collected the data at a rate of two measurements per second over the sampling time, and during the sample purge to record the baseline values before each cycle's respiration measurement. The soils were incubated and the emitted CO_2 was measured during 50 days. After the incubation period, the soils were air-dried and submitted to soil organic matter fractionation.

2.7 Soil organic matter characterization by ^{13}C CP/MAS NMR spectroscopy

Soil clay fractions (< 2 μm) of four soil profiles of precipitation levels across the climate gradient were chosen for NMR spectroscopy (approximately 1700, 2000, 2200, and 2300 mm $year^{-1}$, respectively). The light and heavy fractions of Study 3 were also analyzed.

I performed solid-state ^{13}C NMR spectroscopy (Biospin DSX 200 NMR spectrometer, Bruker, Rheinstetten, Germany) of the < 2 μm clay fractions from the subsoil (0.4–0.6 m) with a contact time of 0.001 sec with a pulse delay of 0.4 sec. At least 100,000 accumulated scans were performed. The spectra were integrated using four major chemical shift regions: 0 to 45 ppm (alkyl-C), 45 to 110 ppm (O/N-alkyl-C), 110 to 160 (aryl-C), and 160 to 220 ppm (carboxyl-

C) (Knicker and Lüdemann, 1995). Despite the elevated Fe content, no sample pre-treatment with hydrofluoric acid was necessary in order to obtain a well-resolved spectrum.

2.8 Organo-mineral associations at the microscale by Nano scale secondary ion mass spectrometry (NanoSIMS)

Two contrasting samples from lower (approximately 1800 mm $year^{-1}$) and higher (approximately 2300 mm $year^{-1}$) rainfall levels were chosen for NanoSIMS analysis. Before< 2 μm fraction was freeze-dried, I took aliquots from the soil suspension in deionized water. The aliquots of soil suspensions were diluted 20 times in water, pipetted onto a silica wafer and dried in a desiccator at room temperature for subsequent scanning electron microscopy (SEM) and NanoSIMS analysis.

To elucidate the distribution of the mineral particles on the Si-wafer and to choose regions of interests for subsequent NanoSIMS measurements, the samples were assessed by reflected light microscopy (Axio Imager Z2, Zeiss, Oberkochen - Germany) and SEMSEM (JSM 5900LV, JEOL, Tokyo - Japan). Prior to the measurement the samples were coated with Au/Pd (~30 nm; SCD 005 sputter coater, Baltec GmbH, Germany), and during measurements the electron flood gun was used to compensate for any charging effects (Mueller et al., 2013b). The NanoSIMS imaging was performed using the NanoSIMS 50L (Cameca, Gennevilliers - France) at the Chair of Soil Science of the Technical University of Munich (TUM), Germany, using a high-energy cesium (Cs^+) ion beam (~1.2 pA). We used electron multipliers with a dead time of 44 ns to detect the following secondary ions: $^{16}O^-$, $^{12}C^-$, $^{12}C^{14}N^-$, $^{27}Al^{16}O^-$ and $^{56}Fe^{16}O^-$. Before the analysis, I removed the gold coating layer using a high primary beam current. The beam was focused onto the sample and secondary ions were ejected from the sample surface with a lateral resolution of ~100 nm. The field of view of the measurements was 20 μm · 20 μm (256 · 256 pixels) and the ion images were acquired using a dwell time of 1 ms per pixel with each 40 planes.

2.8.1 M&M: Multi-channel machine-learning segmentation and image analysis

The NanoSIMS measurements were corrected for electron multiplier dead-time by using the OpenMIMS plugin for Fiji (Gormanns et al., 2012). Sum images were created based on auto-alignment of the $^{16}O^-$ distribution across all 40 planes. To differentiate the elemental distributions at the microscale and use these to quantify spatial measures, supervised pixel

classifications was performed based on the machine-learning algorithm implemented in Ilastik 1.2 (Sommer et al., 2011). The $^{16}O^-$ distribution was used to differentiate between soil particles and Si wafer and define training areas for the algorithm. The additional presence of $^{12}C^-$ and $^{12}C^{14}N^-$ on these particles was used to determine OM segments (Hatton et al., 2012; Remusat et al., 2012). In this regard, I use the term soil particles to refer to the total distribution of segments classified as mineral or OM.

The simple segmentation mask based on $^{16}O^-$, $^{12}C^-$, and $^{12}C^{14}N^-$ was used to quantify the spatial arrangement of individual particle and OM segments. Based on the projected area of particle segments and OM segments, their mean size were computed averaged across all sizes and frequency distributions for the size classes <0.1 μm^2, 0.1-0.5 μm^2, 0.5-2 μm^2, and > 2 μm^2. To analyze the relative chemical composition of the OM segments, we determined the normalized CN:C ratio of the individual OM segments based on the simple segmentation mask. To quantify the co-localization of OM^-, Al^-, and Fe-enriched spots, I combined the simple segmentation of mineral and OM segments with the Al and Fe segments into a segmentation mask comprising all possible combinations in 12 material classes. To compare the co-localization of OM with Al and Fe, I computed the relative area contributions of the 4 association classes to the total OM segment area. By transferring the combined segmentation mask to other isotope distributions, I determined the normalized CN:C ratio across all pixels according to the 4 OM association classes.

2.8.2 NanoSIMS analysis in aggregate cross sections (Study 3)

In order to evaluate the presence of input derived OM inside aggregates, I performed cross sectioning of soil macroaggregates according to the method described by Mueller et al. (2013a). Briefly, I have randomly selected macroaggregates of approximately 2 mm size, embedded them in epoxy resin, polished them down until approximately half and performed the nanoscale secondary ion mass spectrometry (NanoSIMS) analysis in their interior. We hypothesized that infiltration through the soil pore system would be the main pathway of organic matter entrance into the soil macroaggregates. Therefore, I have aimed at the interfaces of the pore system (i.e., the space through which the resin has infiltrated during the embedding) and the soil structure. I have made four measurement in two macroaggregates for each treatment in top and subsoil samples, looking for "hot-spots" of $^{12}C^{15}N$ enrichment. By calculating the $^{12}C^{15}N$ / $^{12}C^{14}N$ ratio of the enriched areas, I was able to measure the presence

of amendment derived N-rich organic matter in the soil pore system interfaces. Measurements were processed using the ImageJ software (Abràmoff et al., 2004).

Results and discussion

This section is focusses in an overall discussion from the three main studies performed in this thesis. Detailed information is available online and in the appendices.

3.1 Re-aggregation in the clay fraction at the microscale

I have performed soil organic matter fractionation with different approaches for dispersing the highly stable Andosols samples. The first important fact tested was whether Na saturation prior to soil dispersion was necessary for obtaining clay size fractions < 2 μm. This assumption was made based in recommendations from other studies that performed fractionation in Andosols (Aoyama, 1992; Asano and Wagai, 2014; Kato and Fujisawa, 1973; Yonebayashi et al., 1974). By comparing soil dispersions with and without Na saturation (through addition of 1 M NaCl) our results revealed little influence of this treatment in SOC distributions (lower than 2% of difference for the < 2 μm clay fraction) (Figure. 5).

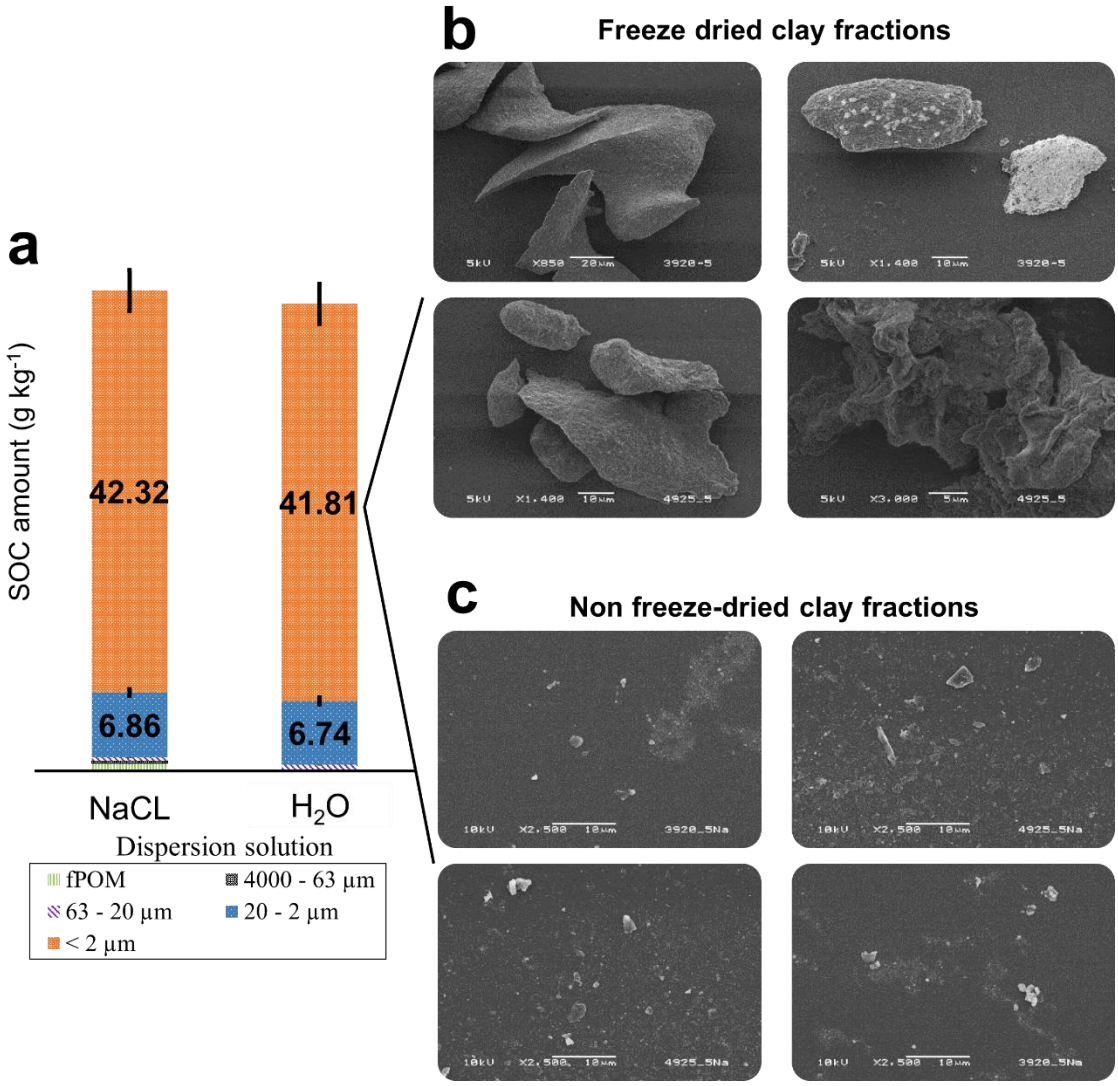

Figure 5: Na saturation on SOC distribution and clay re-aggregation effects of the caused by freeze-drying. **a)** Soil organic matter fractions in subsoil B horizon (0.4–0.6 m) of an Andosol with two dispersion solutions prior to ultrasound sonication, including 1 M NaCl solution and deionized water (H_2O). Numbers in the columns represent the amount of SOC (g kg^{-1}) retained in each fraction. Error bars represent the standard deviation of three laboratory replicates. **b-c)** Scanning electronic microscopy (SEM) images of samples taken from a clay fraction (< 2 µm) water suspension and the same fraction freeze-dried. Source: Adapted from Inagaki et al. (2019).

At the microscale, I observed a clay re-aggregation effect in freeze-dried samples, while this was avoided when sampling directly from the soil suspension (Figure. 5 b-c). Freeze-drying is a common procedure used in different methods including SOM fractionation but also general soil analyzes protocols due to its efficiency in sample preservation (Miller et al., 1999). However, our experimental results demonstrated that for the Andosol used in this

study, this procedure created sample artifacts that can clearly affect the analysis when the objective is to isolate the clay-size fraction, especially with the intent to examine the microscale organic matter surface coverage or the specific surface area (Schweizer et al., 2018; Vogel et al., 2014). The presence of strong binding effects of the poorly crystalline mineral phases in Andosols is likely the primary reason for this effect. Therefore, in future studies, I recommend reserving a small liquid aliquot from soil suspensions after sonication to proceed with microscopy analyzes.

3.2 Discerning the roles of Fe and Al in promoting organo-mineral associations

At the bulk soil scale, I have observed a significant positive correlation between SOC and Fe and Al extracted by ammonium oxalate (OX) throughout the climate gradient (Figure. 6a). The relationships between SOC with either pedogenic Fe or Al (e.g. extracted by OX) along the climate gradient demonstrated the significant role of this proxy for reactive metal oxides in SOC stabilization as supported by several studies (Basile-Doelsch et al., 2007; Schwertmann, 1964; Torn et al., 1997; Wagai et al., 2018). However, despite the slight difference in the significance level of the correlations (Al $p < 0.01$; Fe $p < 0.05$), these extractions at the bulk soil scale alone were not sufficient to discern the differential role of Fe and Al in promoting organo-mineral associations.

On the other hand, when evaluating the < 2 μm clay fractions of soils from contrasting precipitation rates (1800 and 2300 mm $year^{-1}$) at the microscale using NanoSIMS, I could quantify distinct properties of co-localized organic matter (OM) associations (Figure. 6b). Our data revealed more Fe and Fe co-localized with Al on the OM segments under the low precipitation regime compared with high precipitation. Al provided the highest area contribution of co-localized OM under the high precipitation regime.

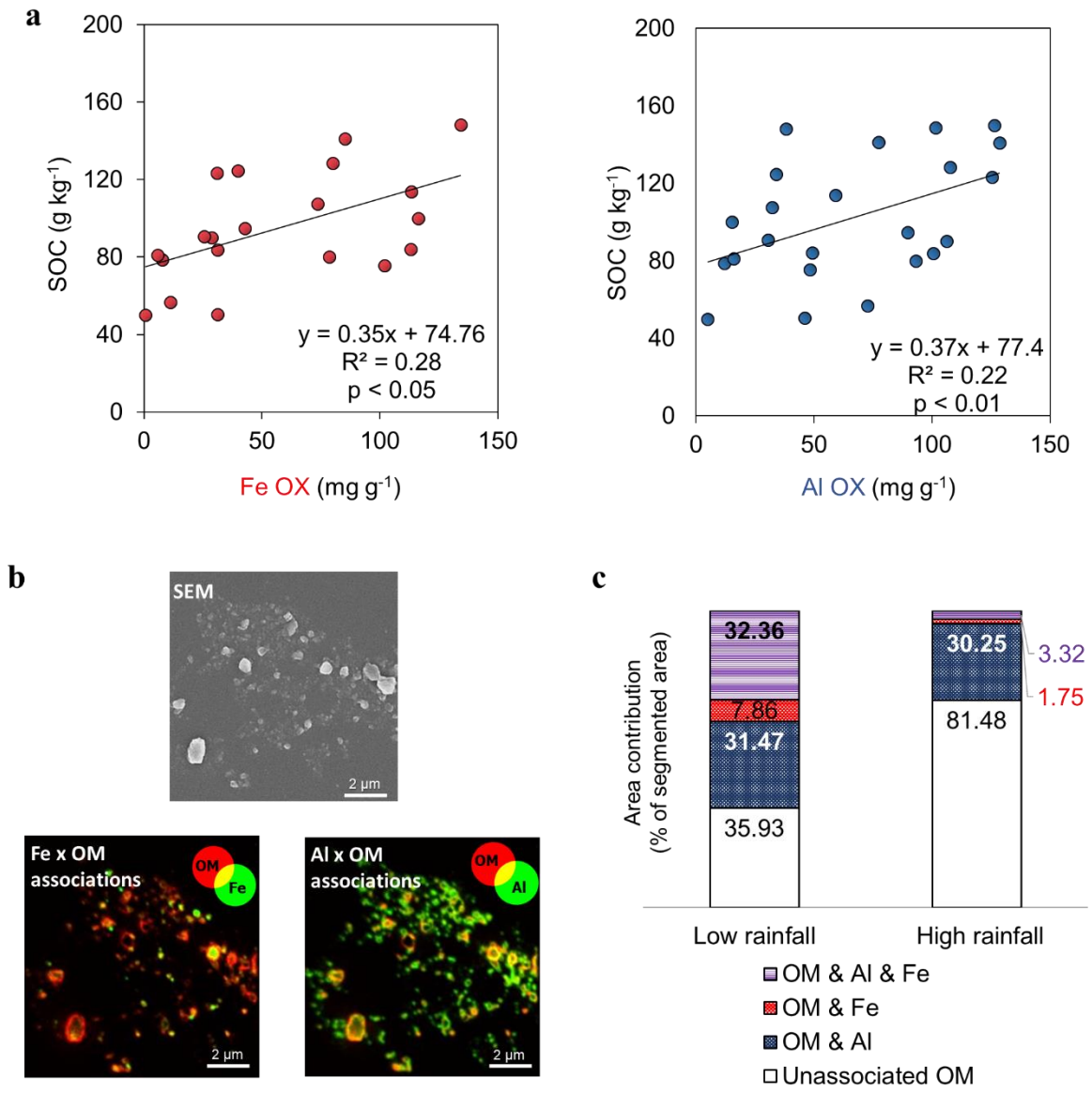

Figure 6: Fe and Al promoting organo-mineral associations at the bulk soil scale and microscale. a) Relationships between Fe and Al extracted by ammonium oxalate (OX) and soil organic carbon (SOC) of 0.4–0.9 m depths along the precipitation gradient. **b)** Composite image of elemental distribution and associations of organic matter ($^{12}C^{14}N^-$) Fe ($^{56}Fe^{16}O^-$) and Al ($^{27}Al^{16}O^-$). **c)** Microspatial associations in < 2 µm clay fraction fractionated. Area contributions of organic matter segment. Source: Adapted from Inagaki et al. (2020).

Our results suggest that a major proportion of the organic matter measured by NanoSIMS at higher rainfall levels (2300 mm year^{-1}) is unassociated with Fe and Al (e.g., 80% of the total segmented area), while most of the remaining organo-mineral interactions are Al-OM associations. This result highlights the importance of Al in promoting overall SOC stabilization especially at higher precipitation regimes. Since the majority of previous studies on mechanisms of organo-mineral interaction focused on Fe associations (Chen et al., 2014; Gu

et al., 1994; Saidy et al., 2012), we emphasize the importance of directing more attention to mechanisms of Al- SOC associations, especially in areas under high precipitation regimes.

3.3 Mechanisms of organo-mineral associations affected by climate factors

Along the precipitation gradient, I have observed maximum levels of SOC and extracted Fe and Al at precipitation rages of 2000 and 2200 mm $year^{-1}$, respectively. These contents declined in higher rainfall regimes (Inagaki et al., 2020). Along the climate gradient, I observed changes in the SOC composition of the clay fraction (<2 mm) as measured by ^{13}C NMR spectroscopy. For instance, I have observed lower levels of Carboxylic-C (5% lower in relative abundance) at higher precipitation ranges of 2300 mm $year^{-1}$. Likewise, at this precipitation level, I have observed changes in Fe speciation to more reduced forms.

These changes in soil organic matter composition and shifts in Fe speciation driven by climate factors may have a direct influence on how organo-mineral associations occur in this gradient. This is because carboxylic C groups play an important role in SOC accrual, since it is responsible for forming associations with minerals through a variety of interactions mechanisms (e.g., cation exchange, ligand exchange) (Aquino et al., 2011). In addition, the Fe reduction can potentially result in a loss of SOC to the aqueous phase mainly by its release from Fe associations as demonstrated by Huang and Hall (2017) in an incubation experiment. According to the authors, this release represents a yet under-appreciated mechanism for SOC destabilization.

In Figure. 7, I demonstrate the overall effects of climate changes on subsoil organo-mineral associations at the macro- and microscale. In this paper, I illustrated under field conditions that the major factors influencing subsoil organo-mineral associations as a function of differences in climate were a combination of lower contents of reactive Fe and changes of Fe and SOC composition. These results demonstrates that the use of microscopic techniques can reveal differences in organo-mineral associations that cannot be observed using bulk soil analyses alone.

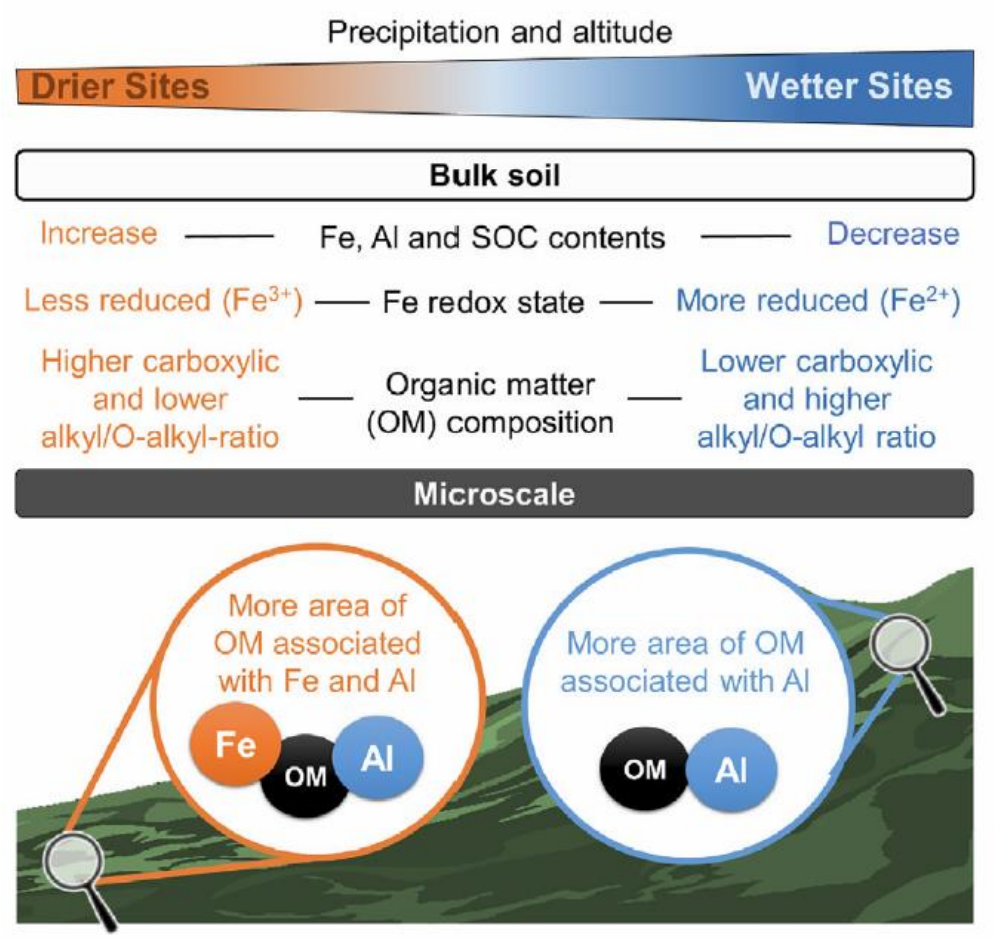

Figure 7: Climate differences on organo-mineral associations. Conceptual illustration demonstrating the overall effects of climate on soil organo-mineral associations at the macro and microscale in subsoil depths along the climate gradient. Source: (Inagaki et al., 2020)

3.4 Influence of microscale spatial distribution on organic matter mineralization and stabilization

In the mineral-rich subsoil at a precipitation of 2100 mm year^{-1}, greater spatial distribution of microbially-derived dissolved organic matter (DOM) on its own increased C sequestration in the heavy fraction (i.e., mineral-associated OM) from 36 to 46% of the total added C (Figure 8a) and decreased cumulative respiration by 17% (Figure 8b). I did not observe a significant influence of the spatial distribution (i.e., point source vs distributed DOM) in the sequestration and mineralization rates in the C-rich topsoil (Figure 8c, Fig. 8d). The significant effect of the spatial distribution of the microbially-derived DOM in the subsoil points towards a yet unrecognized factor affecting C sequestration and mineralization rates. These differences between organic matter inputs may be directly related to lower availability to decomposers.

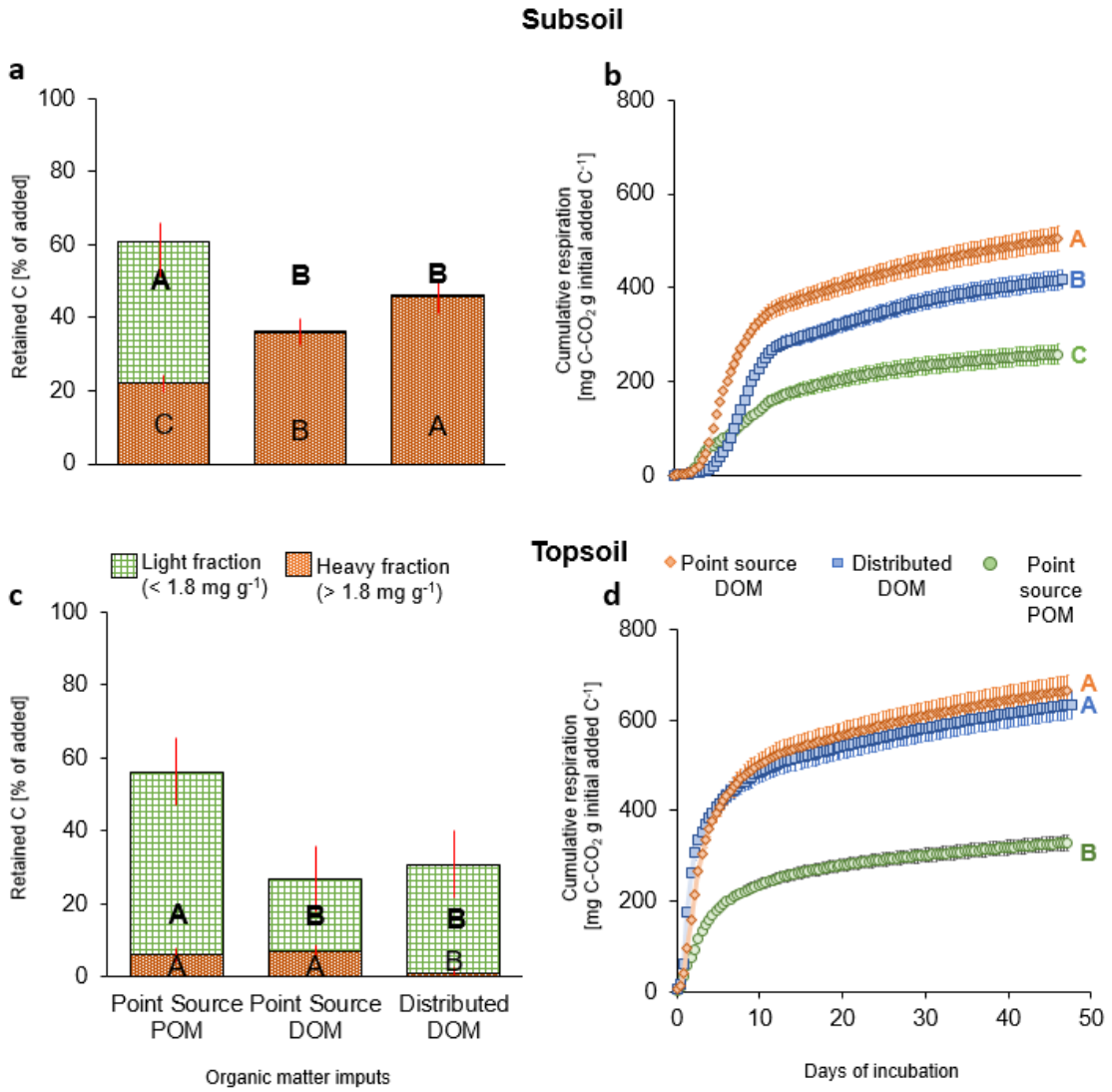

Figure 8: Soil organic carbon (SOC) stabilization and mineralization in top and subsoil. b, d: cumulative respiration rates of the amendment derived C-CO2 during the 50 days of incubation in topsoil (0 – 0.2 m) and subsoil (0.8 – 0.9 m) samples. For a given depth, cumulative respiration rates followed by the same letter do not differ among amendments at $p < 0.05$ (LSD test) a, c: Partitioning of the litter derived C among soil organic matter density fractions: heavy fraction (> 1.8 g cm^{-3}) and light fraction (< 1.8 g cm^{-3}). For a given fraction, means followed by the same letter do not differ among amendments at $p < 0.05$ (LSD test).

In Figure 9, I outline the proposed mechanisms how micro-scale spatial distribution affects the mineralization and sequestration of the microbially-derived DOM. A greater respiration of the point source than the distributed DOM in the subsoil (Figure. 8) indicates that a spatially more concentrated DOM may facilitate the activity of decomposer microorganisms by creating suitable conditions for specialization on a specific substrate and the development of microbial colonies (Dechesne et al., 2007) (Mechanism 2, Fig 9). On the

other hand, the distributed DOM may reduce the ability of the microorganisms to invest in metabolic strategies as also indicated by the delay in peak emissions (Mechanism 1, Figure. 9). In addition, a greater adsorption of distributed than point source DOM plays a role, as the distributed DOM resulted in 46% of the total added OM sequestered in the heavy fraction against 36% of the point source DOM (Figure. 8).

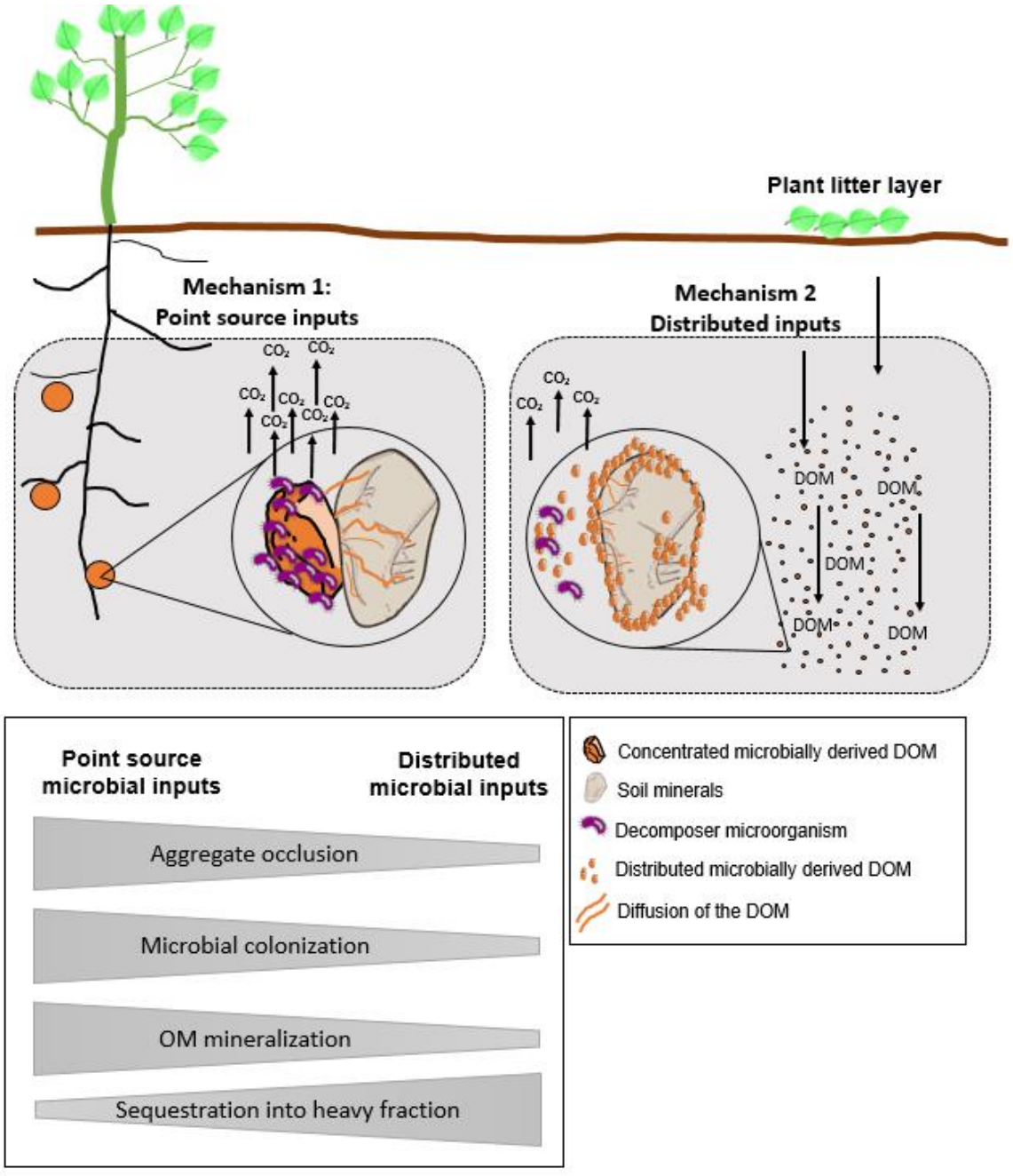

Figure 9: Proposed mechanisms for mineralization and stabilization of point source and distributed inputs of organic matter. The Figure illustrates the colonization of the material by decomposing microorganisms, C sequestration through mineral interactions and the infiltration through the macroaggregates pore system.

Conclusions and outlook

This thesis improves our overall understanding of organo-mineral interactions in soil. I developed important methodological steps to avoid clay re-aggregation in fractionated Andosols. This study demonstrated that Na saturation through the addition of 1 M NaCl solution caused low (less than 2% in SOC amount) clay dispersion (< 2 mm) compared with the dispersion when water alone was used. Direct effects of freeze–drying on Andosol clay fractions at the microscale were also observed, which caused the formation of assemblages larger than 20 mm. The presence of strong binding effects of the poorly crystalline mineral phases in Andosols is likely the primary reason for this effect. Therefore, in future studies, I recommend reserving a small liquid aliquot from soil suspensions after sonication to proceed with microscopy analyzes. These findings can significantly facilitate organic matter fractionation, especially aiming at improving subsequent microscopic and spectromicroscopic analyses.

The findings in the climate gradient contributes to our overall comprehension about the influence of climate differences on organo-mineral associations. I concluded that interactions between reactive metal minerals and SOC at the scale in which mineral interactions occur are of considerable importance to understanding SOC stabilization, and these interactions may not be traceable from analyses at the bulk soil scale. The changes in these associations in subsoils should be taken into consideration when evaluating the impact of climate factors and land use. I recommend that future studies should take the forms of Fe oxides forming at different locations in soil microsites as a function of soil moisture and redox conditions into consideration. In addition, I also encourage researchers to investigate the overall role of Al in promoting SOC accrual, especially under reducing conditions.

The results of our incubation experiment brings novel discoveries about the influence of microscale spatial distribution on organic matter mineralization and stabilization rates. I demonstrated that greater micro-scale spatial distribution of microbially-derived DOM could significantly decrease mineralization rates and increase its stabilization through mineral associations. This yet unrecognized influence could be of great importance for SOC models especially regarding belowground inputs. Therefore, I recommend that future studies take into consideration this fact while evaluating the stabilization mechanisms of organic matter, especially in subsoil depths.

Although this thesis was focused on samples of volcanic soil (Andosols), the results of these studies can be extrapolated to other conditions. Although the Andosols have unique properties, such as a high C storage capacity, the mechanisms observed in our research were similar to those observed in other soils (e.g., Fe-SOC displacement in reduction conditions, changes in Fe and SOC due to climate differences). Therefore, the novelties concluded in our experiments, especially regarding microscale spatial distribution, are likely to apply to other conditions.

References

Abràmoff M.D., Magalhães P.J. and Ram S.J., (2004) Image processing with ImageJ. *Biophotonics international* **11**, 36-42.

Adhikari D. and Yang Y., (2015) Selective stabilization of aliphatic organic carbon by iron oxide. *Scientific reports* **5**, 11214.

Aoyama M., (1992) Accumulated organic matter and its nitrogen mineralization in soil particle size fractions with long-term application of farmyard manure or compost. *Japanese Journal of Soil Science and Plant Nutrition (Japan)*.

Aquino A.J., Tunega D., Schaumann G.E., Haberhauer G., Gerzabek M.H. and Lischka H., (2011) The functionality of cation bridges for binding polar groups in soil aggregates. *International Journal of Quantum Chemistry* **111**, 1531-1542.

Asano M. and Wagai R., (2014) Evidence of aggregate hierarchy at micro- to submicron scales in an allophanic Andisol. *Geoderma* **216**, 62-74.

Asano M., Wagai R., Yamaguchi N., Takeichi Y., Maeda M., Suga H. and Takahashi Y., (2018) In Search of a Binding Agent: Nano-Scale Evidence of Preferential Carbon Associations with Poorly-Crystalline Mineral Phases in Physically-Stable, Clay-Sized Aggregates. *Soil Systems* **2**, 32.

Basile-Doelsch I., Amundson R., Stone W.E.E., Borschneck D., Bottero J.Y., Moustier S., Masin F. and Colin F., (2007) Mineral control of carbon pools in a volcanic soil horizon. *Geoderma* **137**, 477-489.

Baumert V.L., Vasilyeva N., Vladimirov A., Meier I.C., Kögel-Knabner I. and Mueller C.W., (2018) Root exudates induce soil macroaggregation facilitated by fungi in subsoil. *Frontiers in Environmental Science* **6**, 140.

Beare M., McNeill S., Curtin D., Parfitt R., Jones H., Dodd M. and Sharp J., (2014) Estimating the organic carbon stabilisation capacity and saturation deficit of soils: a New Zealand case study. *Biogeochemistry* **120**, 71-87.

Benner R., (2011) Biosequestration of carbon by heterotrophic microorganisms. *Nature Reviews Microbiology* **9**, 75.

Berry A.J., O'Neill H.S.C., Jayasuriya K.D., Campbell S.J. and Foran G.J., (2003) XANES calibrations for the oxidation state of iron in a silicate glass. *American Mineralogist* **88**, 967-977.

Bhattacharyya A., Schmidt M.P., Stavitski E. and Martinez C.E., (2018) Iron speciation in peats: Chemical and spectroscopic evidence for the co-occurrence of ferric and ferrous iron in organic complexes and mineral precipitates. *Organic Geochemistry* **115**, 124-137.

Blagodatsky S. and Richter O., (1998) Microbial growth in soil and nitrogen turnover: a theoretical model considering the activity state of microorganisms. *Soil Biology and Biochemistry* **30**, 1743-1755.

Chen C., Dynes J.J., Wang J. and Sparks D.L., (2014) Properties of Fe-organic matter associations via coprecipitation versus adsorption. *Environmental science & technology* **48**, 13751-13759.

Cotrufo M.F., Wallenstein M.D., Boot C.M., Denef K. and Paul E., (2013) The M icrobial E fficiency-M atrix S tabilization (MEMS) framework integrates plant litter decomposition with soil organic matter stabilization: do labile plant inputs form stable soil organic matter? *Global Change Biology* **19**, 988-995.

Dahlgren R.A., Saigusa M. and Ugolini F.C., (2004) The nature, properties and management of volcanic soils. *Adv Agron* **82**, 113-182.

Dechesne A., Pallud C. and Grundmann G.L., (2007) Spatial distribution of bacteria at the microscale in soil. *the Spatial Distribution of Microbes in the Environment*, 87-107.

DeCiucies S., Whitman T., Woolf D., Enders A. and Lehmann J., (2018) Priming mechanisms with additions of pyrogenic organic matter to soil. *Geochimica et Cosmochimica Acta* **238**, 329-342.

Dungait J.A., Hopkins D.W., Gregory A.S. and Whitmore A.P., (2012) Soil organic matter turnover is governed by accessibility not recalcitrance. *Global Change Biology* **18**, 1781-1796.

Eusterhues K., Rumpel C. and Kogel-Knabner I., (2005) Stabilization of soil organic matter isolated via oxidative degradation. *Organic Geochemistry* **36**, 1567-1575.

Filimonova S., Kaufhold S., Wagner F.E., Hausler W. and Kogel-Knabner I., (2016) The role of allophane nano-structure and Fe oxide speciation for hosting soil organic matter in an allophanic Andosol. *Geochimica Et Cosmochimica Acta* **180**, 284-302.

Giambelluca T.W., Chen Q., Frazier A.G., Price J.P., Chen Y.-L., Chu P.-S., Eischeid J.K. and Delparte D.M., (2013) Online rainfall atlas of Hawai 'i. *Bulletin of the American Meteorological Society* **94**, 313-316.

Golchin A., Oades J., Skjemstad J. and Clarke P., (1994) Study of free and occluded particulate organic matter in soils by solid state 13C CP/MAS NMR spectroscopy and scanning electron microscopy. *Soil Research* **32**, 285-309.

Gormanns P., Reckow S., Poczatek J.C., Turck C.W. and Lechene C., (2012) Segmentation of multi-isotope imaging mass spectrometry data for semi-automatic detection of regions of interest. *PloS one* **7**, e30576.

Gu B., Schmitt J., Chen Z., Liang L. and McCarthy J.F., (1994) Adsorption and desorption of natural organic matter on iron oxide: mechanisms and models. *Environmental Science & Technology* **28**, 38-46.

Harden J.W., (1982) A Quantitative Index of Soil Development from Field Descriptions - Examples from a Chronosequence in Central California. *Geoderma* **28**, 1-28.

Hatton P.J., Remusat L., Zeller B. and Derrien D., (2012) A multi-scale approach to determine accurate elemental and isotopic ratios by nano-scale secondary ion mass spectrometry imaging. *Rapid Communications in Mass Spectrometry* **26**, 1363-1371.

Hong Z.N., Chen W.L., Rong X.M., Cai P., Dai K. and Huang Q.Y., (2013) The effect of extracellular polymeric substances on the adhesion of bacteria to clay minerals and goethite. *Chemical Geology* **360**, 118-125.

Huang W. and Hall S.J., (2017) Elevated moisture stimulates carbon loss from mineral soils by releasing protected organic matter. *Nature communications* **8**, 1774.

Inagaki T.M., Mueller C.W., Lehmann J. and Kögel-Knabner I., (2019) Andosol clay re-aggregation observed at the microscale during physical organic matter fractionation. *Journal of Plant Nutrition and Soil Science* **182**, 145-148.

Inagaki T.M., Possinger A.R., Grant K.E., Schweizer S.A., Mueller C.W., Derry L.A., Lehmann J. and Kögel-Knabner I., (2020) Subsoil organo-mineral associations under contrasting climate conditions. *Geochimica et Cosmochimica Acta* **270**, 244-263.

IUSS Working Group W. (2015) International soil classification system for naming soils and creating legends for soil maps.

Janzen H., (2015) Beyond carbon sequestration: soil as conduit of solar energy. *European Journal of Soil Science* **66**, 19-32.

Kato H. and Fujisawa T., (1973) Studies on the structure of humus-clay complexes (part 1): on the dispersion characteristics. *Jpn. J. Soil Sci. Plant Nutr* **44**, 251-256.

Keiluweit M., Wanzek T., Kleber M., Nico P. and Fendorf S., (2017) Anaerobic microsites have an unaccounted role in soil carbon stabilization. *Nat Commun* **8**, 1771.

Kitagawa Y., (1971) The "unit particle" of allophane. *American Mineralogist: Journal of Earth and Planetary Materials* **56**, 465-475.

Kleber M., Eusterhues K., Keiluweit M., Mikutta C., Mikutta R. and Nico P.S., (2015) Chapter one-mineral–organic associations: formation, properties, and relevance in soil environments. *Advances in agronomy* **130**, 1-140.

Knicker H. and Lüdemann H.D., (1995) N-15 and C-13 Cpmas and Solution Nmr-Studies of N-15 Enriched Plant-Material during 600 Days of Microbial-Degradation. *Organic Geochemistry* **23**, 329-341.

Kögel-Knabner I., Guggenberger G., Kleber M., Kandeler E., Kalbitz K., Scheu S., Eusterhues K. and Leinweber P., (2008) Organo-mineral associations in temperate soils: Integrating biology, mineralogy, and organic matter chemistry. *Journal of Plant Nutrition and Soil Science* **171**, 61-82.

Lavkulich L., (1981) Methods manual, pedology laboratory. *Vancouver, BC, CA: University of British Columbia, Department of Soil Science*.

Lehmann J. and Kleber M., (2015) The contentious nature of soil organic matter. *Nature* **528**, 60-68.

Lehmann J., Solomon D., Kinyangi J., Dathe L., Wirick S. and Jacobsen C., (2008) Spatial complexity of soil organic matter forms at nanometre scales. *Nature Geoscience* **1**, 238-242.

Levard C., Doelsch E., Basile-Doelsch I., Abidin Z., Miche H., Masion A., Rose J., Borschneck D. and Bottero J.-Y., (2012) Structure and distribution of allophanes, imogolite and proto-imogolite in volcanic soils. *Geoderma* **183**, 100-108.

Liang C., Amelung W., Lehmann J. and Kästner M., (2019) Quantitative assessment of microbial necromass contribution to soil organic matter. *Global change biology*.

Liang C., Schimel J.P. and Jastrow J.D., (2017) The importance of anabolism in microbial control over soil carbon storage. *Nature Microbiology* **2**, 17105.

Marin-Spiotta E., Chadwick O.A., Kramer M. and Carbone M.S., (2011) Carbon delivery to deep mineral horizons in Hawaiian rain forest soils. *Journal of Geophysical Research: Biogeosciences* **116**.

Matus F., Amigo X. and Kristiansen S.M., (2006) Aluminium stabilization controls organic carbon levels in Chilean volcanic soils. *Geoderma* **132**, 158-168.

McNally S.R., Beare M.H., Curtin D., Meenken E.D., Kelliher F.M., Calvelo Pereira R., Shen Q. and Baldock J., (2017) Soil carbon sequestration potential of permanent pasture and continuous cropping soils in New Zealand. *Global change biology* **23**, 4544-4555.

Mehra O. and Jackson M. (1958) Iron oxide removal from soils and clays by a dithionite-citrate system buffered with sodium bicarbonate, National conference on clays and clays minerals, pp. 317-327.

Mueller C.W., Weber P.K., Kilburn M.R., Hoeschen C., Kleber M. and Pett-Ridge J., (2013a) Advances in the Analysis of Biogeochemical Interfaces: NanoSIMS to Investigate Soil Microenvironments. *Adv Agron* **121**, 1-46.

Mueller C.W., Weber P.K., Kilburn M.R., Hoeschen C., Kleber M. and Pett-Ridge J. (2013b) Advances in the Analysis of Biogeochemical Interfaces: NanoSIMS to Investigate Soil Microenvironments, in: Sparks, D.L. (Ed.), Advances in Agronomy, Vol 121, pp. 1-46.

Nanzyo M., Dahlgren R. and Shoji S. (1993) Chemical characteristics of volcanic ash soils, Developments in Soil Science. Elsevier, pp. 145-187.

O'Gorman P.A., (2015) Precipitation extremes under climate change. *Current climate change reports* **1**, 49-59.

Parfitt R. and Childs C., (1988) Estimation of forms of Fe and Al-a review, and analysis of contrasting soils by dissolution and Mossbauer methods. *Soil Research* **26**, 121-144.

Prietzel J., Thieme J., Eusterhues K. and Eichert D., (2007) Iron speciation in soils and soil aggregates by synchrotron-based X-ray microspectroscopy (XANES, μ-XANES). *European Journal of Soil Science* **58**, 1027-1041.

Remusat L., Hatton P.-J., Nico P.S., Zeller B., Kleber M. and Derrien D., (2012) NanoSIMS study of organic matter associated with soil aggregates: advantages, limitations, and combination with STXM. *Environmental science & technology* **46**, 3943-3949.

Rennert T., (2019) Wet-chemical extractions to characterise pedogenic Al and Fe species–a critical review. *Soil research* **57**, 1-16.

Reynolds A.M., Dutta T.K., Curtis R.H., Powers S.J., Gaur H.S. and Kerry B.R., (2010) Chemotaxis can take plant-parasitic nematodes to the source of a chemo-attractant via the shortest possible routes. *Journal of the Royal Society Interface* **8**, 568-577.

Saidy A., Smernik R., Baldock J., Kaiser K., Sanderman J. and Macdonald L., (2012) Effects of clay mineralogy and hydrous iron oxides on labile organic carbon stabilisation. *Geoderma* **173**, 104-110.

Schimel J. and Schaeffer S.M., (2012) Microbial control over carbon cycling in soil. *Frontiers in microbiology* **3**, 348.

Schweizer S.A., Hoeschen C., Schlüter S., Kögel-Knabner I. and Mueller C.W., (2018) Rapid soil formation after glacial retreat shaped by spatial patterns of organic matter accrual in microaggregates. *Global change biology* **24**, 1637-1650.

Schwertmann U., (1964) Differenzierung der Eisenoxide des Bodens durch Extraktion mit Ammoniumoxalat-Lösung. *Journal of Plant Nutrition and Soil Science* **105**, 194-202.

Schwertmann U. and Cornell R.M. (2008) Iron oxides in the laboratory: preparation and characterization. John Wiley & Sons.

Silva J.H.S., Deenik J.L., Yost R.S., Bruland G.L. and Crow S.E., (2015) Improving clay content measurement in oxidic and volcanic ash soils of Hawaii by increasing dispersant concentration and ultrasonic energy levels. *Geoderma* **237**, 211-223.

Six J., Conant R.T., Paul E.A. and Paustian K., (2002) Stabilization mechanisms of soil organic matter: Implications for C-saturation of soils. *Plant and Soil* **241**, 155-176.

Sommer C., Straehle C., Koethe U. and Hamprecht F.A. (2011) Ilastik: Interactive learning and segmentation toolkit, 2011 IEEE international symposium on biomedical imaging: From nano to macro. IEEE, pp. 230-233.

Souza I.F., Archanjo B.S., Hurtarte L.C., Oliveros M.E., Gouvea C.P., Lidizio L.R., Achete C.A., Schaefer C.E. and Silva I.R., (2017) Al-/Fe-(hydr) oxides–organic carbon associations in Oxisols—From ecosystems to submicron scales. *Catena* **154**, 63-72.

Steffens M., Rogge D.M., Mueller C.W., Hoschen C., Lugmeier J., Kolbl A. and Kogel-Knabner I., (2017) Identification of Distinct Functional Microstructural Domains Controlling C Storage in Soil. *Environ Sci Technol* **51**, 12182-12189.

Stucki J.W., Golden D. and Roth C.B., (1984) Preparation and handling of dithionite-reduced smectite suspensions. *Clays and Clay Minerals* **32**, 191-197.

Thompson A., Rancourt D.G., Chadwick O.A. and Chorover J., (2011) Iron solid-phase differentiation along a redox gradient in basaltic soils. *Geochimica et Cosmochimica Acta* **75**, 119-133.

Torn M.S., Trumbore S.E., Chadwick O.A., Vitousek P.M. and Hendricks D.M., (1997) Mineral control of soil organic carbon storage and turnover. *Nature* **389**, 170-173.

Trenberth K.E., (2011) Changes in precipitation with climate change. *Climate Research* **47**, 123-138.

Van Haastert P.J. and Bosgraaf L., (2009) Food searching strategy of amoeboid cells by starvation induced run length extension. *PloS one* **4**, e6814.

Vogel C., Mueller C.W., Hoschen C., Buegger F., Heister K., Schulz S., Schloter M. and Kogel-Knabner I., (2014) Submicron structures provide preferential spots for carbon and nitrogen sequestration in soils. *Nat Commun* **5**, 2947.

von Lützow M., Kögel-Knabner I., Ekschmitt K., Matzner E., Guggenberger G., Marschner B. and Flessa H., (2006) Stabilization of organic matter in temperate soils: mechanisms and their relevance under different soil conditions - a review. *European Journal of Soil Science* **57**, 426-445.

Wagai R., Kajiura M., Uchida M. and Asano M., (2018) Distinctive Roles of Two Aggregate Binding Agents in Allophanic Andisols: Young Carbon and Poorly-Crystalline Metal Phases with Old Carbon. *Soil Systems* **2**, 29.

Wiesmeier M., Urbanski L., Hobley E., Lang B., von Lützow M., Marin-Spiotta E., van Wesemael B., Rabot E., Ließ M., Garcia-Franco N., Wollschläger U., Vogel H.-J. and Kögel-Knabner I., (2019) Soil organic carbon storage as a key function of soils - A review of drivers and indicators at various scales. *Geoderma* **333**, 149-162.

Wolfe E.W. and Morris J. (1996) Geologic map of the Island of Hawaii.

Yonebayashi K., Kawaguchi K. and Kyuma K., (1974) Characterization of the organic matter in the soil organo-mineral complexes. *Journal of the Science of Soil and Manure*.

CV
THIAGO M. INAGAKI

Link to online profiles:
Researchgate
Linkedin
Google Scholar
Publons

ABOUT ME

I am a Bachelor and Master in Agronomy with experience in Soil Science. I have been involved in different projects focused on the influence of land use changes and fertilization practices on soil organic matter in tropical and subtropical soils. Currently in my PhD program, I work studying mechanisms for soil organic matter stabilization through mineral interactions in soils.

EDUCATION / EXPERIENCE

2016 – 2020

PhD Candidate
Technical University of Munich (TUM), Freising, Germany
I studied for soil organic matter protection through mineral interactions in soils, advised by Prof. Ingrid Kögel-Knabner and Prof. Johannes Lehmann. I was hired through the TUM-IAS Hans Fischer Senior Fellowship program. In the first part of the project, we studied methodological aspects regarding the soil organic matter fractionation of Andosols, we have figured out important insights in respect to the use of microscopy techniques in these soils. In the second part, we studied the influence of a climate gradient and consequent changes in mineralogy on subsoil organo-mineral associations at the macro and microscale. In the third part of the project, we studied the mineralization and stabilization mechanisms of different ^{13}C and ^{15}N labeled residues including leaves and dissolved organic carbon (DOC). In this study, we were able to identify the influence of the organic matter arrangement (point source or distributed C) on its mineralization and stabilization rates.

2017
(2 months)

Visiting Researcher
Cornell University - USA
I worked as a Visiting Researcher in the department of Soil and Crop Sciences. I developed part of my PhD research working on isotope labeling (^{13}C and ^{15}N) and synchrotron-based techniques (XANES/NEXAFS) advised by Prof. Johannes Lehmann.

2015-2017
(2 years)

Teaching assistant
Agropro Brasil
I worked as a collaborator/freelancer for Agropro, a technology company dedicated to the development of solutions for agribusiness. I worked as an assistant in online courses with focus on no-tillage system in tropical and subtropical regions. My tasks were as follow:
- Assisting students with questions regarding soil fertility and soil use and management.
- Producing soil science teaching materials for the courses.

- Writing regular texts for the company's blog about soil science in an accessible language for farmers and the non-scientific community.

2014-2016
(2 years)

Master Degree in Agronomy:
State University of Ponta Grossa (UEPG), PR, Brazil
During my master degree, I studied the use of lime and gypsum as a strategy to provide carbon sequestration in agriculture advised by Prof. João Carlos de Moraes Sá and Prof. Eduardo F. Caires. During this period, I also worked as teaching assistant performing lectures in Soil Fertility and advising undergraduate students with their research projects. I could acquire a good expertise in soil fertility analysis (nutrient determinations, crop yield evaluations) and soil organic matter fractionation.

2013
(4 months)

Internship Student
Ohio State University (OARDC-OSU), Wooster, OH, USA
As part of an international mobility program, I worked as a summer intern at the Ohio Agriculture Research and Development Center (OARDC) from the Ohio State University (OSU) advised by Prof. Warren Dick. During this period, I had the opportunity to work in different research projects focused mainly in greenhouse gases emissions and soil enzyme analysis. At the end of the program, I performed an oral presentation in an undergraduate research conference.

2012-2013
(9 months)

Study abroad (non-degree student)
University of Illinois at Urbana Champaign (UIUC), IL, USA.
I was selected to participate of an international scientific mobility program from the Brazilian Government called “Science without Borders”. In this program, I attended two semesters of classes at the UIUC (Fall 2012, Spring 2013) in the major of Crop Sciences as a non-degree student**.** I had the opportunity to know different aspects of agriculture in the USA focused on grain and horticultural production.

2009 – 2013
(5 years)

Bachelor degree in Agronomy:
State University of Ponta Grossa (UEPG), PR, Brazil
During my bachelor degree, I worked as a research assistant (i.e., Scientific Initiation Scholarship from the Brazilian Government) advised by Prof. João Carlos de Moraes Sá. I participated of different research projects in the area of land use and management in tropical and subtropical agriculture. During this period, I acquired a good experience in laboratory analysis (i.e., general soil chemistry analysis and organic matter fractionation) and field sampling. I also performed several oral and poster presentations in conferences.

REFERECES

Prof. Ingrid Kögel-Knabner
PhD Advisor
Technical University of Munich
Email: koegel@wzw.tum.de

Prof. Johannes Lehmann
PhD Advisor
Cornell University
Email: cl273@cornell.edu

Prof. João Carlos de M. Sá
Bachelor/Master Advisor
State University of Ponta Grossa
Email: jcmsa@uepg.br

COURSES (INTERPERSONAL SKILLS AND TECHNIQUES)

Year	Course name	Instructors	Institution of the course
2019	Survival Guide to Peer Review (8h)	Ulrike Müller	TU München
2019	360-Degree-Leadership (6h)	Brooke Gazdag	TU München
2019	Statistical modelling and regressions using R for soil scientists. (8h)	Bernard Ludwig	Uni. Kassel
2018	The Imposter Syndrome: Why successful people often feel like frauds. (3h)	Hugh Kearns	TU München
2017	Communication in Teams and difficult Situations (14h)	Monika Thiel	TU München
2017	Scientific Writing - High impact practices (32h)	Ulrike Müller	TU München
2017	Teaching in the laboratory (4h)	Judit Tuschak	TU München
2017	Fit for Teaching (3h)	Judit Tuschak	TU München
2016	Writing Scientific English for Publication (25h)	John Guess	TU München
2016	Making Effective Scientific Presentations in English (20h)	John Guess	TU München
2015	Soil quality indicators (45h)	George Brown / Patrick Lavelle / Elena Velasquez	Federal University of Parana

REVIEWS FOR JOURNALS

Soil Research (2)
Geoderma (6)
Catena (2)
Soil Science Society of America Journal (1)
Science of the Total Environment (1)
Agronomy for Sustainable Development (1)
Land Degradation & Development (1)
Acta Oecologica (1)
Journal of Environmental Management (1)
Carbon Management (2)

AWARDS

2018 "*Best talk*". Best oral presentation at the 4th HEF-Agrar PhD Symposium. Hans Eisenmann-Zentrum für Agrarwissenschaften. Technical University of Munich - Germany

2017 "*Excellent review*" - Soil Research (CSIRO PUBLISHING), Publons.

2012 "*Science without borders Scholarship*". Scientific Mobility Program grant in the USA (1 year). Brazilian Government.

2010 "*Highlighted presentation*". Best oral presentation at the Scientific Initiation Meeting. Centro de Ensino Superior dos Campos Gerais (CESCAGE) Ponta Grossa, Brazil.

2009 "*Scientific Initiation Scholarship*" – Undergrad research assistant grant (3 years). Brazilian Government.

2009 "*Highlighted presentation*". Best research presentation at the 18º Annual Meeting of Scientific Initiation. Universidade Estadual de Londrina (UEL) Londrina – Brazil.

LANGUAGES

Portuguese	Native Speaker
English	Fluent: 93/120 Toefl ibt (2015)
German	Intermediate

FULL PUBLICATION RECORD

Publications in per-reviewed journals

2019

Inagaki, T. M., Possinger, A., Grant, K., Schweizer, S. A., Mueller, C. W., Derry, L. A., Lehmann, J., Kogel-Knabner, I. Subsoil organo-mineral associations under contrasting climate conditions. **Geochimica et Cosmochimica Acta**, 2019 (accepted).

Auler, A. C., Romaniw, J., Sá, J.C.M., Pires, Luiz F., Harmann, D. C., Inagaki, T. M., Rosa, J. A. Solid slaughterhouse organic waste applied as a crop fertilization, in southern Brazil, improvement on soil carbon pools, water retention, soil structure and fertility. **International journal of recycling of organic waste in agriculture**, 2019 (accepted).

Inagaki T. M., Mueller C. W., Lehmann J., Kögel-Knabner I. Andosol clay re-aggregation observed at the microscale during physical organic matter fractionation. **Journal of Plant Nutrition and Soil Science.** Vol 182. pp 145-148. 2019. DOI: 10.1002/jpln.201800421

Gonçalves DR, de Moraes Sá JC, Mishra U, Furlan FJ, Ferreira LA, Inagaki TM, Romaniw J, de Oliveira Ferreira A, Briedis C. Conservation agriculture based on diversified and high-performance production system leads to soil carbon sequestration in subtropical environments. **Journal of Cleaner Production.** DOI: 10.1016/j.jclepro.2019.01.263

2018

Gonçalves DR, de Moraes Sá JC, Mishra U, Furlan FJ, Ferreira LA, Inagaki TM, Romaniw J, de Oliveira Ferreira A, Briedis C. (2018) Soil carbon inventory to quantify the impact of land use change to mitigate greenhouse gas emissions and ecosystem services. **Environmental Pollution**. 25. DOI: 10.1016/j.envpol.2018.07.068

Briedis, C., de Moraes Sá, J.C., Lal, R., Tivet, F., Franchini, J.C., de Oliveira Ferreira, A., da Cruz Hartman, D., Schimiguel, R., Bressan, P.T., Inagaki, T.M., Romaniw, J. & Gonçalves, D.R.P. (2018) How does no-till deliver carbon stabilization and saturation in highly weathered soils? **Catena**, 163, 13-23. DOI: 10.1016/j.catena.2017.12.003

Sá, J.C.M., Potma Goncalves, D.R., Ferreira, L.A., Mishra, U., Inagaki, T.M., Ferreira Furlan, F.J., Moro, R.S., Floriani, N., Briedis, C. & Ferreira, A.d.O. (2018) Soil carbon fractions and biological activity based indices can be used to study the impact of land management and ecological successions. **Ecological Indicators**, 84, 96-105. DOI: 10.1016/j.ecolind.2017.08.029

Ferreira, A.d.O., Carneiro Amado, T.J., Rice, C.W., Ruiz Diaz, D.A., Briedis, C., Inagaki, T.M. & Potma Goncalves, D.R. (2018a) Driving factors of soil carbon accumulation in Oxisols in long-termno-till systems of South Brazil. **Science of the total environment**, 622, 735-742. DOI: 10.1016/j.scitotenv.2017.12.019

Ferreira, A.d.O., de Moraes Sa, J.C., Lal, R., Tivet, F., Briedis, C., Inagaki, T.M., Potma Goncalves, D.R. & Romaniw, J. (2018b) Macroaggregation and soil organic carbon restoration in a highly weathered Brazilian Oxisol after two decades under no-till. **Science of the total environment**, 621, 1559-1567. DOI: 10.1016/j.scitotenv.2017.10.072

Garcia, L.C., Frare, I., Inagaki, T., Neto, P.H.W., Martins, M., Melo, M.H., Nadolny, L., Rogenski, M.K., Seifert Filho, N. & de Oliveira, E.B. (2018) Spacing between Soybean Rows. **American Journal of Plant Sciences**, 9, 711. DOI: 10.4236/ajps.2018.94056

Hok, L., de Moraes Sá, J.C., Reyes, M., Boulakia, S., Tivet, F., Leng, V., Kong, R., Briedis, C., da Cruz Hartman, D., Ferreira, L.A., Inagaki, T.M., Gonçalves, D.R.P. & Bressan, P.T. (2018) Enzymes and C pools as indicators of C build up in short-term conservation agriculture in a savanna ecosystem in Cambodia. **Soil and Tillage Research**, 177, 125-133. DOI: doi.org/10.1016/j.still.2017.11.015

Mainardes, E.L., Garcia, L.C., Weirich Neto, P.H., Rocha, C.H., Inagaki, T., de Souza, N.M., Pedrollo Mazer, G., Gomes, J.A., Furmann Moura, I.C. & Zeny, É.P. Economic Feasibility of Canola

Production in the Region of Campos Gerais, Parana;, Brazil. **American Journal of Plant Sciences**, 09, 958-965. DOI: 10.4236/ajps.2018.95073

2017

Engels, C., Rodrigues, F., Ferreira, A., Inagaki, T. & Nepomuceno, A. (2017) Drought Effects on Soybean Cultivation - A Review. **Annual Research & Review in Biology**, 16, 1-13. DOI: 10.9734/ARRB/2017/35232

Inagaki, T.M., de Moraes Sa, J.C., Caires, E.F. & Potma Goncalves, D.R. (2017) Why does carbon increase in highly weathered soil under no-till upon lime and gypsum use? **Science of the total environment**, 599, 523-532. DOI: doi.org/10.1016/j.scitotenv.2017.04.234

2016

Ferreira, A.d.O., Amado, T., Ric, C.W., Diaz, D.A.R., Keller, C. & Inagaki, T.M. (2016) Can no-till grain production restore soil organic carbon to levels natural grass in a subtropical Oxisol? **Agriculture Ecosystems & Environment,** 229, 13-20. DOI: 10.1016/j.agee.2016.05.016

Inagaki, T.M., de Moraes Sa, J.C., Caires, E.F. & Potma Goncalves, D.R. (2016a) Lime and gypsum application increases biological activity, carbon pools, and agronomic productivity in highly weathered soil. **Agriculture Ecosystems & Environment**, 231, 156-165. DOI: 10.1016/j.agee.2016.06.034

Inagaki, T.M., Romaniw, J., Sá, J.C.d.M., Ferreira, A.D.O., Briedis, C. & Tivet, F. (2016b) Macroagregados como indicadores de qualidade em sistema plantio direto. **Revista Plantio Direto**, 1, 32.

Romaniw, J., Sá, J.C.d.M., Ferreira, A.d.O. & Inagaki, T.M. (2016) C-CO_2 Emissions, Carbon Pools and Crop Productivity Increased upon Slaughterhouse Organic Residue Fertilization in a No-Till System. **Intech - Organic Fertilizers: From Basic Concepts to Applied Outcomes**. Vol 1. pp 223-239. DOI: 10.5772/63123

2015

Ferreira, A.D.O., Sá, J.C.M., Dos Santos, J.B., Briedis, C. & Inagaki, T.M. (2015) Correction Equations for Wet Combustion Carbon Determination at Different Depths and Management Systems of a Rhodic Hapludox. **Journal of Agriculture and Crops**, 1, 75-82.

2012

Briedis, C., de Moraes Sá, J.C., Caires, E.F., de Fátima Navarro, J., Inagaki, T.M., Boer, A., de Oliveira Ferreira, A., Neto, C.Q., Canalli, L.B. & Bürkner dos Santos, J. (2012a) Changes in Organic Matter Pools and Increases in Carbon Sequestration in Response to Surface Liming in an Oxisol under Long-Term No-Till. **Soil Science Society of America Journal**, 76, 151-160. DOI: 10.2136/sssaj2011.0128

Briedis, C., de Moraes Sa, J.C., Caires, E.F., Navarro, J.d.F., Inagaki, T.M., Boer, A., Neto, C.Q., Ferreira, A.d.O., Canalli, L.B. & dos Santos, J.B. (2012b) Soil organic matter pools and carbon-protection mechanisms in aggregate classes influenced by surface liming in a no-till system. **Geoderma**, 170, 80-88. DOI: 10.1016/j.geoderma.2011.10.011

Briedis, C., Sá, J.C.d.M., Caires, E.F., Navarro, J.d.F., Inagaki, T.M. & Ferreira, A.d.O. (2012c) Carbono do solo e atributos de fertilidade em resposta à calagem superficial em plantio direto. **Pesquisa Agropecuária Brasileira**, 47, 1007-1014.

Tivet, F., de Moraes Sa, J.C., Borszowskei, P.R., Letourmy, P., Briedis, C., Ferreira, A.O., dos Santos, J.B. & Inagaki, T.M. (2012) Soil Carbon Inventory by Wet Oxidation and Dry Combustion Methods: Effects of Land Use, Soil Texture Gradients, and Sampling Depth on the Linear Model of

C-Equivalent Correction Factor. **Soil Science Society of America Journal**, 76, 1048-1059. DOI: 10.2136/sssaj2011.0328

Conference abstracts and presentations

2019

Inagaki, T. M.; Possinger, A.; Grant, K.; Derry, L. A.; Lehmann, J.; Kögel-Knabner, I. Soil organic matter stabilization in top and subsoil. **European Geosciences Union General Assembly (EGU**) Vienna – Austria. 2019 (Poster presentation)

Almeida, L. F. J.; Inagaki, T. M.; Hurtarte, L. C. C.; Souza, I. F.; Silva, I. R.; Mueller, C.; Plant litter biochemistry controls C partitioning into CO_2 and soil organic matter fractions. **European Geosciences Union General Assembly (EGU)** Vienna – Austria. 2019 (Poster presentation)

Inagaki, T. M.; Kögel-Knabner, I.; Lehmann, J. Soil organic carbon stabilization promoted by mineral interactions. **Institute for Advanced Study (IAS-TUM) General Assembly.** Burghausen – Germany 2019. (Poster presentation).

2018

Inagaki, T. M.; Possinger, A.; Grant, K.; Derry, L. A.; Lehmann, J.; Kögel-Knabner, I. Mechanisms for SOC stabilization in a Volcanic Andosol: topsoil vs subsoil. **European Geosciences Union General Assembly (EGU)** Vienna – Austria. 2018. (Oral presentation).

Inagaki, T. M.; Kögel-Knabner, I.; Lehmann, J. Soil organic matter stabilization provided by mineral interactions in soils under changing rainfall levels **4th HEZagrar PhD Symposium**, Freising – Germany 2018. (Oral presentation).

Inagaki, T. M.; Kögel-Knabner, I.; Lehmann, J. Organic matter protection through mineral interactions in soil. **Institute for Advanced Study (IAS) General Assembly.** Garching – Germany 2018. (Poster presentation).

2017

Inagaki, T. M.; Grant, K. ; Mueller, C. W. ; Lehmann, J. ; Derry, L. A. ; Kögel-Knabner, I. Organic matter protection through mineral interactions in soil. **Institute for Advanced Study (IAS) General Assembly**. Raitenhaslach – Germany 2017. (Poster presentation).

Inagaki, T. M.; Grant, K. ; Mueller, C. W. ; Lehmann, J. ; Derry, L. A. ; Kogel-Knabner, I. . Distinctive soil organic matter composition in a precipitation contrast of a Hawaiian Andosol. In: **European Geosciences Union General Assembly (EGU)**. Vienna – Austria. 2017. (Oral presentation)

Inagaki, T. M.; Grant, K. ; Mueller, C. W. ; Lehmann, J. ; Derry, L. A. ; Kögel-Knabner, Distinct soil organic matter properties across a Fe and rainfall gradient In: **Goldschmidt**, Paris – France 2017. (Oral presentation).

Inagaki, T. M.; Grant, K. ; Mueller, C. W. ; Lehmann, J. ; Derry, L. A. ; Kögel-Knabner, I. Organic matter protection through mineral interactions in soil. **Technical University of Munich (TUM) Kick-off Seminar**. Raitenhaslach – Germany 2017. (Poster presentation).

2015

Inagaki, T. M.; Sa, J. C. M.; Caires, E. F. Calcário e gesso conduzem aumento da atividade biológica e do c orgânico do solo em sistema plantio direto de longa duração In: **IV Reunião Paranaense de Ciência do Solo**, 2015, Cascavel. (Poster presentation)

Inagaki, T M; Sa, J C M; Caires, E. F. Calcário e gesso conduzem aumento da atividade biológica e do c orgânico do solo em sistema plantio direto de longa duração In: **XXXV Congresso Brasileiro de Ciência do Solo,** 2015, Natal - RN. (Poster presentation)

2013

Inagaki, T. M.; Dick, W. A.; Chen, L. Tillage and Crop Rotation Impacts on Greenhouse Gas Emissions from Ohio Soils. In: Wooster – OH. **Ohio State University OARD Internship program**. 2013. (Oral presentation).

Inagaki, T. M.; Briedis, C.; Sa, J C M. Sistemas de manejo e a respiração basal do solo em ambiente tropical e subtropical In: 22° EAIC e 3° EAITI, 2013, Foz do Iguaçu. **22° EAIC e 3° EAITI**. (Oral presentation).

2012

Hartman, D. C.; Inagaki, T. M.; Santos, J. Z.; Briedis, C. Evidências de saturação de carbono em solos sob plantio direto em agro-ecosistemas sub-tropical e tropical no brasil. **In: XXI Encontro Anual de Iniciação Científica**, 2012**,** Maringá. (Oral presentation)

2011

Borszowskei, P. R.; Sa, J C M; Tivet, F. E.; Navarro, J F; Nadolny Junior, M.; Hartman, D. C.; Eurich, G.; Inagaki, T. M.; Farias, A.; Briedis, C; Santos, J. B.; Rosa, J. A. Alterações no compartimento oxidável e recalcitrante da matéria orgânica do solo devido ao manejo associado a sistemas de produção em ambiente subtropical e tropical In: **II Reunião Paranaense de Ciência do Solo**, 2011. (Poster presentation)

Briedis, C; Sa, J C M; Navarro, J F; Inagaki, T. M.; Ferreira, A. O. Associação de cálcio com carbono para estabilização da matéria orgânica do solo In **II Reunião Paranaense de Ciência do Solo**. Curitiba: Universidade Federal do Paraná, Curitiba, 2011. (Poster presentation)

Tivet, F. E.; Sa, J C M; Borszowskei, P. R.; Hartman, D. C.; Eurich, G.; Navarro, J F; Nadolny Junior, M.; Inagaki, T. M.; Farias, A.; Rosa, J. A. Aumento do conteúdo de polissacarídeos e carbono orgânico dissolvido sob plantio direto devido a sistemas de produção com elevado aporte de carbono em região subtropical e tropical. In: **II Reunião Paranaense de Ciência do Solo**, 2011, Curitiba. Universidade Federal do Paraná. (Poster presentation)

Briedis, C; Sa, J C M; Navarro, J F; Inagaki, T. M.; Ferreira, A. O. Aumento no carbono do solo com a calagem e sua relação com atributos de fertilidade In: II Reunião Paranaense de Ciência do Solo, 2011, Curitiba. **II Reunião Paranaense de Ciência do Solo**. , 2011. (Poster presentation)

Briedis, C; Sa, J C M; Inagaki, T. M.; Navarro, J F; Ferreira, A. O. Calagem superficial aumenta o conteúdo de polissacarídeos e carbono orgânico dissolvido melhorando a agregação do solo em sistema plantio direto de longa duração In: **II Reunião Paranaense de Ciência do Solo**. Curitiba: Universidade Federal do Paraná, 2011. (Poster presentation)

Tivet, F. E.; Sa, J C M; Borszowskei, P. R.; Farias, A.; Briedis, C; Santos, J. B.; Inagaki, T. M.; Hartman, D. C.; Eurich, G.; Navarro, J F; Nadolny Junior, M.; Rosa, J. A. Estoque de c na fração particulada e associada aos minerais afetadas pelo manejo do solo e sistemas de produção em região subtropical e tropical In: **II Reunião Paranaense de Ciência do Solo**, 2011, Curitiba. Universidade Federal do Paraná, 2011. (Poster presentation)

Inagaki, T. M.; Tivet, F. E.; Borszowskei, P. R.; Briedis, C; Hartman, D. C.; Sa, J C M Estoque e taxas de sequestro de carbono afetados pelo manejo do solo associado a sistemas de produção com elevado aporte de carbono em região subtropical e tropical In Ponta Grossa. **Salão de Iniciação Científica 2011 Cescage**. (Oral presentation)

Inagaki, T. M Sa, J C M; Tivet, F. E.; Borszowskei, P. R.; Farias, A.; Hartman, D. C.; Eurich, G.; Navarro, J F; Nadolny Junior, M.; Rosa, J. A. Estoque e taxas sequestro de carbono afetado pelo

manejo do solo associado a sistemas de produção com elevado aporte de c em região subtropical e tropical In: **II Reunião Paranaense de Ciência do Solo, 2011**, Curitiba. (Poster presentation)

Borszowskei, P. R.; Sa, J C M; Tivet, F. E.; Eurich, G.; Briedis, C; Santos, J. B.; Farias, A.; Nadolny Junior, M.; Navarro, J F; Inagaki, T. M.; Hartman, D. C.; Rosa, J. A. Estoques de carbono na fração lábil e associada aos minerais afetados pela conversão da vegetação natural em área agrícola em diferentes ecossistemas In: **II Reunião Paranaense de Ciência do Solo, 2011**, Curitiba. (Poster presentation)

Sa, J C M; Borszowskei, P. R.; Tivet, F. E.; Letourmy, P.; Briedis, C; Ferreira, A. O.; Santos, J. B.; Inagaki, T. M**.** Monitoramento do carbono em ambientes subtropicais e tropicais por via húmida e seca: efeito do uso da terra, gradiente textural e profundidade de amostragem In: **II Reunião Paranaense de Ciência do Solo**, 2011, Curitiba. (Poster presentation)

Sa, J C M; Tivet, F. E.; Borszowskei, P. R.; Nadolny Junior, M.; Briedis, C; Santos, J. B.; Inagaki, T. M.; Hartman, D. C.; Eurich, G.; Navarro, J F; Farias, A.; Rosa, J. A. Potencial de sistemas de produção com elevado aporte de carbono na preservação da agregação e da matéria orgânica do solo em plantio direto em região subtropical e tropical In: **II Reunião Paranaense de Ciência do Solo**, 2011, Curitiba. (Poster presentation)

Boer, A; Briedis, C; Navarro, J F; Inagaki, T. M.; Ferreira, A. O. Compartimentos da matéria orgânica do solo afetados por calagem superficial em sistema plantio direto. In: **IX Encontro de Pesquisa e III Simpósio de Pós-Graduação - UEPG**, 2010, Ponta Grossa. (Oral presentation)

Inagaki, T. M.; Tivet, F. E.; Borszowskei, P. R.; Sa, J C M; Fonseca, A. F. Influência da capacidade de troca catiônica sobre compartimentos da matéria orgânica em diferentes sistemas de manejo em ambiente subtropical In: XX Encontro Anual de Iniciação Científica, 2011, Ponta Grossa. **XX Encontro Anual de Iniciação Científica**. (Oral presentation)

2010

Inagaki, T. M.; Briedis, C; Ferreira, A. O.; Navarro, J F; Boer, A; Sa, J C M Polissacarídeos e carbono extraído em água quente afetados pela calagem superficial em sistema de plantio direto In: IX Encontro de Pesquisa e III Simpósio de Pós Graduação - UEPG, 2010, Ponta Grossa. **IX Encontro de Pesquisa e III Simpósio de Pós-Graduação - UEPG**. (Oral presentation)

Navarro, J F; Briedis, C; Boer, A; Inagaki, T. M.; Ferreira, A. O.; Sa, J C M Sequestro de carbono em macroagregados afetado pela calagem superficial In: IX Encontro de Pesquisa e III Simpósio de Pós-Graduação - UEPG, 2010, Ponta Grossa. **IX Encontro de Pesquisa e III Simpósio de Pós-Graduação - UEPG**. (Oral presentation)

Sa, J C M; Ferreira, A. O.; Santos, J. B.; Briedis, C; Inagaki, T. M.; Quadros Netto, C. Q. Equivalência do conteúdo de carbono determinado por combustão úmida e seca em um Latossolo Vermelho sob diferentes sistemas de manejo In: **II Simpósio de Graduação e Pós-graduação em Química da UEPG**, 2010, Ponta Grossa. (Oral presentation)

Boer, A; Briedis, C; Sa, J C M; Inagaki, T. M.; Navarro, J F; Ferreira, A. O. Formas de carbono do solo afetados por calagem superficial em sistema de plantio direto In: **XIX Encontro Anual de Iniciação Científica**, 2010, Guarapuava. (Oral presentation)

Inagaki, T. M.; Sa, J C M; Briedis, C; Navarro, J F Polissacarídeos e carbono extraído em água quente afetados pela calagem superficial em sistema de plantio direto In: Ponta Grossa. **Salão de Iniciação Científica 2010 Cescage**. (Oral presentation)

Inagaki, T. M.; Briedis, C; Sa, J C M; Navarro, J F; Boer, A; Ferreira, A. O. Polissacarídeos e carbono extraído em água quente afetados pela calagem superficial em sistema de plantio direto In: Guarapuava. **XIX Encontro Anual de Iniciação Científica**. , 2010. (Oral presentation)

Navarro, J F; Briedis, C; Sa, J C M; Inagaki, T. M.; Boer, A; Ferreira, A. O. Sequestro de carbono em macroagregados afetado pela calagem superficial In: **XIX Encontro Anual de Iniciação**

Científica, 2010, Guarapuava. (Oral presentation)

2009

Navarro, J F; Briedis, C; Ferreira, A. O.; Quadros Netto, C. Q.; Inagaki, T. M.; Boer, A; Sa, J C M agregação do solo e seqüestro de carbono afetado pela calagem superficial em sistema plantio direto In: **VIII Encontro de Pesquisa, II Simpósio de Pós-Graduação,** 2009, Ponta Grossa. (Oral presentation)

Inagaki, T. M.; Ferreira, A. O.; Santos, J. B.; Briedis, C; Quadros Netto, C. Q.; Sa, J C M Fator de correção de COT (Walkley-Black) para COT (LECO-Combustão seca) em diferentes sistemas de manejo In: **VIII Encontro de Pesquisa, II SImpósio de Pós-Graduação**, 2009, Ponta Grossa - PR. (Oral presentation)

Sa, J C M; Ferreira, A. O.; Santos, J. B.; Inagaki, T. M.; Briedis, C; Quadros Netto, C. Q. Equações de correção de carbono orgânico em diferentes profundidades e sistemas de manejo de um latossolo na região dos campos gerais In: **XXXII Congresso Brasileiro de Ciência do Solo**, 2009, Fortaleza. (Oral presentation)

Inagaki, T. M.; Ferreira, A. O.; Santos, J. B.; Briedis, C; Quadros Netto, C. Q.; Sa, J C M. Equações de correção para carbono orgânico total em diferentes sistemas de manejo de um latossolo da região dos campos gerais In: **XVIII Encontro Anual de Iniciação Científica**, 2009, Londrina. (Oral presentation)

Briedis, C; Sa, J C M; Navarro, J F; Boer, A; Inagaki, T. M.; Quadros Netto, C. Q.; Ferreira, A. O.; Caires, E F estabilidade de agregados em água afetada pela calagem superficial em plantio direto In: **XXXII Congresso Brasileiro de Ciência do Solo**, 2009, Fortaleza. (Poster presentation)

Navarro, J F; Briedis, C; Ferreira, A. O.; Quadros Netto, C. Q.; Inagaki, T. M.; Boer, A; Sa, J C M Estabilidade de agregados em água afetada pela calagem superficial em plantio direto. In: **XVIII Encontro Anual de Iniciação Científica, 2009**, Londrina.

Appendix

Study 1

Thiago M. Inagaki Carsten W. Mueller Johannes Lehmann Ingrid Kögel-Knabner
Andosol clay re-aggregation observed at the microscale during physical organic matter fractionation
Journal of Plant Nutrition and Soil Science,
Volume 182,
Pages 145 – 148,
2020,
ISSN: 1522-2624
https://doi.org/10.1002/jpln.201800421
(https://onlinelibrary.wiley.com/doi/abs/10.1002/jpln.201800421)

Study 2
Thiago M. Inagaki, Angela R. Possinger, Katherine E. Grant, Steffen A. Schweizer, Carsten W. Mueller, Louis A. Derry, Johannes Lehmann, Ingrid Kögel-Knabner,
Subsoil organo-mineral associations under contrasting climate conditions,
Geochimica et Cosmochimica Acta,
Volume 270,
2020,
Pages 244-263,
ISSN 0016-7037,
https://doi.org/10.1016/j.gca.2019.11.030
(http://www.sciencedirect.com/science/article/pii/S0016703719307380)

Study 3
Thiago M. Inagaki, Angela R. Possinger, Katherine E. Grant, Carsten W. Mueller, Louis A. Derry, Ingrid Kögel-Knabner, Johannes Lehmann
To be submitted.

JOHN WILEY AND SONS LICENSE
TERMS AND CONDITIONS

Jan 24, 2020

This Agreement between Technical University of Munich -- Thiago Massao Inagaki ("You") and John Wiley and Sons ("John Wiley and Sons") consists of your license details and the terms and conditions provided by John Wiley and Sons and Copyright Clearance Center.

License Number	4755240555761
License date	Jan 24, 2020
Licensed Content Publisher	John Wiley and Sons
Licensed Content Publication	Journal of Plant Nutrition and Soil Science
Licensed Content Title	Andosol clay re-aggregation observed at the microscale during physical organic matter fractionation
Licensed Content Author	Ingrid Kögel-Knabner, Johannes Lehmann, Carsten W. Mueller, et al
Licensed Content Date	Feb 4, 2019
Licensed Content Volume	182
Licensed Content Issue	2
Licensed Content Pages	4
Type of use	Dissertation/Thesis
Requestor type	Author of this Wiley article

Format	Print and electronic
Portion	Full article
Will you be translating?	No
Title of your thesis / dissertation	Organic matter protection through mineral interactions in soils
Expected completion date	Apr 2020
Expected size (number of pages)	100
Requestor Location	Technical University of Munich Emil-Ramann-Straße 2 Lehrstuhl für Bodenkunde Freising, 85354 Germany Attn: Technical University of Munich
Publisher Tax ID	EU826007151
Total	0.00 EUR

Terms and Conditions

TERMS AND CONDITIONS

This copyrighted material is owned by or exclusively licensed to John Wiley & Sons, Inc. or one of its group companies (each a"Wiley Company") or handled on behalf of a society with which a Wiley Company has exclusive publishing rights in relation to a particular work (collectively "WILEY"). By clicking "accept" in connection with completing this licensing transaction, you agree that the following terms and conditions apply to this transaction (along with the billing and payment terms and conditions established by the Copyright Clearance Center Inc., ("CCC's Billing and Payment terms and conditions"), at the time that you opened your RightsLink account (these are available at any time at http://myaccount.copyright.com).

Terms and Conditions

- The materials you have requested permission to reproduce or reuse (the "Wiley Materials") are protected by copyright.

- You are hereby granted a personal, non-exclusive, non-sub licensable (on a stand-alone basis), non-transferable, worldwide, limited license to reproduce the Wiley Materials for the purpose specified in the licensing process. This license, **and any CONTENT (PDF or image file) purchased as part of your order,** is for a one-time use only and limited to any maximum distribution number specified in the license. The first instance of republication or reuse granted by this license must be completed within two years of the date of the grant of this license (although copies prepared before the end date may be distributed thereafter). The Wiley Materials shall not be used in any other manner or for any other purpose, beyond what is granted in the license. Permission is granted subject to an appropriate acknowledgement given to the author, title of the material/book/journal and the publisher. You shall also duplicate the copyright notice that appears in the Wiley publication in your use of the Wiley Material. Permission is also granted on the understanding that nowhere in the text is a previously published source acknowledged for all or part of this Wiley Material. Any third party content is expressly excluded from this permission.

- With respect to the Wiley Materials, all rights are reserved. Except as expressly granted by the terms of the license, no part of the Wiley Materials may be copied, modified, adapted (except for minor reformatting required by the new Publication), translated, reproduced, transferred or distributed, in any form or by any means, and no derivative works may be made based on the Wiley Materials without the prior permission of the respective copyright owner.**For STM Signatory Publishers clearing permission under the terms of the STM Permissions Guidelines only, the terms of the license are extended to include subsequent editions and for editions in other languages, provided such editions are for the work as a whole in situ and does not involve the separate exploitation of the permitted figures or extracts,** You may not alter, remove or suppress in any manner any copyright, trademark or other notices displayed by the Wiley Materials. You may not license, rent, sell, loan, lease, pledge, offer as security, transfer or assign the Wiley Materials on a stand-alone basis, or any of the rights granted to you hereunder to any other person.

- The Wiley Materials and all of the intellectual property rights therein shall at all times remain the exclusive property of John Wiley & Sons Inc, the Wiley Companies, or their respective licensors, and your interest therein is only that of having possession of and the right to reproduce the Wiley Materials pursuant to Section 2 herein during the continuance of this Agreement. You agree that you own no right, title or interest in or to the Wiley Materials or any of the intellectual property rights therein. You shall have no rights hereunder other than the license as provided for above in Section 2. No right, license or interest to any trademark, trade name, service mark or other branding ("Marks") of WILEY or its licensors is granted hereunder, and you agree that you shall not assert any such right, license or interest with respect thereto

- NEITHER WILEY NOR ITS LICENSORS MAKES ANY WARRANTY OR REPRESENTATION OF ANY KIND TO YOU OR ANY THIRD PARTY, EXPRESS, IMPLIED OR STATUTORY, WITH RESPECT TO THE MATERIALS OR THE ACCURACY OF ANY INFORMATION CONTAINED IN THE MATERIALS, INCLUDING, WITHOUT LIMITATION, ANY IMPLIED WARRANTY OF MERCHANTABILITY, ACCURACY, SATISFACTORY QUALITY, FITNESS FOR A PARTICULAR PURPOSE, USABILITY, INTEGRATION OR NON-INFRINGEMENT AND ALL SUCH WARRANTIES ARE HEREBY EXCLUDED BY WILEY AND ITS LICENSORS AND WAIVED BY YOU.

- WILEY shall have the right to terminate this Agreement immediately upon breach of this Agreement by you.

- You shall indemnify, defend and hold harmless WILEY, its Licensors and their respective directors, officers, agents and employees, from and against any actual or threatened claims, demands, causes of action or proceedings arising from any breach of this Agreement by you.

- IN NO EVENT SHALL WILEY OR ITS LICENSORS BE LIABLE TO YOU OR ANY OTHER PARTY OR ANY OTHER PERSON OR ENTITY FOR ANY SPECIAL, CONSEQUENTIAL, INCIDENTAL, INDIRECT, EXEMPLARY OR PUNITIVE DAMAGES, HOWEVER CAUSED, ARISING OUT OF OR IN CONNECTION WITH THE DOWNLOADING, PROVISIONING, VIEWING OR USE OF THE MATERIALS REGARDLESS OF THE FORM OF ACTION, WHETHER FOR BREACH OF CONTRACT, BREACH OF WARRANTY, TORT, NEGLIGENCE, INFRINGEMENT OR OTHERWISE (INCLUDING, WITHOUT LIMITATION, DAMAGES BASED ON LOSS OF PROFITS, DATA, FILES, USE, BUSINESS OPPORTUNITY OR CLAIMS OF THIRD PARTIES), AND WHETHER OR NOT THE PARTY HAS BEEN ADVISED OF THE POSSIBILITY OF SUCH DAMAGES. THIS LIMITATION SHALL APPLY NOTWITHSTANDING ANY FAILURE OF ESSENTIAL PURPOSE OF ANY LIMITED REMEDY PROVIDED HEREIN.

- Should any provision of this Agreement be held by a court of competent jurisdiction to be illegal, invalid, or unenforceable, that provision shall be deemed amended to achieve as nearly as possible the same economic effect as the original provision, and the legality, validity and enforceability of the remaining provisions of this Agreement shall not be affected or impaired thereby.

- The failure of either party to enforce any term or condition of this Agreement shall not constitute a waiver of either party's right to enforce each and every term and condition of this Agreement. No breach under this agreement shall be deemed waived or excused by either party unless such waiver or consent is in writing signed by the party granting such waiver or consent. The waiver by or consent of a party to a breach of any provision of this Agreement shall not operate or be construed as a waiver of or consent to any other or subsequent breach by such other party.

- This Agreement may not be assigned (including by operation of law or otherwise) by you without WILEY's prior written consent.

- Any fee required for this permission shall be non-refundable after thirty (30) days from receipt by the CCC.

- These terms and conditions together with CCC's Billing and Payment terms and conditions (which are incorporated herein) form the entire agreement between you and WILEY concerning this licensing transaction and (in the absence of fraud) supersedes all prior agreements and representations of the parties, oral or written. This Agreement may not be amended except in writing signed by both parties. This Agreement shall be binding upon and inure to the benefit of the parties' successors, legal representatives, and authorized assigns.

- In the event of any conflict between your obligations established by these terms and conditions and those established by CCC's Billing and Payment terms and conditions, these terms and conditions shall prevail.

- WILEY expressly reserves all rights not specifically granted in the combination of (i) the license details provided by you and accepted in the course of this licensing transaction, (ii) these terms and conditions and (iii) CCC's Billing and Payment terms and conditions.

- This Agreement will be void if the Type of Use, Format, Circulation, or Requestor Type was misrepresented during the licensing process.

- This Agreement shall be governed by and construed in accordance with the laws of the State of New York, USA, without regards to such state's conflict of law rules. Any legal action, suit or proceeding arising out of or relating to these Terms and Conditions or the breach thereof shall be instituted in a court of competent jurisdiction in New York County in the State of New York in the United States of America and each party hereby consents and submits to the personal jurisdiction of such court, waives any objection to venue in such court and consents to service of process by registered or certified mail, return receipt requested, at the last known address of such party.

WILEY OPEN ACCESS TERMS AND CONDITIONS

Wiley Publishes Open Access Articles in fully Open Access Journals and in Subscription journals offering Online Open. Although most of the fully Open Access journals publish open access articles under the terms of the Creative Commons Attribution (CC BY) License only, the subscription journals and a few of the Open Access Journals offer a choice of Creative Commons Licenses. The license type is clearly identified on the article.

The Creative Commons Attribution License

The Creative Commons Attribution License (CC-BY) allows users to copy, distribute and transmit an article, adapt the article and make commercial use of the article. The CC-BY license permits commercial and non-

Creative Commons Attribution Non-Commercial License

The Creative Commons Attribution Non-Commercial (CC-BY-NC)License permits use, distribution and reproduction in any medium, provided the original work is properly cited and is not used for commercial purposes.(see below)

Creative Commons Attribution-Non-Commercial-NoDerivs License

The Creative Commons Attribution Non-Commercial-NoDerivs License (CC-BY-NC-ND) permits use, distribution and reproduction in any medium, provided the original work is properly cited, is not used for commercial purposes and no modifications or adaptations are made. (see below)

Use by commercial "for-profit" organizations

Use of Wiley Open Access articles for commercial, promotional, or marketing purposes requires further explicit permission from Wiley and will be subject to a fee.

Further details can be found on Wiley Online Library
http://olabout.wiley.com/WileyCDA/Section/id-410895.html

Other Terms and Conditions:

v1.10 Last updated September 2015

Questions? customercare@copyright.com or +1-855-239-3415 (toll free in the US) or

+1-978-646-2777.

Andosol clay re-aggregation observed at the microscale during physical organic matter fractionation

Thiago M. Inagaki* [a,d`], Carsten W. Mueller [a], Johannes Lehmann [b,d], Ingrid Kögel-Knabner [a,d].

*corresponding author: thiago.inagaki@wzw.tum.de

a Chair of Soil Science, Technical University of Munich, Emil-Ramann-Straße 2, Freising, Germany. 85354

b Soil and Crop Sciences, Cornell University, 909 Bradfield Hall, Ithaca NY, USA 14853

d Institute for Advanced Study, Technical University of Munich, Lichtenbergstraße 2a Garching, Germany. 85748

Abstract

The high aggregate stability of Andosols and the direct effects of sample drying led to several inconsistencies during physical soil organic matter fractionation. We have determined that NaCl addition displayed little influence on clay dispersion. At the microscale, we observed the re-aggregation of the clay fraction caused by freeze-drying. This issue was avoided by analyzing aliquots of soil suspension. Thus, we recommend reserving a small soil liquid aliquot to be subjected to microscopy analysis.

Introduction

Soil organic matter (SOM) fractionation is an important tool used to investigate the distribution and composition of differently stabilized C pools; thus, it provides important insight into its persistence and turnover (Golchin *et al.*, 1994; Six *et al.*, 2002). Fine mineral soil fractions (i.e., fine silt and clay size) are used to separate long-term protected OM, as they contain the majority of organo-mineral associations (Kögel-Knabner *et al.*, 2008). However, separating fine fractions especially from allophanic Andosols by physical fractionation was shown to be critical because the dispersion of such soils is hampered by the high stability of microaggregates (<63 µm), which is derived from strong interactions between organic matter, Al oxides, and Fe oxides (Asano and Wagai, 2014; Matus *et al.*, 2014). Silva *et al.* (2015) demonstrated that high levels of ultrasonic dispersion (i.e., up to 1600 J ml^{-1}) were necessary to achieve clay (<2 µm) dispersion depending on the soil weathering stage and concentration of Al and Fe oxides. Studies that sought to obtain even smaller fractions such as fine clay (< 0.2 µm) (Asano and Wagai, 2014) or nano-clay (<10 nm) (Calabi-Floody *et al.*, 2011) required even higher levels of dispersion. In addition, soil

saturation with sodium (i.e., “Na saturation”) has been used to increase dispersion (Kyuma *et al.*, 1969; Yonebayashi *et al.*, 1974). However, studies examining the combined effects of Na saturation with ultrasonic dispersion are still relatively rare.

In addition, clay flocculation after soil dispersion is a common artifact reported in studies that focused on the fractionation of Andosols, and performing the procedure within a single day has been recommended to avoid biases in SOM distribution between fractions (Asano and Wagai, 2014; Asano *et al.*, 2018; Wagai *et al.*, 2018). However, this effect becomes even more important for analyses at the microscale because it can potentially preclude spectromicroscopic analysis (e.g., nanoscale secondary ion mass spectrometry–NanoSIMS) when the aim is to investigate clay-size particles due to the formation of sample topography (Mueller *et al.*, 2013). However, there is still a lack of studies evaluating this flocculation effect at the microscale.

Therefore, SOM fractionation was performed with and without Na saturation prior to ultrasonic dispersion in an allophanic Andosol to evaluate the effects of fractionation on clay dispersion. Two different approaches were employed to avoid clay flocculation at the microscale and analyzed using scanning electron microscopy (SEM), including the standard method of using freeze-dried samples and taking a liquid aliquot from the clay suspension during the final step of fractionation.

2. Material and Methods

2.1 Soil samples

We focused on obtaining clay-size fractions to study the composition and amount of organo-mineral associated OC in Andosols. Therefore, a subsoil sample with a lower content of light particulate fractions (to reduce possible bias from particulate

73 OM) from an Andosol localized in the Kohala region in northern Hawaii (20°4'14.16"N,
74 155°43'21.94"E) was used in this study. The soil was collected from a B horizon at a
75 depth of approximately 0.5–0.6 m that contained 50.4 g kg^{-1} of total C (SOC). It was
76 sieved to 4 mm mesh size and maintained under field moisture conditions at 4°C until
77 the analyses were performed.
78
79 *2.2 Soil organic matter fractionation*
80 The procedure was adapted from the SOM fractionation method described by
81 Golchin *et al.* (1994), which tested three different dispersion agents followed by
82 ultrasonic dispersion. All analyzes were performed in triplicate, and a schematic
83 diagram of the method is presented in Figure 1.
84 We used 10 g of field-moist soil (i.e., dry equivalent, sieved to 4 mm), which
85 were gently saturated with the specific fractionation solutions at a solid-to-liquid ratio
86 of 1 to 2.5, and two different solutions were as follows: (1) 1 M solution of NaCl and (2)
87 deionized water. After allowing the saturated samples to equilibrate overnight, the
88 free particulate organic matter (fPOM) was removed from the supernatant using an
89 electric vacuum pump.
90 Thereafter, ultrasonic dispersion (SonopulsHD2200, Bandelin, Berlin - Germany)
91 was performed using an energy input of 1500 MJ m^{-3}. The chosen energy level was
92 considered sufficient for providing clay (< 2 µm) dispersion of the highly-stable Andosol
93 without causing damage to the primary mineral structure (Silva *et al.*, 2015).
94 To remove the residual salt, each fraction was rinsed with deionized water until
95 the electrical conductivity dropped below 0.001 S m^{-1}. Later, the soil was sieved with
96 20-µm sized mesh to separate the sand and coarse silt fractions; subsequently the

97 residue was subjected to sedimentation to separate the medium silt and clay fractions
98 of 20–2 μm and <2 μm, respectively, and SOC recovery was 99.4 and 98.0% for the
99 NaCl and H_2O treatments, respectively. OC content in the bulk soil sample and each
100 fraction were measured in duplicate by dry combustion (CHNSO Elemental Analyzer,
101 Hekatech, Wegberg–Germany).
102
103 *2.3 Microscopy analysis*
104 To observe clay flocculation artifacts at the microscale on samples with and
105 without freeze-drying, the clay-size fraction (< 2 μm) was analyze using both
106 fractionation procedures (e.g., NaCl and H_2O) using SEM (JSM 5900LV, JEOL, Tokyo -
107 Japan). Two different sample preparation approaches were employed, including: (1)
108 freeze-drying of the clay-size fraction; and (2) direct deposition of the clay-size mineral
109 suspension from the last step of physical fractionation. Samples were suspended in
110 water at a proportion of 1 x 10,000, pipetted onto a silica wafer, and dried in a
111 desiccator at room temperature for subsequent SEM analyzes.
112
113 **3. Results and Discussion**
114 *3.1 Effectiveness of sodium saturation on clay dispersion*
115 Regardless of the fractionation solution used, for both soils, the greatest
116 amount (i.e., more than 95%) of SOC was concentrated in the mineral fractions of <2
117 μm and 20–2 μm (Figure 2). Such distribution was likely due to the sampling depth
118 (i.e., below 0.4 m). In subsoil layers, there is normally a lower concentration of light
119 fractions recovered as particulate organic matter and the greatest amount of OC was
120 concentrated in the mineral fractions (Golchin *et al.*, 1994).

Overall, the dispersion treatment resulted in a comparable SOC distribution among fractions. We expected that NaCl would increase the <2 µm clay dispersion, but the difference in the SOC amount of this fraction between the NaCl and the H_2O treatments was lower than 2%. The addition of NaCl solution prior to fractionation, also referred to as "Na saturation," has been a common procedure used to obtain higher soil dispersion (Yonebayashi *et al.*, 1974). The weakening of Ca and Mg cation bridges and the expansion of the double layer on the soil particle surface are the primary reasons for the enhanced capacity of NaCl to disperse soils (Edwards and Bremner, 1967; Kato and Fujisawa, 1973).

When evaluating Andosol aggregation using different fractionation procedures, Asano and Wagai (2014) also concluded that saturation with NaCl was necessary to achieve maximum dispersion and to obtain fractions smaller than 0.2 µm. However, in this study, for clay particles <2 µm, the NaCl addition did not cause a significant difference when compared with dispersion only in water. The latter method has the main advantage of being less time consuming, as salt washing is unnecessary.

3.2 Re-aggregation effects at the microscale

At the microscale, we observed a clay re-aggregation effect in freeze-dried samples, while this was avoided when sampling directly from the soil suspension (Figure 3). Although the samples were diluted in the same proportion, the freeze-drying procedure created assemblages larger than 20 µm that did not represent the size of the respective fraction. On the other hand, aliquots from the soil suspension were predominantly composed of clay-size particles that were 2 µm or smaller. This re-

aggregation was very likely a result of the strong binding effects of Fe and Al oxides in Andosols (Asano *et al.*, 2018; Wagai *et al.*, 2018).

Freeze-drying is a common procedure used in different methods including SOM fractionation but also general soil analyzes protocols due to its efficiency in sample preservation (Miller *et al.*, 1999). However, our experimental results demonstrated that for the Andosol used in this study, this procedure created sample artifacts that can clearly affect the analysis when the objective is to isolate the clay-size fraction, especially with the intent to examine the microscale organic matter surface coverage or the specific surface area (Vogel *et al.*, 2014; Schweizer *et al.*, 2018).

Over the last decade, investigating microenvironments using spectromicroscopy has provided important discoveries with respect to SOM turnover and C sequestration mechanisms (Lehmann *et al.*, 2008; Mueller *et al.*, 2012; Steffens *et al.*, 2017). Among the different process, the formation of organo-mineral associations occurring at a small spatial scale are considered as key for C protection in soils (Kögel-Knabner *et al.*, 2008). In this way, Andosols are a particularly ideal soil for investigating such interactions, given their high concentration of short-range order minerals (Dahlgren *et al.*, 2004). Therefore, avoiding artifacts at the microscale is extremely important to fully explore microenvironments and understand their enhanced OC stabilization capacity in soils.

Results of this study indicated that artifacts such as re-aggregation could easily be avoided by taking liquid aliquots from the soil suspension at the final step of fractionation. Therefore, we recommend the separation of a small liquid portion for microscopic analysis to avoid biases when exploring microenvironments.

4. Conclusions

This study demonstrated that Na saturation through the addition of 1 M NaCl solution caused low (less than 2% in SOC amount) clay dispersion (<2 µm) compared with the dispersion when water alone was used. Direct effects of freeze-drying on Andosol clay fractions at the microscale were also observed, which caused the formation of assemblages larger than 20 µm. The presence of strong binding effects of the poorly crystalline mineral phases in Andosols is likely the primary reason for this effect. Therefore, in future studies, we recommend reserving a small liquid aliquot from soil suspensions after sonication to proceed with microscopy analyzes.

5. Acknowledgments

The authors would like to thank *Prof. Louis Derry* and *Katherine Grant* from Cornell University for providing the Andosol sample used in this study and the technicians, *Maria Greiner* and *Bärbel Angres*, from the Technical University of Munich for their support with the laboratory analysis. This research was supported by the Institute for Advanced Study (IAS–TUM) through the Hans Fischer Senior Fellowship.

6. References

Asano, M., Wagai, R., (2014). Evidence of aggregate hierarchy at micro- to submicron scales in an allophanic Andisol. *Geoderma* 216, 62–74.

Asano, M.; Wagai, R.; Yamaguchi, N.; Takeichi, Y.; Maeda, M.; Suga, H.; Takahashi, Y. (2018): In search of a binding agent: Nano-scale evidence of preferential carbon associations with poorly-crystalline mineral phases in physically-stable, clay-sized aggregates. *Soil Syst.* 2, 32–50.

192 *Calabi-Floody, M., Bendall, J.S., Jara, A.A., Welland, M.E., Theng, B.K.G., Rumpel, C., Mora,*
193 *M.D.,* (2011). Nanoclays from an Andisol: Extraction, properties and carbon stabilization.
194 Geoderma 161, 159–167.
195 *Dahlgren, R., Saigusa, M., Ugolini, F.,* (2004). The nature, properties and management of
196 volcanic soils. *Adv. Agr.* 82, 113–182.
197 *Edwards, A., Bremner, J.,* (1967). Dispersion of soil particles by sonic vibration. *J Soil Sci* 18, 47–
198 63.
199 *Golchin, A., Oades, J., Skjemstad, J., Clarke, P.,* (1994). Study of free and occluded particulate
200 organic matter in soils by solid state 13C CP/MAS NMR spectroscopy and scanning
201 electron microscopy. *Soil Res.* 32, 285–309.
202 *Kato, H., Fujisawa, T.,* (1973). Studies on the structure of humus-clay complexes (part 1): on
203 the dispersion characteristics. *J. Plant Nutr. Soil Sci.* 44, 251–256.
204 *Kögel-Knabner, I., Guggenberger, G., Kleber, M., Kandeler, E., Kalbitz, K., Scheu, S., Eusterhues,*
205 *K., Leinweber, P.,* (2008). Organo-mineral associations in temperate soils: Integrating
206 biology, mineralogy, and organic matter chemistry. *J. Plant Nutr. Soil Sci.* 171, 61–82.
207 *Kyuma, K., Hussain, A., Kawaguchi, K.,* (1969). The nature of organic matter in soil organo-
208 mineral complexes. *J. Plant Nutr. Soil Sci.* 15, 149–155.
209 *Lehmann, J., Solomon, D., Kinyangi, J., Dathe, L., Wirick, S., Jacobsen, C.,* (2008). Spatial
210 complexity of soil organic matter forms at nanometer scales. *Nat. Geo*. 1, 238–242.
211 *Matus, F., Rumpel, C., Neculman, R., Panichini, M., Mora, M.L.,* (2014). Soil carbon storage and
212 stabilisation in andic soils: A review. *Catena*. 120, 102–110.
213 *Miller, D., Bryant, J., Madsen, E., Ghiorse, W.,* (1999). Evaluation and optimization of DNA
214 extraction and purification procedures for soil and sediment samples. *Appl. Environ.*
215 *Microbiol.* 65, 4715–4724.

Mueller, C.W., Kölbl, A., Hoeschen, C., Hillion, F., Heister, K., Herrmann, A.M., Kögel-Knabner, I., (2012). Submicron scale imaging of soil organic matter dynamics using NanoSIMS–from single particles to intact aggregates. Organic geochemistry 42, 1476–1488.

Mueller, C.W., Weber, P.K., Kilburn, M.R., Hoeschen, C., Kleber, M., Pett-Ridge, J., (2013). Advances in the Analysis of Biogeochemical Interfaces: NanoSIMS to Investigate Soil Microenvironments. *Adv. Agr.,* 121, 1–46.

Schweizer, S.A., Hoeschen, C., Schlüter, S., Kögel-Knabner, I., Mueller, C.W., (2018). Rapid soil formation after glacial retreat shaped by spatial patterns of organic matter accrual in microaggregates. *Global Change Biol*. 24, 1637–1650.

Silva, J.H.S., Deenik, J.L., Yost, R.S., Bruland, G.L., Crow, S.E., (2015). Improving clay content measurement in oxidic and volcanic ash soils of Hawaii by increasing dispersant concentration and ultrasonic energy levels. *Geoderma* 237, 211–223.

Six, J., Conant, R., Paul, E., Paustian, K., (2002). Stabilization mechanisms of soil organic matter: implications for C-saturation of soils. *Plant soil* 241, 155–176.

Steffens, M., Rogge, D.M., Mueller, C.W., Höschen, C., Lugmeier, J., Kölbl, A., Kögel-Knabner, I., (2017). Identification of distinct functional microstructural domains controlling C storage in soil. *Environ Sci Technol* 51, 12182–12189.

Vogel, C., Mueller, C.W., Hoschen, C., Buegger, F., Heister, K., Schulz, S., Schloter, M., Kogel-Knabner, I., (2014). Submicron structures provide preferential spots for carbon and nitrogen sequestration in soils. *Nat Commun* 5, 2947.

Wagai, R., Kajiura, M., Uchida, M., Asano, M., (2018). Distinctive Roles of Two Aggregate Binding Agents in Allophanic Andisols: Young Carbon and Poorly-Crystalline Metal Phases with Old Carbon. *Soil Systems* 2, 29.

Yonebayashi, K., Kawaguchi, K., Kyuma, K., (1974). Characterization of the organic matter in the soil organo-mineral complexes*. J. Sci. Soil Man*. 1, 34–39.

242 **Figures captions**

243 Figure 1: Schematic figure of the soil organic matter fractionation procedure. White
244 boxes represent the different fractions separated by the procedure (i.e., light
245 particulate organic matter–fPOM; occluded particulate organic matter–oPOM; mineral
246 fractions of 4000–64 µm, 63–20 µm, 20–2 µm and <2 µm). Dashed arrows and
247 observations represent the procedures performed for conducting each step.
248

249 Figure 2: Soil organic matter fractions in subsoil B horizon (0.4–0.6 m) of an Andosol
250 with two dispersion solutions prior to ultrasound sonication, including 1 M NaCl
251 solution and deionized water (H_2O). Numbers in the columns represent the amount of
252 SOC (g kg^{-1}) retained in each fraction. Error bars represent the standard deviation of
253 three laboratory replicates.
254

255 Figure 3: Scanning electronic microscopy(SEM) images of samples taken from a clay
256 fraction (<2 µm) water suspension and the same fraction freeze-dried.
257

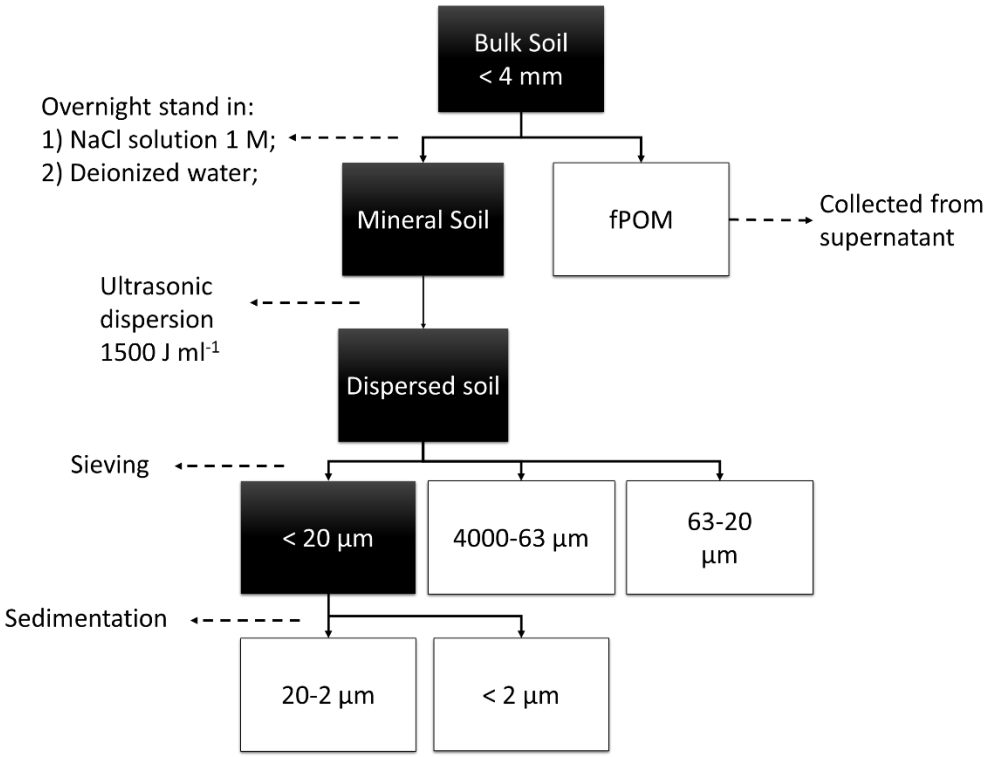

258

259 Figure 1

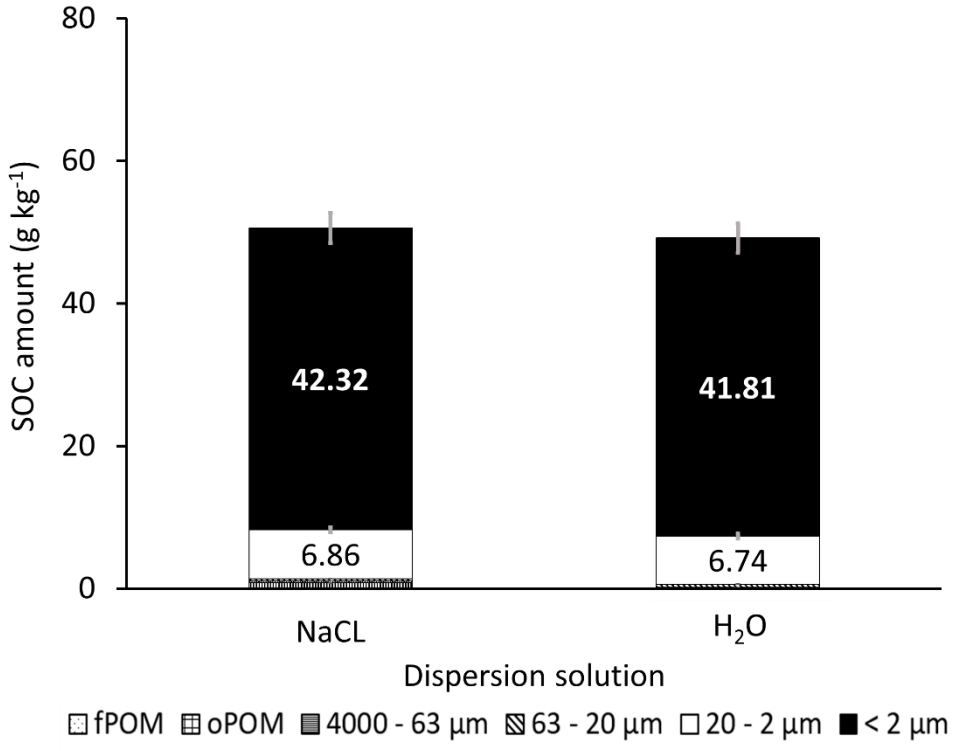

260

261 Figure 2

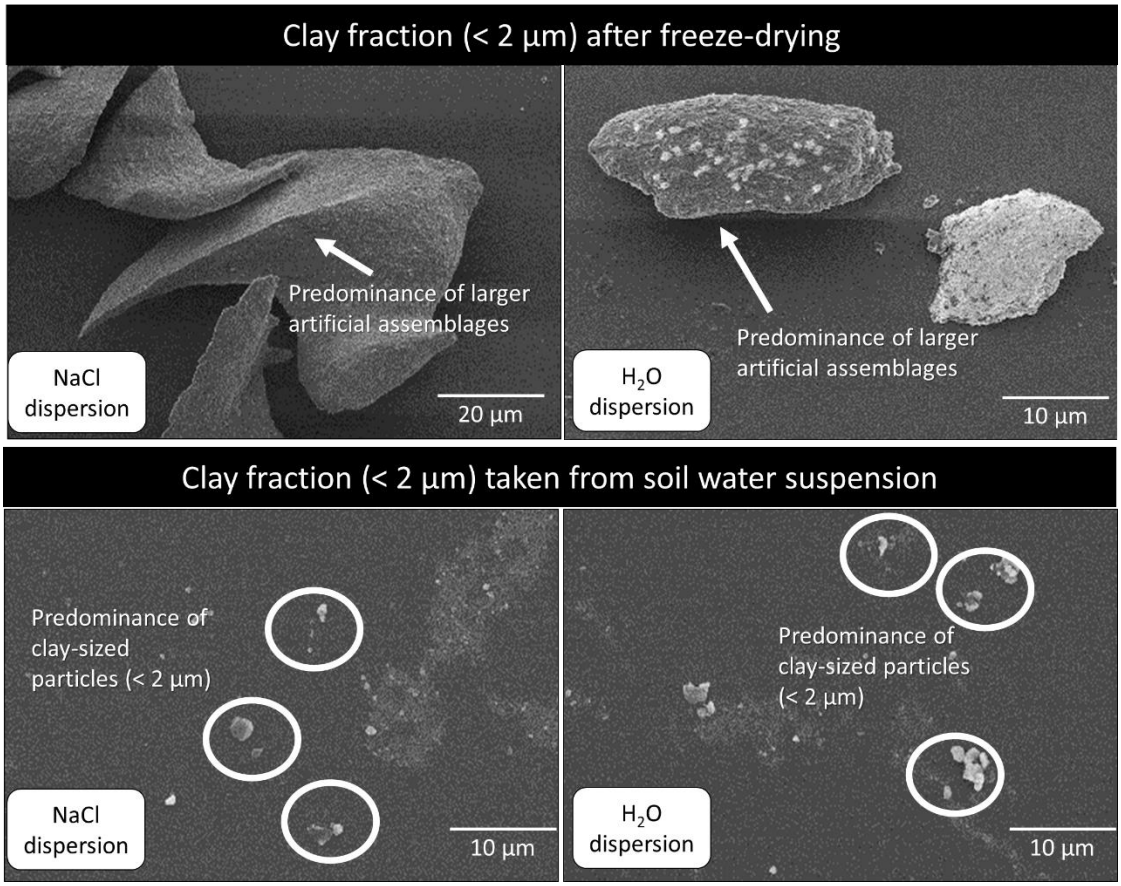
Clay fraction (< 2 µm) after freeze-drying
Predominance of larger artificial assemblages
NaCl dispersion
20 µm
Predominance of larger artificial assemblages
H2O dispersion
10 µm
Clay fraction (< 2 µm) taken from soil water suspension
Predominance of clay-sized particles (< 2 µm)
NaCl dispersion
10 µm
Predominance of clay-sized particles (< 2 µm)
H2O dispersion
10 µm

Figure 3

ELSEVIER LICENSE
TERMS AND CONDITIONS

Jan 24, 2020

This Agreement between Technical University of Munich -- Thiago Massao Inagaki ("You") and Elsevier ("Elsevier") consists of your license details and the terms and conditions provided by Elsevier and Copyright Clearance Center.

License Number	4755241157802
License date	Jan 24, 2020
Licensed Content Publisher	Elsevier
Licensed Content Publication	Geochimica et Cosmochimica Acta
Licensed Content Title	Subsoil organo-mineral associations under contrasting climate conditions
Licensed Content Author	Thiago M. Inagaki,Angela R. Possinger,Katherine E. Grant,Steffen A. Schweizer,Carsten W. Mueller,Louis A. Derry,Johannes Lehmann,Ingrid Kögel-Knabner
Licensed Content Date	Feb 1, 2020
Licensed Content Volume	270
Licensed Content Issue	n/a
Licensed Content Pages	20
Start Page	244

End Page	263
Type of Use	reuse in a thesis/dissertation
Portion	full article
Circulation	1
Format	both print and electronic
Are you the author of this Elsevier article?	No
Will you be translating?	No
Title	Organic matter protection through mineral interactions in soils
Institution name	Technical University of Munich
Expected presentation date	Apr 2020
Requestor Location	Technical University of Munich Emil-Ramann-Straße 2 Lehrstuhl für Bodenkunde Freising, 85354 Germany Attn: Technical University of Munich
Publisher Tax ID	GB 494 6272 12
Total	0.00 USD

Terms and Conditions

INTRODUCTION

1. The publisher for this copyrighted material is Elsevier. By clicking "accept" in connection with completing this licensing transaction, you agree that the following terms and conditions apply to this transaction (along with the Billing and Payment terms and conditions

established by Copyright Clearance Center, Inc. ("CCC"), at the time that you opened your Rightslink account and that are available at any time at http://myaccount.copyright.com).

GENERAL TERMS

2. Elsevier hereby grants you permission to reproduce the aforementioned material subject to the terms and conditions indicated.

3. Acknowledgement: If any part of the material to be used (for example, figures) has appeared in our publication with credit or acknowledgement to another source, permission must also be sought from that source. If such permission is not obtained then that material may not be included in your publication/copies. Suitable acknowledgement to the source must be made, either as a footnote or in a reference list at the end of your publication, as follows:

"Reprinted from Publication title, Vol /edition number, Author(s), Title of article / title of chapter, Pages No., Copyright (Year), with permission from Elsevier [OR APPLICABLE SOCIETY COPYRIGHT OWNER]." Also Lancet special credit - "Reprinted from The Lancet, Vol. number, Author(s), Title of article, Pages No., Copyright (Year), with permission from Elsevier."

4. Reproduction of this material is confined to the purpose and/or media for which permission is hereby given.

5. Altering/Modifying Material: Not Permitted. However figures and illustrations may be altered/adapted minimally to serve your work. Any other abbreviations, additions, deletions and/or any other alterations shall be made only with prior written authorization of Elsevier Ltd. (Please contact Elsevier at permissions@elsevier.com). No modifications can be made to any Lancet figures/tables and they must be reproduced in full.

6. If the permission fee for the requested use of our material is waived in this instance, please be advised that your future requests for Elsevier materials may attract a fee.

7. Reservation of Rights: Publisher reserves all rights not specifically granted in the combination of (i) the license details provided by you and accepted in the course of this licensing transaction, (ii) these terms and conditions and (iii) CCC's Billing and Payment terms and conditions.

8. License Contingent Upon Payment: While you may exercise the rights licensed immediately upon issuance of the license at the end of the licensing process for the transaction, provided that you have disclosed complete and accurate details of your proposed use, no license is finally effective unless and until full payment is received from you (either by publisher or by CCC) as provided in CCC's Billing and Payment terms and conditions. If full payment is not received on a timely basis, then any license preliminarily granted shall be deemed automatically revoked and shall be void as if never granted. Further, in the event that you breach any of these terms and conditions or any of CCC's Billing and Payment terms and conditions, the license is automatically revoked and shall be void as if never granted. Use of materials as described in a revoked license, as well as any use of the materials beyond the scope of an unrevoked license, may constitute copyright infringement and publisher reserves the right to take any and all action to protect its copyright in the materials.

9. Warranties: Publisher makes no representations or warranties with respect to the licensed material.

10. Indemnity: You hereby indemnify and agree to hold harmless publisher and CCC, and their respective officers, directors, employees and agents, from and against any and all claims arising out of your use of the licensed material other than as specifically authorized pursuant to this license.

11. No Transfer of License: This license is personal to you and may not be sublicensed, assigned, or transferred by you to any other person without publisher's written permission.

12. No Amendment Except in Writing: This license may not be amended except in a writing signed by both parties (or, in the case of publisher, by CCC on publisher's behalf).

13. Objection to Contrary Terms: Publisher hereby objects to any terms contained in any purchase order, acknowledgment, check endorsement or other writing prepared by you, which terms are inconsistent with these terms and conditions or CCC's Billing and Payment terms and conditions. These terms and conditions, together with CCC's Billing and Payment terms and conditions (which are incorporated herein), comprise the entire agreement between you and publisher (and CCC) concerning this licensing transaction. In the event of any conflict between your obligations established by these terms and conditions and those established by CCC's Billing and Payment terms and conditions, these terms and conditions shall control.

14. Revocation: Elsevier or Copyright Clearance Center may deny the permissions described in this License at their sole discretion, for any reason or no reason, with a full refund payable to you. Notice of such denial will be made using the contact information provided by you. Failure to receive such notice will not alter or invalidate the denial. In no event will Elsevier or Copyright Clearance Center be responsible or liable for any costs, expenses or damage incurred by you as a result of a denial of your permission request, other than a refund of the amount(s) paid by you to Elsevier and/or Copyright Clearance Center for denied permissions.

LIMITED LICENSE

The following terms and conditions apply only to specific license types:

15. **Translation**: This permission is granted for non-exclusive world **English** rights only unless your license was granted for translation rights. If you licensed translation rights you may only translate this content into the languages you requested. A professional translator must perform all translations and reproduce the content word for word preserving the integrity of the article.

16. **Posting licensed content on any Website**: The following terms and conditions apply as follows: Licensing material from an Elsevier journal: All content posted to the web site must maintain the copyright information line on the bottom of each image; A hyper-text must be included to the Homepage of the journal from which you are licensing at http://www.sciencedirect.com/science/journal/xxxxx or the Elsevier homepage for books at http://www.elsevier.com; Central Storage: This license does not include permission for a scanned version of the material to be stored in a central repository such as that provided by Heron/XanEdu.

Licensing material from an Elsevier book: A hyper-text link must be included to the Elsevier homepage at http://www.elsevier.com . All content posted to the web site must maintain the copyright information line on the bottom of each image.

Posting licensed content on Electronic reserve: In addition to the above the following clauses are applicable: The web site must be password-protected and made available only to bona fide students registered on a relevant course. This permission is granted for 1 year only. You may obtain a new license for future website posting.

17. **For journal authors:** the following clauses are applicable in addition to the above:

Preprints:

A preprint is an author's own write-up of research results and analysis, it has not been peer-reviewed, nor has it had any other value added to it by a publisher (such as formatting, copyright, technical enhancement etc.).

Authors can share their preprints anywhere at any time. Preprints should not be added to or enhanced in any way in order to appear more like, or to substitute for, the final versions of articles however authors can update their preprints on arXiv or RePEc with their Accepted Author Manuscript (see below).

If accepted for publication, we encourage authors to link from the preprint to their formal publication via its DOI. Millions of researchers have access to the formal publications on ScienceDirect, and so links will help users to find, access, cite and use the best available version. Please note that Cell Press, The Lancet and some society-owned have different preprint policies. Information on these policies is available on the journal homepage.

Accepted Author Manuscripts: An accepted author manuscript is the manuscript of an article that has been accepted for publication and which typically includes author-incorporated changes suggested during submission, peer review and editor-author communications.

Authors can share their accepted author manuscript:

- immediately
    - via their non-commercial person homepage or blog
    - by updating a preprint in arXiv or RePEc with the accepted manuscript
    - via their research institute or institutional repository for internal institutional uses or as part of an invitation-only research collaboration work-group
    - directly by providing copies to their students or to research collaborators for their personal use
    - for private scholarly sharing as part of an invitation-only work group on commercial sites with which Elsevier has an agreement
- After the embargo period
    - via non-commercial hosting platforms such as their institutional repository
    - via commercial sites with which Elsevier has an agreement

In all cases accepted manuscripts should:

- link to the formal publication via its DOI
- bear a CC-BY-NC-ND license - this is easy to do
- if aggregated with other manuscripts, for example in a repository or other site, be shared in alignment with our hosting policy not be added to or enhanced in any way to appear more like, or to substitute for, the published journal article.

Published journal article (JPA): A published journal article (PJA) is the definitive final record of published research that appears or will appear in the journal and embodies all value-adding publishing activities including peer review co-ordination, copy-editing, formatting, (if relevant) pagination and online enrichment.

Policies for sharing publishing journal articles differ for subscription and gold open access articles:

Subscription Articles: If you are an author, please share a link to your article rather than the full-text. Millions of researchers have access to the formal publications on ScienceDirect, and so links will help your users to find, access, cite, and use the best available version.

Theses and dissertations which contain embedded PJAs as part of the formal submission can be posted publicly by the awarding institution with DOI links back to the formal publications on ScienceDirect.

If you are affiliated with a library that subscribes to ScienceDirect you have additional private sharing rights for others' research accessed under that agreement. This includes use for classroom teaching and internal training at the institution (including use in course packs and courseware programs), and inclusion of the article for grant funding purposes.

Gold Open Access Articles: May be shared according to the author-selected end-user license and should contain a CrossMark logo, the end user license, and a DOI link to the formal publication on ScienceDirect.

Please refer to Elsevier's posting policy for further information.

18. **For book authors** the following clauses are applicable in addition to the above: Authors are permitted to place a brief summary of their work online only. You are not allowed to download and post the published electronic version of your chapter, nor may you scan the printed edition to create an electronic version. **Posting to a repository:** Authors are permitted to post a summary of their chapter only in their institution's repository.

19. **Thesis/Dissertation**: If your license is for use in a thesis/dissertation your thesis may be submitted to your institution in either print or electronic form. Should your thesis be published commercially, please reapply for permission. These requirements include permission for the Library and Archives of Canada to supply single copies, on demand, of the complete thesis and include permission for Proquest/UMI to supply single copies, on demand, of the complete thesis. Should your thesis be published commercially, please reapply for permission. Theses and dissertations which contain embedded PJAs as part of the formal submission can be posted publicly by the awarding institution with DOI links back to the formal publications on ScienceDirect.

Elsevier Open Access Terms and Conditions

You can publish open access with Elsevier in hundreds of open access journals or in nearly 2000 established subscription journals that support open access publishing. Permitted third party re-use of these open access articles is defined by the author's choice of Creative Commons user license. See our open access license policy for more information.

Terms & Conditions applicable to all Open Access articles published with Elsevier:

Any reuse of the article must not represent the author as endorsing the adaptation of the article nor should the article be modified in such a way as to damage the author's honour or reputation. If any changes have been made, such changes must be clearly indicated.

The author(s) must be appropriately credited and we ask that you include the end user license and a DOI link to the formal publication on ScienceDirect.

If any part of the material to be used (for example, figures) has appeared in our publication with credit or acknowledgement to another source it is the responsibility of the user to ensure their reuse complies with the terms and conditions determined by the rights holder.

Additional Terms & Conditions applicable to each Creative Commons user license:

CC BY: The CC-BY license allows users to copy, to create extracts, abstracts and new works from the Article, to alter and revise the Article and to make commercial use of the Article (including reuse and/or resale of the Article by commercial entities), provided the user gives appropriate credit (with a link to the formal publication through the relevant DOI), provides a link to the license, indicates if changes were made and the licensor is not represented as endorsing the use made of the work. The full details of the license are available at http://creativecommons.org/licenses/by/4.0.

CC BY NC SA: The CC BY-NC-SA license allows users to copy, to create extracts, abstracts and new works from the Article, to alter and revise the Article, provided this is not done for commercial purposes, and that the user gives appropriate credit (with a link to the formal publication through the relevant DOI), provides a link to the license, indicates if changes were made and the licensor is not represented as endorsing the use made of the work. Further, any new works must be made available on the same conditions. The full details of the license are available at http://creativecommons.org/licenses/by-nc-sa/4.0.

CC BY NC ND: The CC BY-NC-ND license allows users to copy and distribute the Article, provided this is not done for commercial purposes and further does not permit distribution of the Article if it is changed or edited in any way, and provided the user gives appropriate credit (with a link to the formal publication through the relevant DOI), provides a link to the license, and that the licensor is not represented as endorsing the use made of the work. The full details of the license are available at http://creativecommons.org/licenses/by-nc-nd/4.0. Any commercial reuse of Open Access articles published with a CC BY NC SA or CC BY NC ND license requires permission from Elsevier and will be subject to a fee.

Commercial reuse includes:

- Associating advertising with the full text of the Article
- Charging fees for document delivery or access
- Article aggregation
- Systematic distribution via e-mail lists or share buttons

Posting or linking by commercial companies for use by customers of those companies.

20. **Other Conditions**:

v1.9

Questions? customercare@copyright.com or +1-855-239-3415 (toll free in the US) or +1-978-646-2777.

Journal Pre-proofs

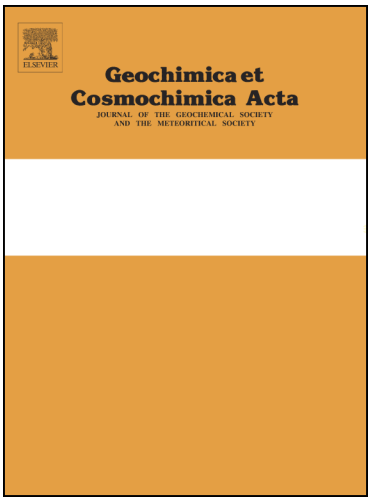

Subsoil organo-mineral associations under contrasting climate conditions

Thiago M. Inagaki, Angela R. Possinger, Katherine E. Grant, Steffen A. Schweizer, Carsten W. Mueller, Louis A. Derry, Johannes Lehmann, Ingrid Kögel-Knabner

PII: S0016-7037(19)30738-0
DOI: https://doi.org/10.1016/j.gca.2019.11.030
Reference: GCA 11542

To appear in: *Geochimica et Cosmochimica Acta*

Received Date: 3 October 2018
Revised Date: 21 October 2019
Accepted Date: 21 November 2019

Please cite this article as: Inagaki, T.M., Possinger, A.R., Grant, K.E., Schweizer, S.A., Mueller, C.W., Derry, L.A., Lehmann, J., Kögel-Knabner, I., Subsoil organo-mineral associations under contrasting climate conditions, *Geochimica et Cosmochimica Acta* (2019), doi: https://doi.org/10.1016/j.gca.2019.11.030

Subsoil organo-mineral associations under contrasting climate conditions

Thiago M. Inagaki* [a,d], Angela R. Possinger [b], Katherine E. Grant [c], Steffen A. Schweizer [a], Carsten W. Mueller [a], Louis A. Derry [c], Johannes Lehmann [b,d], Ingrid Kögel-Knabner [a,d].

*corresponding author: thiago.inagaki@wzw.tum.de

[a] Chair of Soil Science, Technical University of Munich, Emil-Ramann-Straße 2, Freising, Germany. 85354

[b] Soil and Crop Sciences, Cornell University, 909 Bradfield Hall, Ithaca NY, USA 14853

[c] Earth and Atmospheric Sciences, 4140 Snee Hall, Cornell University, Ithaca NY, USA 14853

[d] Institute for Advanced Study, Technical University of Munich, Lichtenbergstraße 2a Garching, Germany. 85748

Abstract

Climate differences can induce profound changes in organo-mineral associations in soils. However, the magnitude of these modifications, whether as a direct effect of climate conditions or an indirect effect through changes in soil mineralogy, are still not fully understood. In this study, we aimed to improve understanding of how climate and resultant changes in soil mineralogy affect subsoil (i.e., 0.4–0.9 m) organo-mineral interactions at the macro- and microscale. A set of subsoil samples were collected throughout an elevation gradient (approximately 1800 to 2400 mm precipitation year^{-1} and 15 to 24ºC) on Kohala Mountain, Hawaii. We carried out a combined approach of bulk soil analyses with mineral extractions and spectroscopic and spectromicroscopic analyses. Significant positive correlations ($p < 0.05$) between soil organic carbon (SOC) with extracted Fe and Al (dithionite citrate bicarbonate – DCB and ammonium oxalate – OX) at the bulk soil scale supported prior research showing also concurrent decline of subsoil Fe, Al and SOC above a precipitation level of ~2000 - ~2200 mm year^{-1}. However, divergence in microscale organo-mineral associations identified using NanoSIMS allowed us to discern the relative roles of Fe and Al in promoting organo-mineral associations. At the lower precipitation range (~1800 mm year^{-1}), the clay fraction < 2 µm showed higher amounts of organic matter (OM) co-localized with Fe & Al compared with the higher precipitation level (~2300 mm year^{-1}), where OM was mostly unassociated or only associated with Al. While Fe contributed to approximately 40% of the microscale organo-mineral associations in the lower precipitation site (quantified by co-localizations with OM segments), this contribution at the higher rainfall regime was only 5%. In contrast, the contribution of Al was approximately the same in both rainfall levels (approximately 30%). Therefore, associations with Al may be more important than Fe for OM stabilization under reducing climate conditions. The normalized CN:C ratio based on individual pixels was found to be higher when co-localized with Al, Fe, or both, especially under the high precipitation regime. This fact points towards the importance of Fe and Al to stabilize more N-rich OM, especially at high rainfall levels. In addition, subsoil from higher rainfall conditions exhibited more reduced forms of Fe (assessed by Fe K-edge

XANES) and lower proportions of carboxyl-C (5% lower in the relative abundance) as well as higher alkyl/O-alkyl ratios determined by CP-MAS ^{13}C NMR. Such differences in composition may directly influence the organo-mineral associations at both locations, as differences in Fe reduction and the presence of carboxyl-C groups are recognized to play a role in OM stabilization. We conclude that spatial relationships between Fe and Al with SOC at the microscale show a shift towards Al-dominated SOC associations at higher precipitation that could not be ascertained from bulk measurements alone. Therefore, they are of fundamental importance to understand the impact of climate change on SOC stabilization.

Key words: Fe, Al, short-range order minerals, Andosols, organo-mineral associations.

Abbreviations: soil organic carbon (SOC), dithionite citrate bicarbonate (DCB), ammonium oxalate (OX).

1. Introduction

Soils have the capacity to store more organic carbon than the global vegetation and atmosphere combined (Lehmann and Kleber, 2015). Therefore, the capacity of soils to foster carbon storage for climate and food security has become increasingly important due to Earth's changing climate (Rumpel et al., 2018). Organo-mineral associations are recognized as one of the most important mechanisms for providing long-term soil organic carbon (SOC) stabilization (Kögel-Knabner et al., 2008). Likewise, soil development and concomitant changes in mineralogy are known to be crucial factors in this process (Harden, 1982). According to Torn et al. (1997), when considering long timescales, changes of mineral-stabilized OC in subsoils provide the largest changes in the quantity and turnover of SOC stocks. Many studies have used proxies of reactive metals, such as Fe and Al extracted by dithionite citrate bicarbonate (DCB), and acid ammonium oxalate (OX) to assess SOC storage potential (Filimonova et al., 2016; Giardina et al., 2014; Keiluweit et al., 2017; Torn et al., 1997). Such phases of minerals are considered essential for the promotion of soil

aggregation and SOC protection (Souza et al., 2017). However, the differences in how each element (e.g. Fe and Al) acts in providing SOC stabilization are still unclear. In addition, bulk extractions may not represent the scale at which the organo-mineral associations occur (e.g., micro no nanoscale). Recently, the investigation of microenvironments in soils revealed several novel insights into SOC turnover and sequestration, adding more mechanistic understanding of the measurements performed at the bulk soil scale (Lehmann et al., 2008; Mueller et al., 2017; Netzer et al., 2018; Pohl et al., 2018; Remusat et al., 2012; Schweizer et al., 2018; Steffens et al., 2017; Wiesheu et al., 2018). Although clay size aggregates < 2 μm or even smaller fractions are mainly responsible for SOC storage in reactive Fe and Al-rich soils (e.g., Andosols) (Asano and Wagai, 2014), spatially-resolved assessments at the microscale are still relatively rare for studying organo-mineral associations.

In addition, soil moisture stands out as one of five major factors affecting interactions between organic matter and minerals in soil (Kleber et al., 2015). Higher moisture levels promote biological processes, functioning as a solvent for several microbial reactions that enhance organo-mineral associations (Hong et al., 2013). In a recent study, Keiluweit et al. (2017) demonstrated that the formation of anaerobic microsites under higher moisture levels could be an important mechanism for SOC stabilization. On the other hand, excessive moisture promotes loss of SOC from minerals by releasing protected organic matter (Huang and Hall, 2017). It is not yet clear through which mechanisms higher moisture levels can affect organo-mineral interactions in soils. As many studies have already demonstrated, climate change is influencing precipitation amounts and variability worldwide (Madsen et al., 2014; O'Gorman, 2015; Trenberth, 2011). However, most precipitation studies cover large areas, encompassing different biomes and environmental conditions (O'Gorman, 2015; Trenberth, 2011). There are relatively few studies demonstrating the impact of variable climate conditions on mineral associations within soils of similar mineralogy, particularly taking into consideration soil microenvironments.

Here we present a study of mineral-SOC interaction processes across a precipitation gradient of approximately 1800 to 2400 mm $year^{-1}$. The goal of this study was to understand

how different climate conditions impact subsoil organo-mineral associations at the macro- and microscales. We hypothesized that climate-induced changes, either qualitative or quantitative, in association of SOC with reactive metals, especially Fe oxides, are differently expressed between observations at the bulk and microscale.

2. Materials and Methods

2.1 Experimental area and soil sampling

The study was carried out in the Kohala region (20°4'14.16"N, 155°43'21.94"E) of northern Hawaii in a rainfall gradient varying from approximately 1800 to 2400 mm year^{-1}, with annual temperatures ranges of 15 to 24ºC, depending on elevation (Giambelluca *et al.,* 2013). The vegetation canopy at the sites changes with elevation. The native vegetation constituted of mixed ohi'a (*Metrosideros polymorpha* Gaudich.) and koai'a (*Acacia koaia* Hillebr.) in the lower part of the transect, grading to a o'hia and mixed fern vegetation at higher parts of the transect (hapu'u - *Cybotium spp.*- and uluhe – *Dicronopteris linearis* Burm.). In the 20th century, the mid elevation forest (up to 1400 m at this site) was largely cleared and replaced by kikuyu pasture grasses (*Pennisetum clandestinum* Hochst.).

We used eleven sites in this study along the climate gradient, six collected from grassland and five from forest vegetation (*Metrosideros polymorpha)*. Soil profiles were excavated by hand and sampled by genetic horizon until approximately 1 m depth. Since the main objective of this study was to evaluate subsoil organic carbon stabilization, we focused mainly on 23 samples from 0.4–0.9 m B subsoil horizons across the rainfall gradient. We also included 23 samples from the respective 0.2 m A topsoil horizons to evaluate the influence of aboveground biomass and vegetation change on topsoil layers. The complete set of samples with respective location and depth can be found in Table 1.

2.2 Soil mineralogy and organic matter distribution along the climate gradient

The soil is characterized as an Andosol derived from alkalic lavas of the 350 ka Pololu basalt that likely also received ash deposition from the younger (150 ka) Hawi basalt

series (Wolfe and Morris, 1996). The soils were sieved (4-mm mesh). In order to maintain field-moist conditions, we kept the samples in boxes with ice bags while they were transported to the laboratory and stored in climate-controlled rooms at 4ºC. All analyses (in Section 2.2) were performed in duplicate and the results were corrected by the respective moisture level of each sample. Soil organic carbon contents were measured by dry combustion (CHNSO Elemental Analyzer, Hekatech, Wegberg – Germany). Due to the high rainfall regime and soil pH < 7, ($CaCl_2$), no pre-treatment for carbonate removal was necessary. Pre-tests conducted with 1 M HCl solution also demonstrated no reaction in the samples.

We determined what we call proxy for “reactive metals” in this study, which refers to Fe and Al extractable from soil by selective dissolution techniques of acid ammonium oxalate and citrate-dithionite. These reactive phases include monomeric metal cations related to organic ligands, short-range order minerals such as allophane- and imogolite-type minerals, amorphous metal phases, and minor fractions of crystalline Fe oxides, hydroxides and oxyhydroxides (Levard et al., 2012; Parfitt and Childs, 1988; Thompson et al., 2011; Wagai et al., 2018).

We performed extractions of Fe and Al in parallel with dithionite-citrate following the method of Mehra and Jackson (1958) and with NH_4 oxalate at pH 3 according to the method described by Schwertmann (1964). Soil pH was measured in 0.01 M $CaCl_2$ solution (1 : 2.5 soil : solution ratio) using a pH meter (Orion Star A111, ThermoFisher Scientific, Waltham – MA, USA) and exchangeable Ca, Mg, and K were extracted using the NH_4OAc method at pH 7 (Lavkulich, 1981). All the extracted elements were measured by inductively coupled plasma optical emission spectroscopy (ICP-OES) (Vista-Pro CCD simultaneous, Varian, Darmstadt - Germany). In addition, we analyzed the mineralogy of the fine clay fraction (< 2 µm) (Section 2.3) by X-ray diffraction (PW 1830, Phillips, Amsterdam - Netherlands; X-ray source: Co K alpha).

2.3 Fe speciation by Iron K-edge X-ray Absorption Near Edge Structure (XANES) spectroscopy

To assess the presence of reducing conditions at higher precipitation levels, we performed Fe K-edge XANES measurements at the Cornell High Energy Synchrotron Source (CHESS) F3 beamline on two bulk subsoil samples of approximately 2200 and 2300 mm precipitation $year^{-1}$, respectively. The F3 beamline uses a hard-bend magnet source with a silicon (111) monochromator tunable to hard X-ray energies (6–18 keV) and a silicon drift X-ray detector. Data were collected for the Fe K-edge in fluorescence mode, with a spot size of approximately 0.5 × 4 mm. The F3 end station is operated at room temperature and under ambient pressure. The Fe K-edge (E_0) was set to 7.112 keV (Prietzel et al., 2007), and scans were collected for the pre-edge region (6.912–7.092 keV) with 0.005 keV step size and 1 s dwell time. For the near-edge (7.092–7.142 eV) region we used a 0.001 keV step size and 2 s dwell time. Multiple scans were collected for each sample; specifically, we collected 2–3 scans for Fe standards and 5 scans for soil samples. Elemental Fe foil was used to collect simultaneous Fe K-edge alignment measurements for each scan.

Fe-organic complex standards (previously published in Bhattacharyya et al. (2018)) included Fe (III) EDTA, Fe (III) citrate, and Fe (II) citrate. Commercially obtained mineral standards include elemental Fe^0 (energy calibration), goethite, and fayalite. All the ssamples, including the standards, were stored air-dry prior to XAS analysis. Additionally, Fe^{2+}-substituted nontronite and ferrihydrite were prepared for this experiment following standard protocols. Briefly, structural Fe^{3+} in nontronite was reduced using the dithionite method described by Stucki et al. (1984). Fe^{2+}-substituted nontronite was stored in an anaerobic environment in ultrapure water suspension prior to XAS analysis. Ferrihydrite ($Fe^{3+}_2O_3 \bullet 0.5H_2O$) was prepared by titration of Fe (III) nitrate (0.005 M) by addition of base (0.05 M KOH) to pH 7 and purification by dialysis (1000D MWCO) and subsequent rinsing and re-suspension in water until XANES analysis (modified from Schwertmann and Cornell (2008)). Samples were prepared for XANES measurements by deposition of ~2.5 g material

on polyimide tape (1-mil) thickness. Reduced Fe samples were prepared and stored anaerobically prior to analysis.

Initial processing of scans was completed using Athena in Demeter v. 0.9.25 (Ravel and Newville 2005). Scans were flattened and third-order normalization was performed with a pre-edge normalization range of −150 to −30 eV and post-edge range of +150 to ~400 eV relative to E_0 = 7112. Energy calibration was performed for individual scans with reference Fe foil, and aligned scans were merged. The pre-edge centroid and white line energy positions for the normalized probability of X-ray absorbance (μ(E)) were determined by using the peak detection function in Fityk v 0.9.8 (Wojdyr, 2010) for energy ranges of 7110–7118 eV (pre-edge centroid) and 7119–7160 eV (white line). The Fe K-edge position (E_0) (i.e. the edge inflection point) was identified by the maximum of the first derivative of normalized μ(E).

Additionally, the relative contribution of Fe^{2+} to the total Fe XANES spectrum was described using the first derivative of normalized μ(E). In the first derivative μ(E) spectrum, the area of the peak assigned to the 1s-4s transition (~7120 eV) can be used to estimate relative Fe^{2+} (Berry et al., 2003). The ~7120 eV peak area relative to total area was determined by fitting four Gaussian functions at 7112, 7120, 7124, and 7128 eV to the first derivative μ(E) over the range > 7100 and < 7140 eV using the Levenberg-Marquadt algorithm in Fityk v 0.9.8. (Wojder, 2010), with the function at 7120.0 eV fixed and the remaining functions constrained by ±3*sin(~0) eV. Peak full-width half-maximum was constrained to 2 ±1*sin(~0) eV and peak height was unconstrained. The fitted area of the 7120 eV peak was divided by the sum of all four-peak areas to determine relative contribution to the total XANES spectrum.

2.4 Isolation of clay-sized fraction

In order to obtain a pure clay-sized fraction that was free of particulate organic matter, we performed clay isolation. The separation of the clay-sized fraction allows studying the organo-mineral associations at the micrometer scale without the interference of other components that are not directly associated with soil mineral surfaces.

The procedure was adapted from the soil organic matter fractionation method described by Golchin et al. (1994), using 4-mm sieved soils under field-moist conditions. In our tests for choosing an isolation method, we assessed three different approaches to disperse the soil: 1) using a 1 M NaCl solution, 2) using deionized water, and 3) using a sodium polytungstate solution (density of 1.8 g cm^{-3}). Overall, no differences were observed regarding the SOC distribution using the different solutions (Inagaki et al., 2019). This was mainly a result of the fact that the subsoil samples analyzed in our study contained an insignificant amount of particulate organic matter (less than 1% of the total SOC amount). Therefore, we opted to proceed using deionized water for clay separation. The complete procedure is described as follows.

First, we gently saturated the soil by adding deionized water yielding a suspension of 1 : 2.5 soil : water volume. For the dispersion of macroaggregates and larger microaggregates, we utilized ultrasonic dispersion (SonopulsHD2200, Bandelin, Berlin - Germany) with an energy input of 1500 J ml^{-1}. This energy level is considered sufficient for providing dispersion of the highly stable Andosol microaggregates without causing damage to the primary mineral structure (Silva et al., 2015). After centrifuging the suspension (8000 g for 40 min), the floating particulate organic matter was removed from the supernatant using a vacuum pump.

Later, the soil mineral fraction (i.e., free of particulate organic matter) was sieved with a 20-µm sized mesh in order to separate sand and coarse silt-sized fractions. The mineral fraction was then subjected to sedimentation to separate the medium silt and clay-sized fractions of 20-2 µm and < 2 µm, respectively. The < 2 µm clay-sized fraction was subsequently freeze-dried and used for imaging and ^{13}C NMR spectroscopy.

2.5 Soil organic matter characterization by ^{13}C CP/MAS NMR spectroscopy

Soil clay fractions (< 2 µm) of four soil profiles of precipitation levels across the climate gradient were chosen for NMR spectroscopy (approximately 1700, 2000, 2200, and 2300 mm $year^{-1}$, respectively). We performed solid-state ^{13}C NMR spectroscopy (Biospin

DSX 200 NMR spectrometer, Bruker, Rheinstetten, Germany) of the < 2 µm clay fractions from the subsoil (0.4–0.6 m) with a contact time of 0.001 sec with a pulse delay of 0.4 sec. At least 100,000 accumulated scans were performed. The spectra were integrated using four major chemical shift regions: 0 to 45 ppm (alkyl-C), 45 to 110 ppm (O/N-alkyl-C), 110 to 160 (aryl-C), and 160 to 220 ppm (carboxyl-C) (Knicker and Lüdemann, 1995). Despite the elevated Fe content, no sample pre-treatment with hydrofluoric acid was necessary in order to obtain a well-resolved spectrum.

2.6 Organo-mineral associations at the microscale by Nano scale secondary ion mass spectrometry (NanoSIMS)

Two contrasting samples from lower (approximately 1800 mm $year^{-1}$) and higher (approximately 2300 mm $year^{-1}$) rainfall levels were chosen for NanoSIMS analysis. Before the < 2 µm fraction was freeze-dried, we took aliquots from the soil suspension in deionized water. The aliquots of soil suspensions were diluted 20 times in water, pipetted onto a silica wafer and dried in a desiccator at room temperature for subsequent scanning electron microscopy (SEM) and NanoSIMS analysis.

To elucidate the distribution of the mineral particles on the Si-wafer and to choose regions of interests for subsequent NanoSIMS measurements, the samples were assessed by reflected light microscopy (Axio Imager Z2, Zeiss, Oberkochen - Germany) and SEM (JSM 5900LV, JEOL, Tokyo - Japan). Prior to the measurement the samples were coated with Au/Pd (~30 nm; SCD 005 sputter coater, Baltec GmbH, Germany), and during measurements the electron flood gun was used to compensate for any charging effects (Mueller et al., 2013). The NanoSIMS imaging was performed using the NanoSIMS 50L (Cameca, Gennevilliers - France) at the Chair of Soil Science of the Technical University of Munich (TUM), Germany, using a high-energy cesium (Cs^+) ion beam (~1.2 pA). We used electron multipliers with a dead time of 44 ns to detect the following secondary ions: $^{16}O^-$, $^{12}C^-$, $^{12}C^{14}N^-$, $^{27}Al^{16}O^-$ and $^{56}Fe^{16}O^-$. Before the analysis, we removed the gold coating layer using a high primary beam current. The beam was focused onto the sample and secondary

ions were ejected from the sample surface with a lateral resolution of ~100 nm. The field of view of the measurements was 20 µm · 20 µm (256 · 256 pixels) and the ion images were acquired using a dwell time of 1 ms per pixel with each 40 planes.

2.6.1 M&M: Multi-channel machine-learning segmentation and image analysis

We corrected the NanoSIMS measurements for electron multiplier dead-time by using the OpenMIMS plugin for Fiji (Gormanns et al., 2012). Sum images were created based on auto-alignment of the $^{16}O^-$ distribution across all 40 planes. To differentiate the elemental distributions at the microscale (Fig. 1b-d) and use these to quantify spatial measures, we performed supervised pixel classifications based on the machine-learning algorithm implemented in Ilastik 1.2 (Sommer et al., 2011). We used the $^{16}O^-$ distribution to differentiate between soil particles and Si wafer and define training areas for the algorithm. The additional presence of $^{12}C^-$ and $^{12}C^{14}N^-$ on these particles was used to determine OM segments (Hatton et al., 2012; Remusat et al., 2012). In this regard, we use the term soil particles to refer to the total distribution of segments classified as mineral or OM. The supervised classification included multiple image features like intensity, texture, and gradient in all isotope distributions. Further details of the data preparation and underlying segmentation processes are described in Schweizer et al. (2018). In addition to the classification into background, mineral, and OM segments, we computed similar supervised classifications including $^{27}Al^{16}O^-$ to determine spatial Al-enriched segments and $^{56}Fe^{16}O^-$ to determine Fe-enriched segments (Fig. 1f,g).

The simple segmentation mask based on $^{16}O^-$, $^{12}C^-$, and $^{12}C^{14}N^-$ (Fig. 1e) was used to quantify the spatial arrangement of individual particle and OM segments. In total, we detected 333 particles, where 117 were covered by OM, which amounted to 161 OM segments for the soil sample fractionated with H_2O (Appendix, Table A2). We have also performed the same analysis in the clay fraction obtained from the fractionation with NaCl in order to check the data consistency. The latter presented the same trends of the samples fractionated with H_2O and it can be found in the Appendix (Fig. A5, Fig. A6). Particles

including less than 5 pixels (0.2 μm^2) were not included in the further analysis. Based on the projected area of particle segments and OM segments, we computed their mean size averaged across all sizes and frequency distributions for the size classes <0.1 μm^2, 0.1-0.5 μm^2, 0.5-2 μm^2, and > 2 μm^2. To analyze the relative chemical composition of the OM segments, we determined the normalized CN:C ratio of the individual OM segments based on the simple segmentation mask (Fig. 1e). A higher CN:C ratio indicates a relative increase of N-rich compounds, whereas a lower ratio indicates an increase of C-rich compounds. The relationship of $^{12}C^{14}N^-$:$^{12}C^-$ and $^{12}C^{14}N^-$:$^{12}C^{2-}$ with C:N ratios measured by an elemental analyzer was demonstrated to be linear (Alleon et al., 2015; Hatton et al., 2012).

To quantify the co-localization of OM-, Al-, and Fe-enriched spots, we combined the simple segmentation of mineral and OM segments with the Al and Fe segments into a segmentation mask comprising all possible combinations in 12 material classes (Fig. 1h). To compare the co-localization of OM with Al and Fe, we computed the relative area contributions of the 4 association classes to the total OM segment area (Fig. 1i). By transferring the combined segmentation mask to other isotope distributions, we determined the normalized CN:C ratio across all pixels according to the 4 OM association classes.

2.7 Statistical analysis

We performed linear regression analysis using the R software (R Development Core Team, 2014) to evaluate the relationships between Fe and Al at the bulk soil.

3. Results

3.1 Subsoil mineralogy and organic matter content along the climate gradient

At precipitation levels around 2200 mm $year^{-1}$, our analysis revealed a point at which extracted Fe and Al contents in the subsoil decreased after having achieved maximum levels (Appendix Fig. A1). Similarly, the SOC and N contents did not follow a linear trend as a function of the climate gradient (Appendix Fig. A2) and increased until precipitation reached approximately 2000 mm $year^{-1}$ and decreased above that amount. On the other hand, in the

topsoil layers (0–0.2 m), the contents of SOC and N increased along the weather gradient achieving maximum values at the highest evaluated rainfall levels (Appendix Fig. A2). The base saturation (exchangeable Ca, Mg and K) decreased at approximately 2000 mm year^{-1} and then remained the same thereafter, even at the highest precipitation levels. Soil pH was close to neutral (pH = 7) at the lowest rainfall levels and decreased to almost pH 3 at the highest precipitation level. The gravimetric water content increased with measured rainfall from 40 to 80%.

Overall, increases in precipitation promoted decreases in subsoil extractable Fe and Al contents, soil pH, and bases of exchangeable Ca, Mg, and K (Appendix Fig. A1). To evaluate the distribution, we separated the samples into three groups according to precipitation levels. The samples from the lower rainfall level (1800–2000 mm year^{-1}) presented higher soil pH values and base content in general. The highest SOC, Fe, and Al concentrations (extracted by DCB and OX) were found at intermediate precipitation levels (2000–2200 mm year^{-1}). The samples from the highest rainfall levels (2200 – 2400 mm year^{-1}) can be broadly characterized by a large decrease in soil pH, Fe, and Al contents, and by lower SOC contents. Linear regression analyses between bulk subsoil OC with Fe and with Al (DCB and OX extractable) demonstrated significant relationships ($p < 0.05$) for both mineral proxies (Fig. 2).

3.2 Clay mineralogy and Fe speciation along the climate gradient

The four distinct profiles across the climate gradient had similar soil mineralogy as indicated by the XRD spectra (Appendix, Fig. A3). All soil profiles were characterized by low clay crystallinity. Chlorite and illite, promoted by eolian deposition (Kurtz et al., 2001), were found at higher precipitation levels.

Along the climate gradient, we observed changes in the SOC composition of the clay fraction (< 2 µm) as measured by ^{13}C NMR spectroscopy (Fig. 3). Overall, at lower precipitation levels, the samples presented higher relative proportions of carboxyl and O-alkyl-C forms, while samples developed under higher precipitation levels showed higher

proportions of alkyl-C. We also observed an increase for the alkyl-C/O-alkyl-C ratio as a function of the precipitation level. As in the case of SOC, Fe, Al, and bases cations, the relative proportion of the carboxyl-C group also decreased above the SOC peak observed at ~2000 mm year^{-1}.

While Fe-DCB and Fe-OX decreased by 91 and 93%, respectively, between subsoils from sites receiving 2200 and 2300 mm precipitation year^{-1} (Appendix Fig. A1), descriptive data for normalized Fe K-edge XANES did not show appreciable differences in white line, pre-edge centroid, or inflection point (E_0) for soil samples. Energy shifts in reduced Fe standards (Fe^{2+}-substituted nontronite, fayalite, and Fe(II) citrate) were observed (Appendix, Fig. A4 and Table A1). However, using the area of the 1s-4s transition (~7120 eV) peak in the first derivative of normalized μ(E), we identified an increase of reducedFe^{+2} at 2300 vs 2200 mm precipitation year^{-1} (Fig. 4).

3.3 Organo-mineral associations at the microscale observed through NanoSIMS

A supervised classification of the particle and OM segments enabled size comparisons between the precipitation regimes. At the low precipitation regime, we found larger particle sizes compared to the high precipitation, whereas the size of the organic matter (OM) segments did not differ (Fig. 5 a,b). In the high precipitation regime, similar-sized OM segments covered smaller particles, which results in a higher coverage of the mineral surfaces. This reveals that the OM was distributed into a larger area on the mineral surface. The normalized CN:C average across individual OM segments was similar between the precipitation regimes, whereas there were contrasting tendencies between the size classes. In the low precipitation regime, the CN:C ratio was higher for OM segments >0.5 μm^2 whereas in the high precipitation it was lower for OM segments >0.5 μm^2 (Fig. 5c). A similar relationship was shown for the soil fractionated with NaCl (Appendix, Fig. A5c).

By segmenting the OM spots further into associations with Al and Fe, we could compare the two precipitation regimes and quantify distinct properties of co-localized OM associations. Our data revealed more Fe and Fe co-localized with Al on the OM segments

under the low precipitation regime compared with high precipitation (Fig. 6a). Al provided the highest area contribution of co-localized OM under the high precipitation regime (Fig. 6a). However, the majority of OM segments were not associated with either Fe or Al under high precipitation (Fig. 6a). A similar relationship was shown for the soil fractionated with NaCl (Appendix, Fig. A6a).

The normalized CN:C ratio based on individual pixels was found to be higher when co-localized with Al, Fe, or both, especially under the high precipitation regime (Fig. 6b). This points towards the interaction of more N-rich OM compounds with Al and Fe. The pixel-based total mean of the CN:C ratio was lower for the high precipitation regime than for the low precipitation regime (Fig. 6b). This is explained by the higher area contributions of the unassociated OM with a generally more C-rich composition (Fig. 6b).

4. Discussion

4.1 Relative role of Fe and Al in promoting organo-mineral associations at the macro and microscale

Our combined approach using extraction and spectromicroscopic techniques revealed that the organo-mineral associations were differently expressed between bulk soil and microscale. The relationships between SOC with either pedogenic Fe or Al (e.g. extracted by DCB and OX) along the climate gradient demonstrated the significant role of both proxies for reactive metal oxides in SOC stabilization as supported by several studies (Asano et al., 2018; Basile-Doelsch et al., 2007; Schwertmann, 1964; Torn et al., 1997; Wagai et al., 2018). As Torn et al. (1997) demonstrated in their research, the changes in soil mineralogy play a major role controlling SOC accrual in the Kohala region.

The use of chemical extraction methods is widespread because they are inexpensive and do not demand special laboratory infra-structure (Rennert, 2019). In our study, they were a useful tool to demonstrate the overall relationship of Fe and Al proxies with SOC at a landscape scale, given the significant correlations (Fig. 2). Comparisons of the relative role of

Fe and Al in promoting SOC storage vary according to the region and soil type (Wiesmeier et al., 2019). Overall in Andosols, Al seems to be the main driver as demonstrated by Matus et al. (2006), who concluded that Al extracted by acid ammonium acetate was the principal factor controlling SOC stocks in a series of volcanic soils in Chile. In our study, although we observed slight differences in R^2 and p values between the correlations of DCB extracted Fe ($R^2 = 0.11$, $p = 0.02$) and Al ($R^2 = 0.35$, $p < 0.01$) with SOC (Fig. 2a), these parameters did not show a difference in OX extractions (Fe: $R^2 = 0.28$, $p = 0.01$; Al: $R^2 = 0.22$, $p < 0.01$) (Fig 2b). Hence, the relative importance of both elements could not be ascertained from these bulk soil measurements.

In addition, although the use of extractable reactive metals has been recognized as a good indicator of SOC accrual (Asano and Wagai, 2014; Beare et al., 2014; McNally et al., 2017), this metric may not represent the scale at which organo-mineral association processes occur (i.e., micro to nanoscale). In this context, the different patterns of organo-mineral associations observed through NanoSIMS in our study demonstrate the importance of combined assessments including microscale observations in addition to bulk soil analyses. These combined evaluations were a useful tool to disentangle the relative importance of Fe and Al in promoting organo mineral interactions. The differences in the area proportions of Fe-OM, Al-OM and Fe & Al-OM demonstrate the influence of climate, especially reducing conditions, on the subsoil organo-mineral associations at the microscale (Fig. 6). In this way, our findings offer insights regarding the influence of this weather gradient on soil organo-mineral associations, which can serve as important information to understand the effects of climate change on SOC accrual.

4.2 Mechanisms of organo-mineral associations affected by climate factors

Our results suggest that a major proportion of the organic matter measured by NanoSIMS at higher rainfall levels (~2300 mm $year^{-1}$) is unassociated with Fe and Al (e.g., 80% of the total segmented area), while most of the remaining organo-mineral interactions are Al-OM associations (Fig. 6a). This result highlights the importance of Al in promoting

overall SOC stabilization especially at higher precipitation regimes. Since the majority of previous studies on mechanisms of organo-mineral interaction focused on Fe associations (Chen et al., 2014; Chen et al., 2016; Gu et al., 1994; Saidy et al., 2012), we emphasize the importance of directing more attention to mechanisms of Al-SOC association, especially in areas under high precipitation regimes.

While microscale Al-OM associations contributed to a larger extent of organo-mineral associations in both precipitation regimes, the Fe-OM associations were more determined by the climate conditions since they presented lower values at the higher precipitation regime (Fig. 6A). While Fe contributed to approximately 31% of the microscale organo-mineral associations (i.e., Fe-OM and Fe-Al-OM associations), this contribution at the higher rainfall regime was only 6% (Fig. 6a). On the other hand, the contribution of Al-OM associations was approximately the same in both rainfall levels (i.e., approximately 30%). The stronger Al correlations in comparison to Fe observed at the microscale may be influenced by the elements relative proportion (McNally et al., 2017), since the Al contents were higher, especially at the higher precipitation regime.

The shift in Fe speciation may also play a role in causing the differing proportions of Fe-OM and Al-OM associations observed in our study. The Fe reduction in montane tropical regions can be mediated by the presence of bacterial communities responsible for Fe reduction as demonstrated by Dubinsky et al. (2010). Our observations of more reduced Fe forms at the higher precipitation levels are in accordance to the findings of Thompson et al. (2011) who observed a decrease of Fe^{3+} oxides as a function of increased rainfall in the Kohala gradient through Mössbauer spectroscopy. Such Fe reduction can potentially result in a loss of SOC to the aqueous phase. Elevated moisture levels can result in SOC losses mainly by its release from Fe associations as demonstrated by Huang and Hall (2017) and Pan et al. (2016) in incubation experiments. According to the authors, this release represents a yet under-appreciated mechanism for SOC destabilization. Similarly, Adhikari and Yang (2015) observed losses of 5 to 44% of C under reducing conditions in an incubation experiment. According to the authors, the persistence of Fe-OM associations can be

governed by organic matter chemical composition and molecular-level interactions between Fe and C. These observations agree with the lower proportions of Fe co-localized with OM at the microscale in the wetter site (Fig. 6), demonstrating that the climate conditions at this area decreased Fe-OM association.

The increase in the organic matter Alkyl-C / O-N Alkyl ratio observed through NMR spectroscopy (Fig. 3) and the shift in Fe speciation observed through XANES analysis (Fig. 4) demonstrates that differences in climate affected not only the amounts of Fe and SOC but also their composition. At higher precipitation levels, we found the predominance of more aliphatic forms of C (i.e., alkyl-C), lower levels of reactive C groups (i.e., carboxylic-C) as well as more reduced forms of Fe, which are in accordance to the oxygen limitations from increased water saturation (Bartlett and James, 1993; Li et al., 2008).

These changes in soil organic matter composition driven by climate factors may have a direct influence on how organo-mineral associations occur in this gradient. For example, the lower proportion of carboxylic C groups at the higher precipitation level (5% lower in relative abundance, Fig. 3b) may influence organo-mineral associations. The carboxylic C group has a significant role on mechanisms for SOC accrual, since it is responsible for the associating with minerals through a variety of interactions mechanisms (e.g., cation exchange, ligand exchange) (Aquino et al., 2011). In addition, reactions between carboxylic-C and the surface of Fe oxides are considered to be a dominant process affecting organo-mineral associations in soils (Gu et al., 1994). Therefore, the lower amounts of carboxylic-C at the wetter sites (Fig. 3b) may explain the lower frequency of Fe-OM associations observed in our microscale analysis (Fig. 6a).

The higher proportion of aliphatic compounds at the higher precipitation range (0.74 higher in Alkyl/O-Alkyl ratio, Fig. 3c) also demonstrates the preservation of this group at wetter sites. Aromatic-C forms are recognized to be preferentially adsorbed to Fe oxides in soil (Kramer et al., 2012). However, Adhikari and Yang (2015) demonstrated that, under reducing conditions, these associations could be easily released, while associations with aliphatic C were more persistent. However, our analysis at the microscale showed that

approximately 81% of the measured OM in the < 2 μm clay fraction at the higher precipitation regime was not co-localized with Fe and Al, compared to 31% in the lower precipitation rainfall (Fig. 6). This demonstrates that especially interactions of Fe-OM associations may be more important for SOC stabilization at lower precipitation sites. Therefore, the preservation of such organic matter forms at the higher rainfall regimes may be more related to intrinsic C properties such as hydrophobicity (Piccolo and Mbagwu, 1999), which can reduce access for degrading enzymes (von Lutzöw et al., 2006).

In addition, by calculating the normalized CN:C ratio of OM segments, we were able to compare the importance of Fe and Al associations to stabilize N-rich OM under contrasting climate conditions. In our study, most part of the N-rich organic compounds were associated with Fe and Al rather than with unassociated OM (Fig. 6b). This fact indicates the stabilization of microbially processed OM, since most of the organic N in soil is derived from living organisms (Geisseler et al., 2009; Geisseler et al., 2010; Knicker, 2004). Likewise, Kopittke et al. (2018) observed that added microbially-derived compounds were preferentially attached to distinct areas of soil mineral surfaces after a one year incubation. The authors emphasize that differences in mineralogy are important to regulate the sorption of microbial products on mineral surfaces or C dominated moieties. Therefore, we highlight the relative importance of Fe and Al to promote organo mineral associations with N rich organic matter, especially at the wetter sites.

4.3 Implications for overall climate-driven effects on soil pedogenesis

The observed changes in Fe speciation and lower SOC concentrations due to losses to the aqueous solution may be directly related to the overall soil pedogenesis along the climate gradient. As observed in our results (Appendix, Fig. A1 and A2) and in other studies (Chadwick et al., 2003; Li et al., 2017; Torn et al., 1997; Vitousek and Chadwick, 2013), the SOC and reactive metals contents decrease simultaneously under higher precipitation levels above ~2000 mm $year^{-1}$ in the Kohala Hawaiian gradient. Across climate gradients, SOC contents are mainly driven by an optimum combination of temperature and precipitation (Li et

al., 2017). Since the XRD spectra demonstrated few differences along the gradient (Appendix, Fig. A3), the variation of SOC contents appeared to be decoupled from the proportion of semi- or non-crystalline minerals (i.e., both sites are characterized by low clay crystallinity and the presence of amorphous substances) (Kramer and Chadwick, 2016). In this case, the transport of mobile SOC (e.g., colloidal and/or dissolved organic carbon, DOC) through deeper horizons is likely a major driver of pedogenesis at these Andosol sites (Buettner et al., 2014; Marin-Spiotta et al., 2011). In an incubation experiment using soils from the Hawaiian gradient, Buettner et al. (2014) observed that Fe reduction increased DOC content in fractions of < 430 nm. According to the authors, this a colloidal dispersion of SOC during Fe reduction may be a major process responsible for C migration to deeper horizons. The infiltration of DOC through infilling channels in the soil profile has also been pointed out as an important mechanism of DOC transport at higher precipitation ranges in the Hawaiian gradient (Marin-Spiotta et al., 2011).

The transport of DOC throughout the soil profile at the high precipitation ranges also points towards the role of Al in promoting the SOC stabilization under conditions of Fe reduction, since Al is recognized for stabilization of DOC in soils (Scheel et al., 2007; Schwesig et al., 2003). This may explain the overall higher importance of Al in promoting organo-mineral associations compared to Fe in the higher precipitation range (Fig. 6a). In this context, changes in soil pH influenced by climate conditions may also have a significant influence on these mechanisms. Scheel et al. (2007) observed that Al-OM precipitates could be up to 28 times less mineralized than a comparable DOC in an acidic forest soil. This mineralization was even lower at pH 3.8 when compared to pH 4 ($CaCl_2$). The authors mention the precipitation of aromatic and high molecular weight structures under lower pH values, which led to more stable precipitates. Such results agree with the low pH values (e.g., close to pH 3 $CaCl_2$, Appendix Fig. A1) found at the higher precipitation ranges (> ~2300 mm $year^{-1}$). Grybos et al. (2009) observed that increases of soil pH under soil reducing conditions (e.g., from 5.5 to 7.4) can potentially cause organic matter desorption.

Therefore, the low pH values found at the higher precipitation site may be an important factor to maintain the SOC levels and the remaining Al-OM interactions (Fig. 6A) at this region.

For our topsoil layers (0-0.2 m), the continuous increase of SOC is likely driven by a change in vegetation (from pasture to forest), and consequently higher inputs of biomass-C (Torn et al., 1997). On the other hand, such effects of land use change unlikely affect subsoil OC contents, as demonstrated by Kelly et al. (1998) through ^{13}C values of soils formed beneath pastureland and forest. According to the authors, the majority of the subsoil OC (taken at a depth of approximately 0.7 m) is from the pre-pasture forest vegetation. Likewise, Chadwick et al. (2007) demonstrated through ^{14}C radiocarbon analysis that little recent OC has been incorporated into deeper soil horizons following conversion to pasturelands. In addition, in our study, the decreases of SOC contents at higher rainfall levels in the subsoil were observed within the forest area and unrelated to land use change.

Therefore, our results (especially at the microscale) contributes to the overall understanding of the climate influence on soil pedogenesis in this gradient. In Fig. 7, we demonstrate the overall effects of climate changes on subsoil organo-mineral associations at the macro- and microscale. In this paper, we illustrated under field conditions that the major factors influencing subsoil organo-mineral associations as a function of changes in climate were a combination of lower contents of reactive Fe and changes of Fe and SOC composition. Our results show that the combined use of different quantitative and qualitative techniques at the bulk and micro-scale provide important and complimentary information about how organo-mineral interactions are affected by changing climate conditions.

5. Conclusions

We have demonstrated that combined approaches at the bulk soil and microscale can provide important information about how subsoil organo-mineral associations are affected by the climate gradient. The observation at the microscale allowed us to disentangle the relative importance of Fe and Al in promoting organo-mineral associations. This information could not be ascertained only from bulk soil measurements. We observed that Al promoted most part

of the measured microscale organo-mineral associations at the higher rainfall regime compared to Fe, which highlights the importance of this element under reducing conditions. We highlight that changes in organic matter composition (i.e., lower carboxylic-C levels) and shift in Fe redox (i.e., to more reduced forms) can affect organo-mineral associations with Fe at higher rainfall levels. We conclude that interactions between reactive metal minerals and SOC at the scale in which mineral interactions occur are of considerable importance to understand SOC stabilization, and these interactions may not be traceable from analyses at the bulk soil scale. The changes in these associations in subsoils should be taken into consideration when evaluating the impact of climate factors and land use. We recommend that future studies should take in considerations the forms of Fe oxides forming at different locations in soil microsites as a function of soil moisture and redox conditions. In addition, we also encourage researchers to investigate further the overall role of Al in promoting SOC accrual, especially under reducing conditions.

6. Acknowledgements

The authors thank the technicians Maria Greiner and Bärbel Angres for their support with the laboratory analysis. Dr. Carmen Höschen for her support with the NanoSIMS measurements. Dr. Rong Huang for his support with data collection at the CHESS F3 end station. Dr. Werner Häusler for his support with the XRD analysis, and the three anonymous reviewers who helped to improve the quality of this manuscript.

7. Funding

This research was supported by the Institute for Advanced Study (IAS) from the Technical University of Munich (TUM) through the Hans-Fisher Senior Fellowship. CHESS is supported by the NSF and NIH/NIGMS via NSF award DMR-1332208.

8. References

Adhikari D. and Yang Y., (2015) Selective stabilization of aliphatic organic carbon by iron oxide. *Sci. Rep*. **5**, 11214.

Alleon J., Bernard S., Remusat L. and Robert F., (2015) Estimation of nitrogen-to-carbon ratios of organics and carbon materials at the submicrometer scale. *Carbon* **84**, 290-298.

Aquino A.J., Tunega D., Schaumann G.E., Haberhauer G., Gerzabek M.H. and Lischka H., (2011) The functionality of cation bridges for binding polar groups in soil aggregates. *Int. J. Quant. Chem*. **111**, 1531-1542.

Asano M. and Wagai R., (2014) Evidence of aggregate hierarchy at micro- to submicron scales in an allophanic Andisol. *Geoderma* **216**, 62-74.

Asano M., Wagai R., Yamaguchi N., Takeichi Y., Maeda M., Suga H. and Takahashi Y., (2018) In Search of a Binding Agent: Nano-Scale Evidence of Preferential Carbon Associations with Poorly-Crystalline Mineral Phases in Physically-Stable, Clay-Sized Aggregates. *Soil Syst*. **2**, 32.

Bartlett R.J. and James B.R., (1993) Redox Chemistry of Soils. *Adv Agron* **50**, 151-208.

Basile-Doelsch I., Amundson R., Stone W.E.E., Borschneck D., Bottero J.Y., Moustier S., Masin F. and Colin F., (2007) Mineral control of carbon pools in a volcanic soil horizon. *Geoderma* **137**, 477-489.

Beare M., McNeill S., Curtin D., Parfitt R., Jones H., Dodd M. and Sharp J., (2014) Estimating the organic carbon stabilisation capacity and saturation deficit of soils: a New Zealand case study. *Biogeochemistry* **120**, 71-87.

Bhattacharyya A., Schmidt M.P., Stavitski E. and Martinez C.E., (2018) Iron speciation in peats: Chemical and spectroscopic evidence for the co-occurrence of ferric and ferrous iron in organic complexes and mineral precipitates. *Org. Geochem*. **115**, 124-137.

Buettner S.W., Kramer M.G., Chadwick O.A. and Thompson A., (2014) Mobilization of colloidal carbon during iron reduction in basaltic soils. *Geoderma* **221**, 139-145.

Chadwick O.A., Gavenda R.T., Kelly E.F., Ziegler K., Olson C.G., Elliott W.C. and Hendricks D.M., (2003) The impact of climate on the biogeochemical functioning of volcanic soils. *Chem. Geol.* **202**, 195-223.

Chadwick O.A., Kelly E.F., Hotchkiss S.C. and Vitousek P.M., (2007) Precontact vegetation and soil nutrient status in the shadow of Kohala Volcano, Hawaii. *Geomorphology* **89**, 70-83.

Chen C., Dynes J.J., Wang J. and Sparks D.L., (2014) Properties of Fe-organic matter associations via coprecipitation versus adsorption. *Envir. Science & Tech.* **48**, 13751-13759.

Chen K.-Y., Chen T.-Y., Chan Y.-T., Cheng C.-Y., Tzou Y.-M., Liu Y.-T. and Teah H.-Y., (2016) Stabilization of natural organic matter by short-range-order iron hydroxides. *Envir. Science & Tech.* **50**, 12612-12620.

Dubinsky E.A., Silver W.L. and Firestone M.K., (2010) Tropical forest soil microbial communities couple iron and carbon biogeochemistry. *Ecology* **91**, 2604-2612.

Filimonova S., Kaufhold S., Wagner F.E., Hausler W. and Kogel-Knabner I., (2016) The role of allophane nano-structure and Fe oxide speciation for hosting soil organic matter in an allophanic Andosol. *Geochim. Cosmochim. Acta* **180**, 284-302.

Geisseler D., Horwath W.R. and Doane T.A., (2009) Significance of organic nitrogen uptake from plant residues by soil microorganisms as affected by carbon and nitrogen availability. *Soil. Biol. Biochem.* **41**, 1281-1288.

Geisseler D., Horwath W.R., Joergensen R.G. and Ludwig B., (2010) Pathways of nitrogen utilization by soil microorganisms–a review. *Soil. Biol. Biochem.* **42**, 2058-2067.

Giardina C.P., Litton C.M., Crow S.E. and Asner G.P., (2014) Warming-related increases in soil CO 2 efflux are explained by increased below-ground carbon flux. *Nat. Clim. Chang.* **4**, 822.

Gormanns P., Reckow S., Poczatek J.C., Turck C.W. and Lechene C., (2012) Segmentation of multi-isotope imaging mass spectrometry data for semi-automatic detection of regions of interest. *PloS one* **7**, e30576.

Grybos M., Davranche M., Gruau G., Petitjean P. and Pédrot M., (2009) Increasing pH drives organic matter solubilization from wetland soils under reducing conditions. *Geoderma* **154**, 13-19.

Gu B., Schmitt J., Chen Z., Liang L. and McCarthy J.F., (1994) Adsorption and desorption of natural organic matter on iron oxide: mechanisms and models. *Envir. Science & Tech.* **28**, 38-46.

Harden J.W., (1982) A Quantitative Index of Soil Development from Field Descriptions - Examples from a Chronosequence in Central California. *Geoderma* **28**, 1-28.

Hatton P.J., Remusat L., Zeller B. and Derrien D., (2012) A multi-scale approach to determine accurate elemental and isotopic ratios by nano-scale secondary ion mass spectrometry imaging. *Rapid Commun. Mass Spectrom* **26**, 1363-1371.

Hong Z.N., Chen W.L., Rong X.M., Cai P., Dai K. and Huang Q.Y., (2013) The effect of extracellular polymeric substances on the adhesion of bacteria to clay minerals and goethite. *Chem. Geol.* **360**, 118-125.

Huang W. and Hall S.J., (2017) Elevated moisture stimulates carbon loss from mineral soils by releasing protected organic matter. *Nat. Commun.* **8**, 1774.

Inagaki T.M., Mueller C.W., Lehmann J. and Kögel-Knabner I., (2019) Andosol clay re-aggregation observed at the microscale during physical organic matter fractionation. *J. Plant Nutr Soil Sc.* **182**, 145-148.

Keiluweit M., Wanzek T., Kleber M., Nico P. and Fendorf S., (2017) Anaerobic microsites have an unaccounted role in soil carbon stabilization. *Nat Commun* **8**, 1771.

Kelly E.F., Chadwick O.A. and Hilinski T.E., (1998) The effect of plants on mineral weathering. *Biogeochemistry* **42**, 21-53.

Kleber M., Eusterhues K., Keiluweit M., Mikutta C., Mikutta R. and Nico P.S., (2015) Chapter one-mineral–organic associations: formation, properties, and relevance in soil environments. *Adv. Agron.* **130**, 1-140.

Knicker H., (2004) Stabilization of N-compounds in soil and organic-matter-rich sediments—what is the difference? *Mar. Chem.* **92**, 167-195.

Knicker H. and Lüdemann H.D., (1995) N-15 and C-13 Cpmas and Solution Nmr-Studies of N-15 Enriched Plant-Material during 600 Days of Microbial-Degradation. *Org. Geochem.* **23**, 329-341.

Kögel-Knabner I., Guggenberger G., Kleber M., Kandeler E., Kalbitz K., Scheu S., Eusterhues K. and Leinweber P., (2008) Organo-mineral associations in temperate soils: Integrating biology, mineralogy, and organic matter chemistry. *J. Plant Nutr. Soil Sci.* **171**, 61-82.

Kopittke P.M., Hernandez-Soriano M.C., Dalal R.C., Finn D., Menzies N.W., Hoeschen C. and Mueller C.W., (2018) Nitrogen-rich microbial products provide new organo-mineral associations for the stabilization of soil organic matter. *Glob. Chang. Biol.* **24**, 1762-1770.

Kramer M.G. and Chadwick O.A., (2016) Controls on carbon storage and weathering in volcanic soils across a high-elevation climate gradient on Mauna Kea, Hawaii. *Ecology* **97**, 2384-2395.

Kramer M.G., Sanderman J., Chadwick O.A., Chorover J. and Vitousek P.M., (2012) Long-term carbon storage through retention of dissolved aromatic acids by reactive particles in soil. *Glob. Chang. Biol.* **18**, 2594-2605.

Kurtz A.C., Derry L.A. and Chadwick O.A., (2001) Accretion of Asian dust to Hawaiian soils: Isotopic, elemental, and mineral mass balances. *Geochim. Cosmochim. Acta* **65**, 1971-1983.

Lavkulich L., (1981) Methods manual, pedology laboratory. *Vancouver, BC, CA: University of British Columbia, Department of Soil Science*.

Lehmann J. and Kleber M., (2015) The contentious nature of soil organic matter. *Nature* **528**, 60-68.

Lehmann J., Solomon D., Kinyangi J., Dathe L., Wirick S. and Jacobsen C., (2008) Spatial complexity of soil organic matter forms at nanometre scales. *Nat. Geosci.* **1**, 238-242.

Levard C., Doelsch E., Basile-Doelsch I., Abidin Z., Miche H., Masion A., Rose J., Borschneck D. and Bottero J.-Y., (2012) Structure and distribution of allophanes, imogolite and proto-imogolite in volcanic soils. *Geoderma* **183**, 100-108.

Li C.L., Cao Z.Y., Chang J.J., Zhang Y., Zhu G.L., Zong N., He Y.T., Zhang J.J. and He N.P., (2017) Elevational gradient affect functional fractions of soil organic carbon and aggregates stability in a Tibetan alpine meadow. *Catena* **156**, 139-148.

Li J., Richter D.D., Mendoza A. and Heine P., (2008) Four-decade responses of soil trace elements to an aggrading old-field forest: B, Mn, Zn, Cu, and Fe. *Ecology* **89**, 2911-2923.

Madsen H., Lawrence D., Lang M., Martinkova M. and Kjeldsen T.R., (2014) Review of trend analysis and climate change projections of extreme precipitation and floods in Europe. *J. Hydrol.* **519**, 3634-3650.

Marin-Spiotta E., Chadwick O.A., Kramer M. and Carbone M.S., (2011) Carbon delivery to deep mineral horizons in Hawaiian rain forest soils. *J. Geophys. Res. Biogeosci.* **116**.

Matus F., Amigo X. and Kristiansen S.M., (2006) Aluminium stabilization controls organic carbon levels in Chilean volcanic soils. *Geoderma* **132**, 158-168.

McNally S.R., Beare M.H., Curtin D., Meenken E.D., Kelliher F.M., Calvelo Pereira R., Shen Q. and Baldock J., (2017) Soil carbon sequestration potential of permanent pasture and continuous cropping soils in New Zealand. *Glob. Chang. Biol.* **23**, 4544-4555.

Mueller C.W., Hoeschen C., Steffens M., Buddenbaum H., Hinkel K., Bockheim J.G. and Kao-Kniffin J., (2017) Microscale soil structures foster organic matter stabilization in permafrost soils. *Geoderma* **293**, 44-53.

Mueller C.W., Weber P.K., Kilburn M.R., Hoeschen C., Kleber M. and Pett-Ridge J. (2013) Advances in the Analysis of Biogeochemical Interfaces: NanoSIMS to Investigate Soil Microenvironments, in: Sparks, D.L. (Ed.), Advances in Agronomy, Vol 121, pp. 1-46.

Netzer F., Mueller C.W., Scheerer U., Gruner J., Kogel-Knabner I., Herschbach C. and Rennenberg H., (2018) Phosphorus nutrition of Populus x canescens reflects adaptation to high P-availability in the soil. *Tree Physiol* **38**, 6-24.

O'Gorman P.A., (2015) Precipitation extremes under climate change. *Curr. Clim. Change Rep.* **1**, 49-59.

Parfitt R. and Childs C., (1988) Estimation of forms of Fe and Al-a review, and analysis of contrasting soils by dissolution and Mossbauer methods. *Soil Res.* **26**, 121-144.

Piccolo A. and Mbagwu J.S., (1999) Role of hydrophobic components of soil organic matter in soil aggregate stability. *Soil Sci. Soc. Am. J.* **63**, 1801-1810.

Pohl L., Kolbl A., Werner F., Mueller C.W., Hoschen C., Hausler W. and Kogel-Knabner I., (2018) Imaging of Al/Fe ratios in synthetic Al-goethite revealed by nanoscale secondary ion mass spectrometry. *Rapid. Commun. Mass Spectrom.* **32**, 619-628.

R Development Core Team, (2014) R: a language and environment for statistical computing. Vienna, Austria: R Foundation for Statistical Computing; 2012. *Open access available at: http://cran. r-project. org*.

Remusat L., Hatton P.-J., Nico P.S., Zeller B., Kleber M. and Derrien D., (2012) NanoSIMS study of organic matter associated with soil aggregates: advantages, limitations, and combination with STXM. *Environ. Sci. Technol.* **46**, 3943-3949.

Rennert T., (2019) Wet-chemical extractions to characterise pedogenic Al and Fe species–a critical review. *Soil Res.* **57**, 1-16.

Rumpel C., Lehmann J. and Chabbi A., (2018) '4 per 1,000'initiative will boost soil carbon for climate and food security. *Nature* **553**, 27-27.

Saidy A., Smernik R., Baldock J., Kaiser K., Sanderman J. and Macdonald L., (2012) Effects of clay mineralogy and hydrous iron oxides on labile organic carbon stabilisation. *Geoderma* **173**, 104-110.

Scheel T., Dörfler C. and Kalbitz K., (2007) Precipitation of dissolved organic matter by aluminum stabilizes carbon in acidic forest soils. *Soil Sci. Soc. Am. J.* **71**, 64-74.

Schweizer S.A., Hoeschen C., Schluter S., Kogel-Knabner I. and Mueller C.W., (2018) Rapid soil formation after glacial retreat shaped by spatial patterns of organic matter accrual in microaggregates. *Glob. Chang. Biol.* **24**, 1637-1650.

Schwertmann U., (1964) Differenzierung der Eisenoxide des Bodens durch Extraktion mit Ammoniumoxalat-Lösung. *J. Plant Nutr. Soil Sci.* **105**, 194-202.

Schwertmann U. and Cornell R.M. (2008) Iron oxides in the laboratory: preparation and characterization. John Wiley & Sons.

Schwesig D., Kalbitz K. and Matzner E., (2003) Effects of aluminium on the mineralization of dissolved organic carbon derived from forest floors. *Eur. J. Soil Sci.* **54**, 311-322.

Sommer C., Straehle C., Koethe U. and Hamprecht F.A. (2011) Ilastik: Interactive learning and segmentation toolkit, 2011 IEEE international symposium on biomedical imaging: From nano to macro. IEEE, pp. 230-233.

Souza I.F., Archanjo B.S., Hurtarte L.C., Oliveros M.E., Gouvea C.P., Lidizio L.R., Achete C.A., Schaefer C.E. and Silva I.R., (2017) Al-/Fe-(hydr) oxides–organic carbon associations in Oxisols—From ecosystems to submicron scales. *Catena* **154**, 63-72.

Steffens M., Rogge D.M., Mueller C.W., Hoschen C., Lugmeier J., Kolbl A. and Kogel-Knabner I., (2017) Identification of Distinct Functional Microstructural Domains Controlling C Storage in Soil. *Environ. Sci. Technol.* **51**, 12182-12189.

Stucki J.W., Golden D. and Roth C.B., (1984) Preparation and handling of dithionite-reduced smectite suspensions. *Clays Clay Miner.* **32**, 191-197.

Thompson A., Rancourt D.G., Chadwick O.A. and Chorover J., (2011) Iron solid-phase differentiation along a redox gradient in basaltic soils. *Geochim. Cosmochim. Acta* **75**, 119-133.

Torn M.S., Trumbore S.E., Chadwick O.A., Vitousek P.M. and Hendricks D.M., (1997) Mineral control of soil organic carbon storage and turnover. *Nature* **389**, 170-173.

Trenberth K.E., (2011) Changes in precipitation with climate change. *Clim. Res.* **47**, 123-138.

Vitousek P.M. and Chadwick O.A., (2013) Pedogenic Thresholds and Soil Process Domains in Basalt-Derived Soils. *Ecosystems* **16**, 1379-1395.

von Lutzöw M., Kögel-Knabner I., Ekschmitt K., Matzner E., Guggenberger G., Marschner B. and Flessa H., (2006) Stabilization of organic matter in temperate soils: mechanisms and their relevance under different soil conditions - a review. *Eur. J. Soil Sci.* **57**, 426-445.

Wagai R., Kajiura M., Uchida M. and Asano M., (2018) Distinctive Roles of Two Aggregate Binding Agents in Allophanic Andisols: Young Carbon and Poorly-Crystalline Metal Phases with Old Carbon. *Soil Systems* **2**, 29.

Wiesheu A.C., Brejcha R., Mueller C.W., Kogel-Knabner I., Elsner M., Niessner R. and Ivleva N.P., (2018) Stable-isotope Raman microspectroscopy for the analysis of soil organic matter. *Anal. Bioanal. Chem.* **410**, 923-931.

Wiesmeier M., Urbanski L., Hobley E., Lang B., von Lützow M., Marin-Spiotta E., van Wesemael B., Rabot E., Ließ M., Garcia-Franco N., Wollschläger U., Vogel H.-J. and Kögel-Knabner I., (2019) Soil organic carbon storage as a key function of soils - A review of drivers and indicators at various scales. *Geoderma* **333**, 149-162.

Wojdyr M., (2010) Fityk: a general-purpose peak fitting program. *J. of Appl. Crystallogr.* **43**, 1126-1128.

Wolfe E.W. and Morris J. (1996) Geologic map of the Island of Hawaii.

Figure Captions:

Figure 1: Workflow of microscale investigations starting with (a) scanning electron microscopy, (b-d) NanoSIMS measurements, (e-g) segmentations based on machine-learning segmentations, and (h,i) combinations of the simple segmentations to more material classes.

Figure 2: Relationships between Fe and Al extracted by dithionite citrate (DCB) (a) or ammonium oxalate (OX) (b) and subsoil organic carbon (SOC) of 0.4–0.9 m depths along the precipitation gradient.

Figure 3: ^{13}C NMR spectra of the clay fraction (< 2 µm) of subsoil samples collected from distinct positions of the climate gradient (a). Decrease of carboxylic-C relative abundance at the higher precipitation level indicates that reducing conditions promote the decrease of this reactive group (b). Increase of alkyl/O-alkyl-C ratio indicates the presence of less oxygenated C forms at higher precipitation levels (c).

Figure 4: First derivative of normalized µ(E) iron K-edge XANES spectra for the precipitation levels at 2200 mm year^{-1} and 2300 mm year^{-1}.The Gaussian function at 7120.0 eV (red line) associated with the 1s-4s transition (Berry *et al.* 2003) was used as an estimate of the lower-energy shift of the XANES edge associated with increased Fe^{2+} content, indicating more reduced forms of Fe at higher precipitation levels. Additional reference spectra and model fits are included in Appendix Figure A4 and Table A1.

Figure 5: Microspatial properties in coarse clay fraction fractionated with H_2O. (a,b) Frequency distribution of various size classes and mean size of particles and OM

segments (underlying numbers in Appendix Table A6). (c) Mean normalized CN:C ratio and means of various size classes within. The p-value is given in case of significant t-test.

Figure 6: Microspatial properties in < 2 µm clay fraction fractionated with H_2O. (a) Area contributions of OM segment associations. (b) Mean CN:C ratio of all pixels of the various OM segment associations.

Figure 7: Conceptual illustration demonstrating the overall effects of climate on soil organo-mineral associations at the macro and microscale in subsoil depths along the climate gradient.

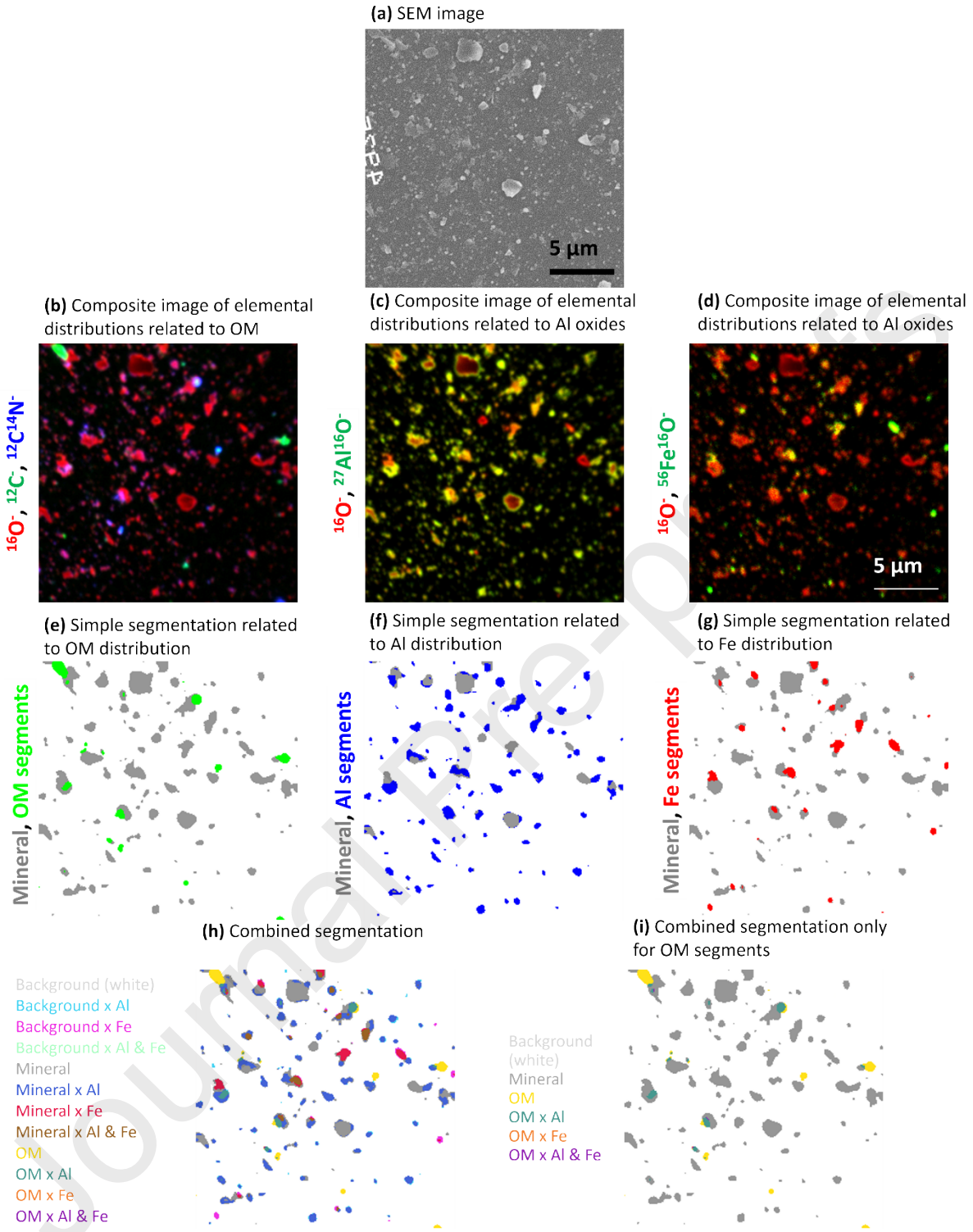
(a) SEM image
5 µm
(b) Composite image of elemental distributions related to OM
$^{16}O^-$, $^{12}C^-$, $^{12}C^{14}N^-$
(c) Composite image of elemental distributions related to Al oxides
$^{16}O^-$, $^{27}Al^{16}O^-$
(d) Composite image of elemental distributions related to Al oxides
$^{16}O^-$, $^{56}Fe^{16}O^-$
5 µm
(e) Simple segmentation related to OM distribution
Mineral, OM segments
(f) Simple segmentation related to Al distribution
Mineral, Al segments
(g) Simple segmentation related to Fe distribution
Mineral, Fe segments
(h) Combined segmentation
Background (white)
Background x Al
Background x Fe
Background x Al & Fe
Mineral
Mineral x Al
Mineral x Fe
Mineral x Al & Fe
OM
OM x Al
OM x Fe
OM x Al & Fe
(i) Combined segmentation only for OM segments
Background (white)
Mineral
OM
OM x Al
OM x Fe
OM x Al & Fe

Figure 1:

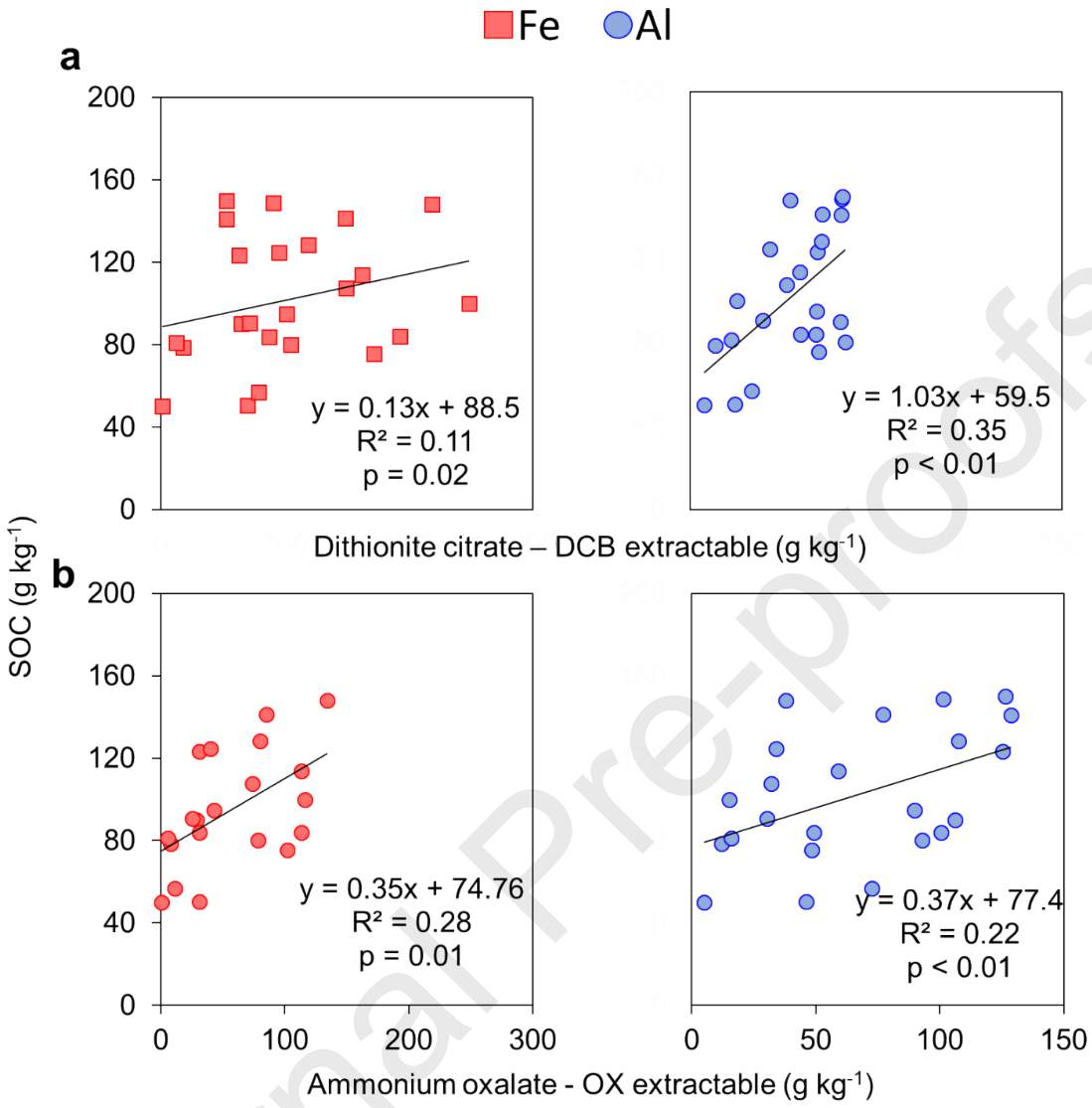

Figure 2:

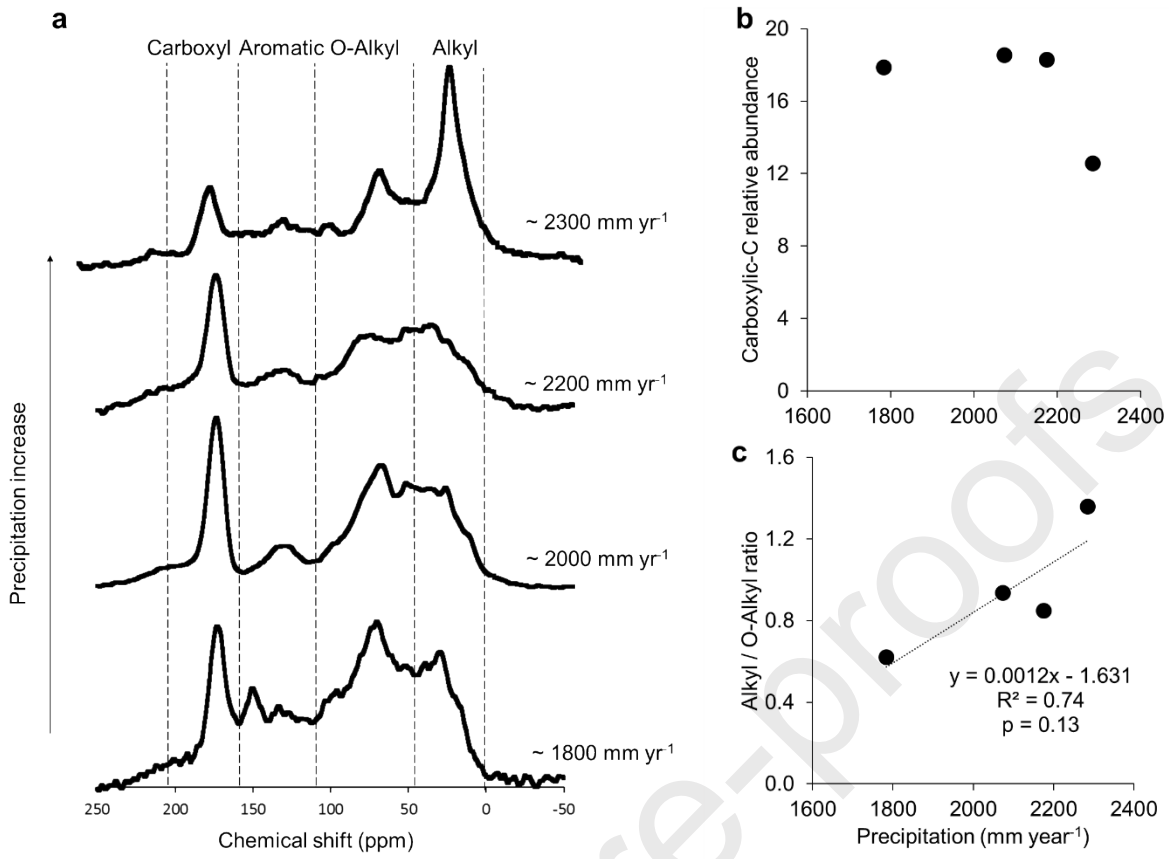

Figure 3:

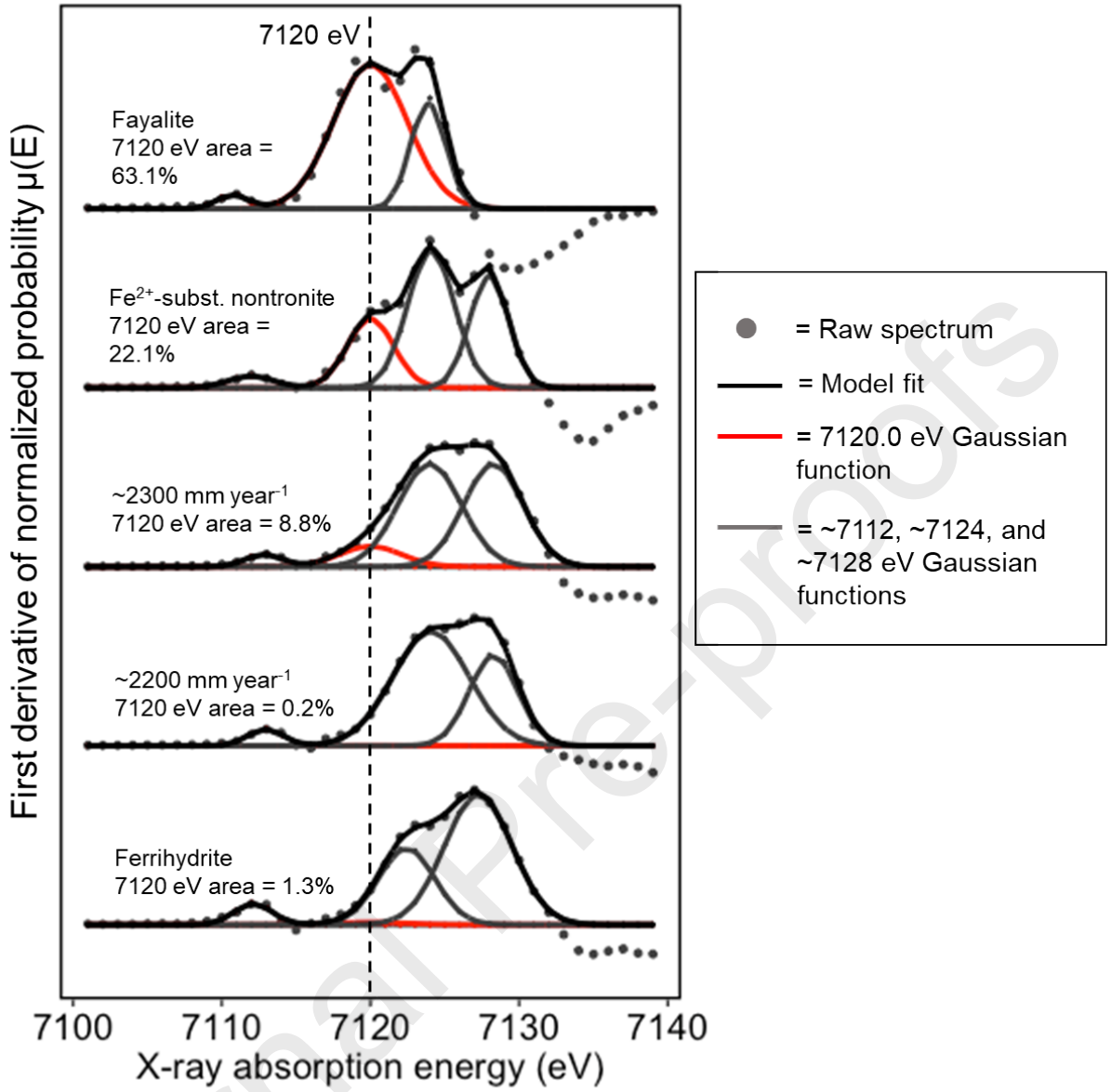

Figure 4:

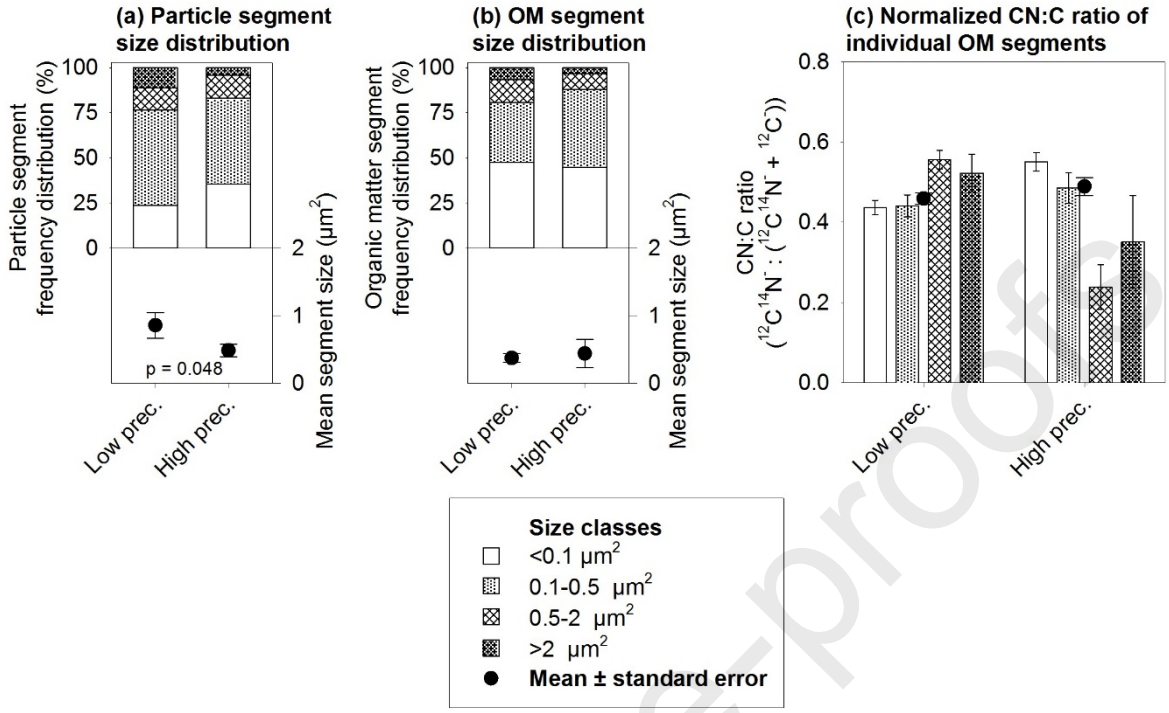

Figure 5:

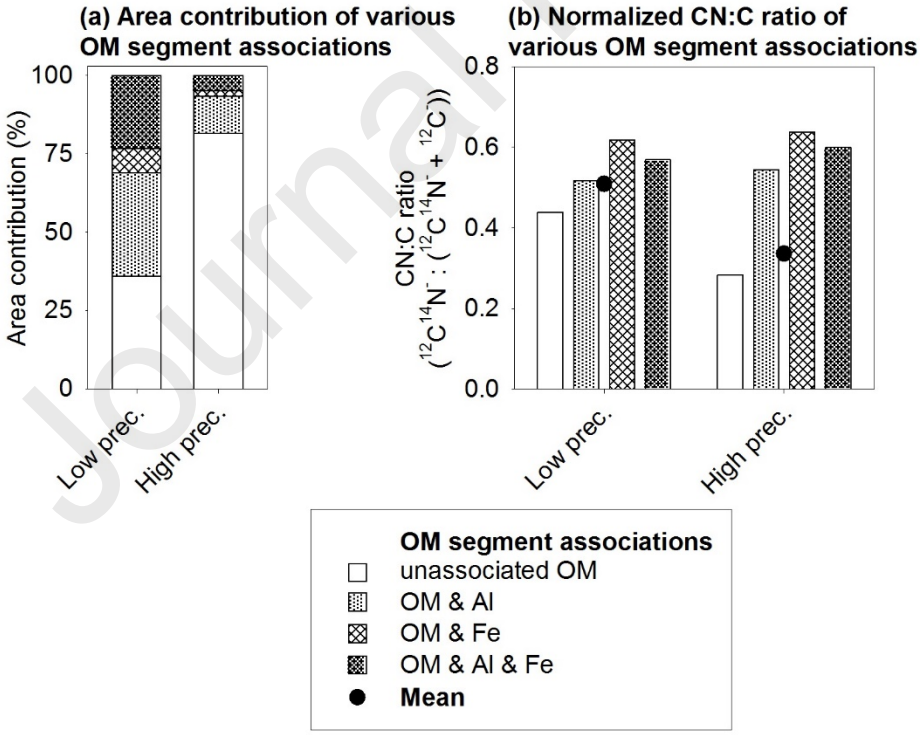

Figure 6:

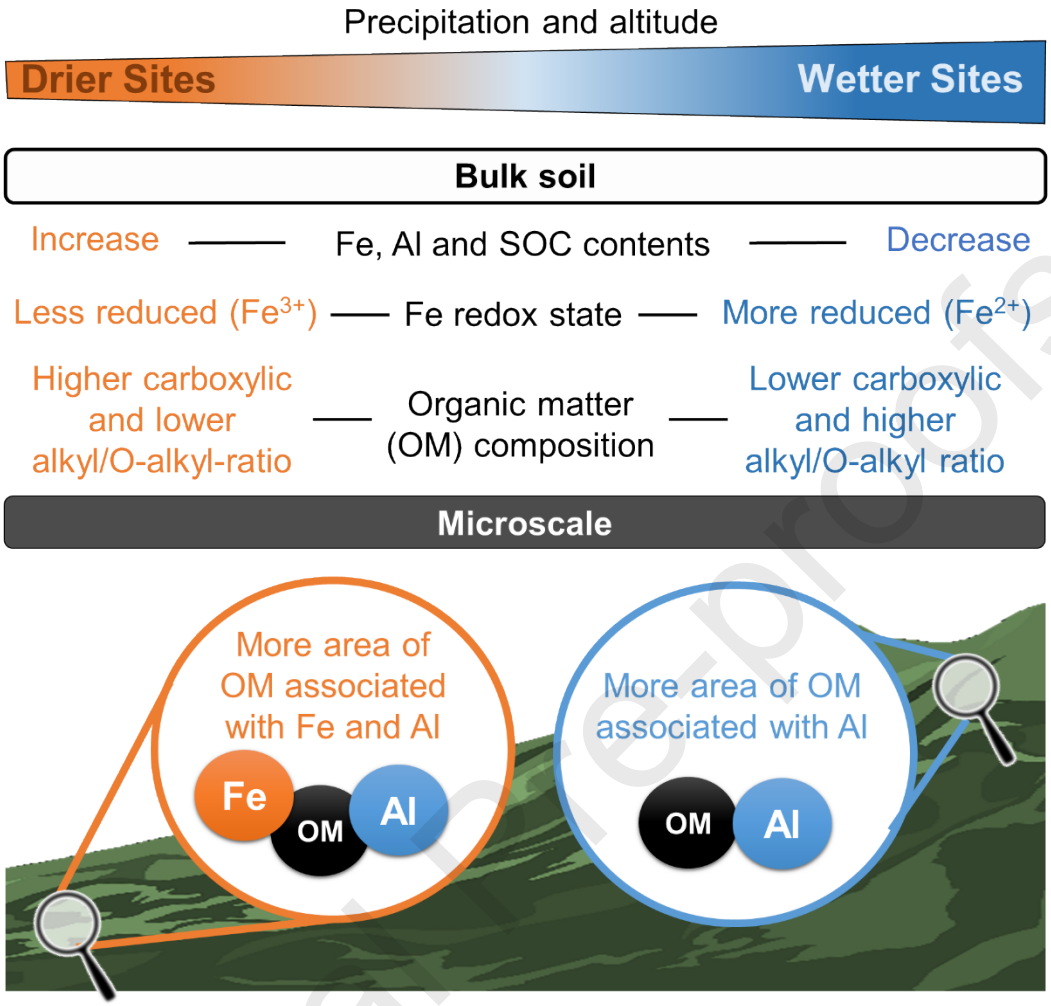

Figure 7:

Table 1: Soil samples collected in distinct elevation levels at top and subsoil depths throughout the precipitation gradient at the Pololu lava flow, Kohala Hawaii.

Altitude (m)	Vegetation	Precipitation (mm year^{-1})*	Coordinates		Depths (m)
1176	Grassland	1800	20°3'35.10"N	155°43'56.82"E	0.0–0.05 0.05–0.25 0.5–0.7 0.7–0.9
1251	Grassland	1900	20°3'44.68"N	155°43'45.55"E	0.0–0.15 0.15–0.25 0.5–0.9 0.7–0.9
1416	Grassland	1900	20°3'48.54"N	155°43'35.30"E	0.0–0.15 0.15–0.25 0.5–0.7 0.7–0.9
1361	Grassland	2000	20°4'13.33"N	155°43'30.83"E	0.0–0.05 0.05–0.25 0.5–0.7 0.6–0.7
1388	Grassland	2000	20°4'4.98"N	155°43'33.24"E	0.0–0.10 0.10–0.16 0.4–0.6 0.6–0.8
1409	Grassland	2100	20°4'8.04"N	155°43'31.65"E	0.0–0.12 0.12–0.20 0.5–0.7 0.6–0.8
1429	Forest	2100	20°4'8.36"N	155°43'28.02"E	0.0-0.03 0.03-0.10 0.4–0.6 0.6–0.8
1440	Forest	2100	20°4'5.54"N	155°43'33.24"E	0.0–0.05 0.05–0.15 0.4–0.5 0.5–0.7
1460	Forest	2200	20°4'14.16"N	155°43'21.94"E	0.0–-0.13 0.13–-0.17 0.4–0.6 0.6–0.7
1478	Forest	2300	20°4'17.40"N	155°43'18.48"E	0.0–-0.08 0.08–-0.15 0.4–0.6

					0.6–0.7
1554	Forest	2400	20°4'25.93"N	155°43'13.84"E	0.0–0.10
					0.10–0.17
					0.4–0.6
					0.6–0.7

* Precipitation values were obtained through interpolation between elevation and the different isoheytes in the Hawaii Rainfall atlas (Giambelluca et al. 2013).

APPENDIX

Subsoil organo-mineral associations in contrasting climate conditions

Thiago M. Inagaki* [a,d], Angela R. Possinger [b], Katherine E. Grant [c], Steffen A. Schweizer [a], Carsten W. Mueller [a], Louis A. Derry [c], Johannes Lehmann [b,d], Ingrid Kögel-Knabner [a,d].

*corresponding author: thiago.inagaki@wzw.tum.de

[a] Chair of Soil Science, Technical University of Munich, Emil-Ramann-Straße 2, Freising, Germany. 85354

[b] Soil and Crop Sciences, Cornell University, 909 Bradfield Hall, Ithaca NY, USA 14853

[c] Earth and Atmospheric Sciences, 4140 Snee Hall, Cornell University, Ithaca NY, USA 14853

[d] Institute for Advanced Study, Technical University of Munich, Lichtenbergstraße 2a Garching, Germany. 85748

Table of contents for appendix

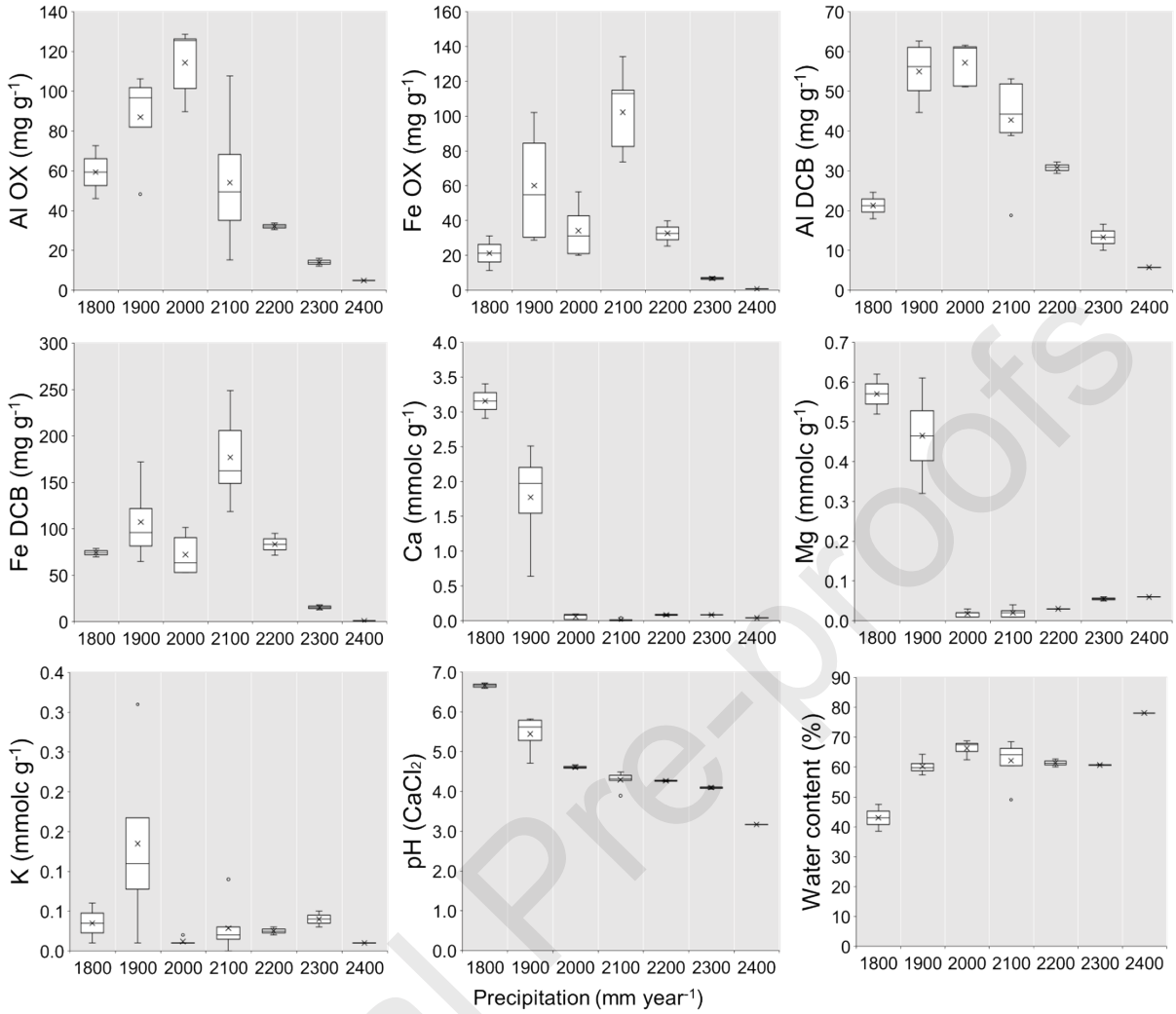

Figure A1: Fe and Al extracted by dithionite citrate (DCB) and ammonium oxalate (OX); soil pH ($CaCl_2$) and gravimetric water content; and exchangeable Ca, Mg, and K at subsoil depths of 0.6–0.9 m in function of the precipitation gradient (mm $year^{-1}$).

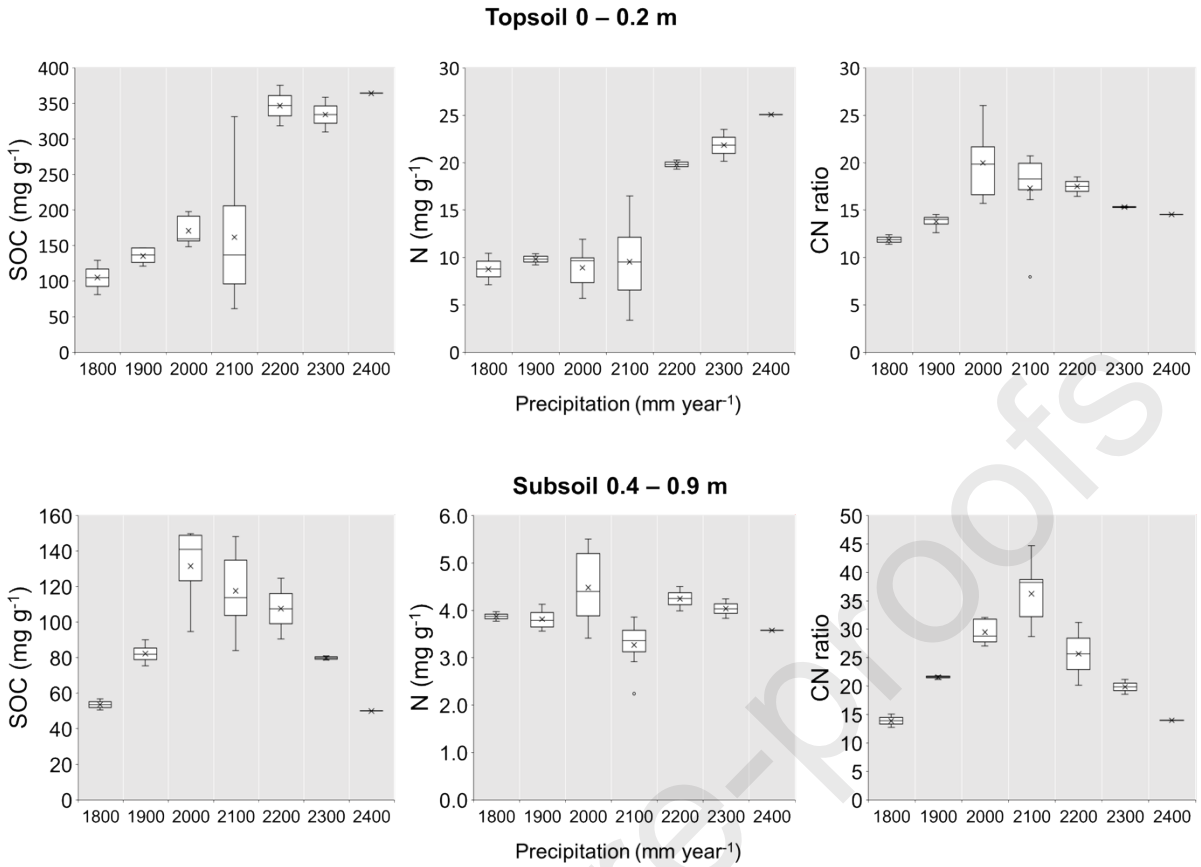

Figure A2: Soil organic carbon (SOC) and nitrogen (N) contents in topsoils (0–0.2 m) (a) and subsoils (0.4–0.9 m) (b), and C:N ratios in top- and subsoil layers in function of the precipitation gradient (mm year^{-1}).

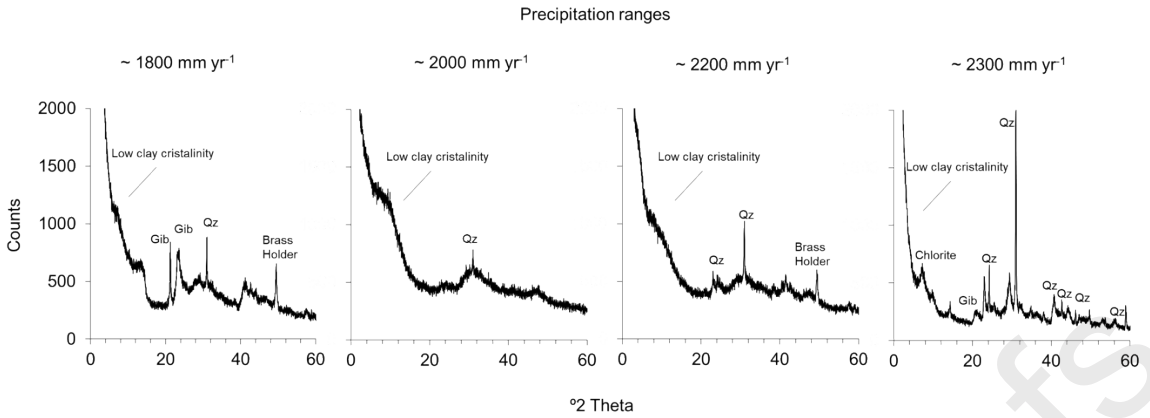

Figure A3: XRD spectra of the fine clay fraction (< 2 µm) of four distinct positions across the rainfall gradient at the depth of 0.4–0.7 m. The “Brass Holder” peak corresponds to the signal that comes from the sample holder, which is made of Brass.

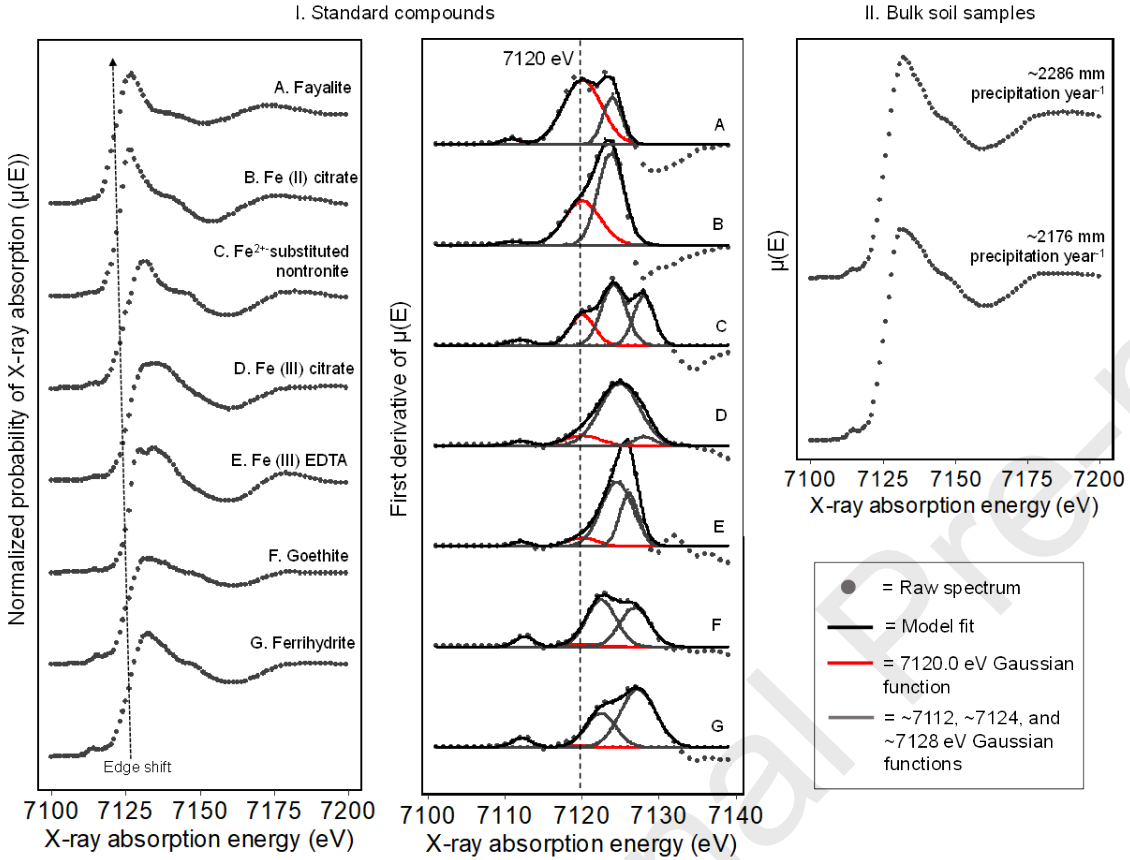

Figure A4. Normalized probability of X-ray absorbance (μ(E)) for standard compounds and subsoil samples (~2200 and ~2300 mm precipitation year^{-1}), showing energy shifts in pre-edge centroid, edge inflection point, and white line for reduced Fe compounds (Fe^{2+}-substituted nontronite, fayalite, iron (II) citrate). The first derivative of normalized μ(E) shows the increasing contribution of the Gaussian function (red curve) fixed at 7120.0 eV associated with the 1s-4s transition as a metric of relative increases in reduced Fe. II. Normalized μ(E) for soil samples, showing no detectable shift in energy position compared to standard compound shifts in I. Values for pre-edge centroid, edge energy (E0), white line energy, and 7120.0 eV peak area are listed in this Appendix in Table A1.

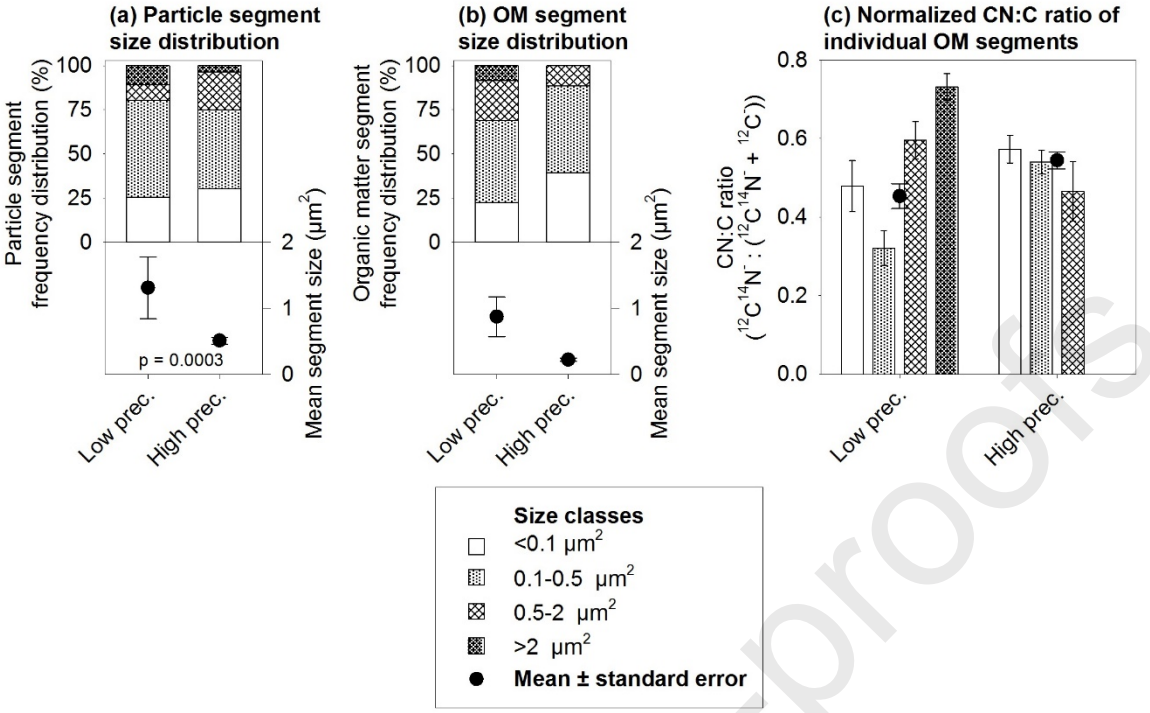

Figure A5 Microspatial properties in coarse clay fraction fractionated with NaCl. (**a,b**) Frequency distribution of various size classes and mean size of particles and OM segments (underlying numbers in Table A3). (**c**) Mean normalized CN:C ratio and means of various size classes within. The p-value is given in case of significant t-test.

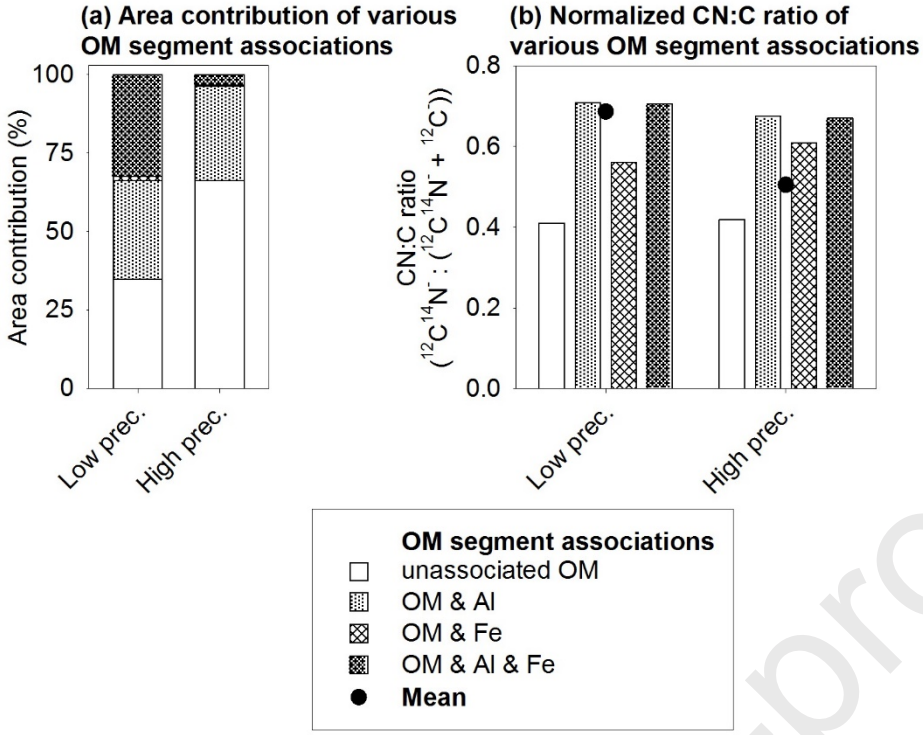

Figure A6 Microspatial properties in coarse clay fraction fractionated with NaCl. (**a**) Area contributions of OM segment associations according to the combined segmentations. (**b**) Mean CN:C ratio of all pixels of the various OM segment associations.S

Table A1: Normalized probability of X-ray absorbance (μ(E)) and first derivative of μ(E) descriptive data for soil samples (~2200 and ~2300 mm precipitation year^{-1}) and standard materials with a range of Fe oxidation state.

	Soil Samples		Fe^{3+} minerals		$Fe^{3+/2+}$ mineral	Fe^{2+} mineral	Fe^{3+}-organic complex		Fe^{2+}-organic
	~2200 mm precip	~2300 mm precip	Goethite	Ferrihydrite	Fe^{2+}-nontronite	Fayalite	Fe (III) citrate	Fe (III) EDTA	Fe (II) citrate
Edge (E_0) (eV)	7127	7127	7123	7127	7124	7123	7125	7126	7124
White line (eV)	7132	7132	7131	7133	7131	7127	7134	7134	7126
Pre-edge centroid (eV)	7115	7115	7114	7114	7113	7112	7114	7113	7113
7120.0 peak area (%)	0.23	8.81	3.17	1.28	22.1	63.13	11.81	7.57	39.43

Table A2 Overview on sample and area sizes of microscale investigations using NanoSIMS.

Precipitation	Dispersion	Number of NanoSIMS measurements	Total particle segment area (μm^2)	Total number of particles	Number of particles co-localized with OM	Total OM segment area (μm^2)	Total number of OM segments
Low	NaCl	5	107.5	82	54	62.1	71
High	NaCl	5	155.6	304	88	23.3	104
Low	H_2O	4	84.1	98	68	38.5	103
High	H_2O	4	114.0	235	49	25.5	58

Table A3: Overview on the number of segments in various size classes (Frequency distribution in 5 a,b).

Precipitation	Dispersion	Number of particle segments				Number of OM segments			
		0–0.1 μm^2	0.1–0.5 μm^2	0.5-2 μm^2	>2 μm^2	0–0.1 μm^2	0.1–0.5 μm^2	0.5-2 μm^2	>2 μm^2
Low	NaCl	21	45	7	9	16	33	16	6
High	NaCl	92	136	65	11	41	51	12	0
Low	H_2O	23	52	12	11	49	34	13	7
High	H_2O	83	112	30	10	26	25	5	2

Declaration of interests

☒ The authors declare that they have no known competing financial interests or personal relationships that could have appeared to influence the work reported in this paper.

☒The authors declare the following financial interests/personal relationships which may be considered as potential competing interests:

Thiago M. Inagaki* [a,d], Angela R. Possinger [b], Katherine E. Grant [c], Steffen A. Schweizer [a], Carsten W. Mueller [a], Louis A. Derry [c,d], Johannes Lehmann [b,d], Ingrid Kögel-Knabner [a,d].

*corresponding author: thiago.inagaki@wzw.tum.de

[a] Chair of Soil Science, Technical University of Munich, Emil-Ramann-Straße 2, Freising, Germany. 85354

[b] Soil and Crop Sciences, Cornell University, 909 Bradfield Hall, Ithaca NY, USA 14853

[c] Earth and Atmospheric Sciences, 4140 Snee Hall, Cornell University, Ithaca NY, USA 14853

[d] Institute for Advanced Study, Technical University of Munich, Lichtenbergstraße 2a Garching, Germany. 85748

Microscale distribution increases microbially derived C stabilization in soils♦

Inagaki, T. M., Possinger, A. R., Grant, K. E., Schweizer, S. A., Mueller, C. W., Derry, L. A., Kögel-Knabner, I., Lehmann J.

*corresponding author: thiago.inagaki@wzw.tum.de

[a] Chair of Soil Science, Technical University of Munich, Emil-Ramann-Straße 2, Freising, Germany. 85354

[b] Soil and Crop Sciences, Cornell University, 909 Bradfield Hall, Ithaca NY, USA 14853

[c] Earth and Atmospheric Sciences, 4140 Snee Hall, Cornell University, Ithaca NY, USA 14853

[d] Institute for Advanced Study, Technical University of Munich, Lichtenbergstraße 2a Garching, Germany. 85748

♦ to be submitted to Nature Geosciences

Organic matter (OM) association with minerals and occlusion in aggregates are thought to be the dominant mechanisms of C sequestration in soil, while the effect of spatial distribution of OM on its own is unclear. Here we use ^{13}C- and ^{15}N-labeled OM to assess the influence of the microscale spatial distribution of microbially-derived dissolved organic matter (DOM) and plant litter on SOC stabilization. We demonstrate that greater spatial distribution of DOM in a mineral-rich subsoil reduced SOC mineralization by 17% and increased the formation of mineral-associated OC by 10% compared to a point source DOM added as easily dissolvable pellets. The stabilization of microbially-derived DOM or plant litter in C-rich topsoil largely occurred without the influence of clay minerals, especially for distributed DOM. Fine-scale spatial analysis in the interior of sectioned macroaggregates from top- and subsoil demonstrated that the distributed DOM promoted 49% less aggregate occlusion than the point-source DOM. This demonstrates that commonly invoked aggregate occlusion may not be a major mechanism for stabilization of distributed DOM in soils. Here we demonstrate that the greater microscale spatial distribution of microbially-derived DOM significantly decreases SOC mineralization and increases sequestration rates.

Soil organic carbon (SOC) sequestration is of extreme importance for climate change mitigation, since soils represent the largest terrestrial C sink and have a recognized role in food production, water quality and biodiversity [1]. The long-term SOC stabilization has been primarily explained by interactions with soil minerals (i.e., organo-mineral interactions) and/or organic matter (OM) occlusion inside aggregates (i.e., soil aggregation)[2]. These processes are recognized to be mediated by microorganisms, reinforcing that the most persistent SOC first passes through microbial biomass [3]. For instance, microbially processed inputs such as leachates of dissolved organic matter (DOM) and rhizosphere exudates have been considered important SOC inputs in addition to plant litter [4, 5, 6]. The influence of the chemical composition of plant litter and DOM inputs has been well studied in soil systems[7, 8, 9]. Nonetheless, such OM inputs can have different spatial distribution ranging from being a point source (e.g., particulate organic matter and root exudates) to being evenly distributed (e.g., leachates) and it is unknown what effect spatial distribution of OM sources has on SOC stabilization.

Interactions of these OM inputs with minerals and microorganisms occur at small scales, as soils are recognized by their high spatial complexity at the nano and micrometer scales[10, 11]. It is recognized that substrate availability to microorganisms plays a key role in SOC turnover[12]. The search of soil microorganisms for food is characterized by a series of methods such as random walks[13] or shortest possible routes[14]. Therefore co-occurrence of substrate and microbes at the same location is considered an important pre-requisite for SOC microbial decomposition [15]. Point-source distribution of microbially-derived OM inputs could potentially favor microbial specialization on specific substrates, due to the higher concentration of a specific food source[16]. This fact could justify, for example, the high presence of fungal communities in root exudates[5]. On the other hand, associations with minerals and aggregates may be reduced when large amounts of OM are present due to C

saturation [17]. However, it remains unknown whether microscale spatial distribution of OM in general can significantly affect their mineralization and stabilization in soil. It is also not fully understood whether the effects of the spatial distribution are more influenced by mineral interactions or characteristics intrinsic to microbial ecology.

Here we investigate the effects of fine-scale spatial distribution of organic matter on its decomposition. We hypothesized that a more homogeneous distribution of organic substrate will decrease mineralization without the need to invoke mineral association. This effect would be enhanced by organo-mineral associations, and therefore more pronounced in soil horizons rich in clay minerals.

Greater fine-scale spatial distribution increases C sequestration in mineral rich soils

In the mineral-rich subsoil (Supplementary Fig. 1), greater spatial distribution of microbially-derived dissolved organic matter (DOM) on its own increased C sequestration in the heavy fraction (i.e., mineral-associated OM) from 36 to 46% of the total C added (Fig. 1a) and decreased cumulative respiration by 17% (Fig. 1b). The daily respiration rates of the distributed DOM were also delayed compared to the point-source DOM, with peak emissions occurring 72 hours later. During the peak respiration of the point-source DOM, respiration of the distributed DOM was 74% lower (Supplementary Fig. 2). The sequestration of the DOM (either point source or distributed) in the subsoil occurred almost entirely (more than 99% of the remaining C) as mineral associated organic matter in the heavy fraction rather than as free OM, demonstrating the capacity of these microbially processed materials to be stabilized in soils through organo-mineral associations.

We did not observe a significant influence of the spatial distribution (i.e., point source vs distributed DOM) on the sequestration and mineralization rates in the C-rich topsoil (Fig. 1c, Fig. 1d). The daily respiration rates of the added DOM in the

topsoil was highest during the second day of incubation and did not show any delay as observed in the subsoil (Supplementary Fig. 2). The cumulative respiration rates of the OM inputs were also significantly higher in the topsoil than in the subsoil (Supplementary Fig. 4). In contrast to the subsoil, most of the DOM irrespective of spatial distribution was sequestered in the light fraction of the topsoil. This demonstrates not only that the spatial distribution of the OM input has a less important influence on C sequestration in a C-rich topsoil with high contents of particulate organic matter isolates than in subsoils, but that the mechanism of retention differs, as well.

The significant effect of the spatial distribution of the microbially-derived DOM in the subsoil points towards a yet unrecognized factor affecting C sequestration and mineralization rates. Since the native SOC (nSOC) mineralization did not increase after addition of the DOM (Supplementary Fig. 3), substrate change (from C input to nSOC) was not the main mechanism responsible for the lower DOM mineralization[18] but rather lower availability to decomposers.

In Fig. 2, we outline the proposed mechanisms how micro-scale spatial distribution affects the mineralization and sequestration of the microbially-derived DOM. A greater respiration of the point source than the distributed DOM in the subsoil (Fig. 1) indicates that a spatially more concentrated DOM may facilitate the activity of decomposer microorganisms by creating suitable conditions for specialization on a specific substrate and the development of microbial colonies[16] (Mechanism 2, Fig 2). On the other hand, the distributed DOM may reduce the ability of the microorganisms to invest in metabolic strategies as also indicated by the delay in peak emissions (Supplementary Fig. 2) (Mechanism 1, Fig. 2). In addition, a greater adsorption of distributed than point source DOM plays a role, as the distributed DOM resulted in 46% of the total added OM sequestered in the heavy fraction against 36% of the point source DOM (Fig. 1).

Spatial distribution on its own plays a lesser role for mineralization and stabilization in C-rich topsoils

The plant-derived POM was retained 50% more and mineralized 49% less (subsoil) than microbially-derived OM in the topsoil, irrespective of being distributed or a point source (average of point source and distributed DOM) (Fig. 1c, Fig. 1d). Since the greatest amount of the point source POM was recovered in the light fraction, also in the subsoil samples, it implies that the remaining POM was mostly composed of undecomposed plant litter remains. This is also observed through the similar organic matter composition of the light-fraction SOC and the added plant-derived POM obtained by nuclear magnetic resonance spectroscopy (NMR) (Supplementary Fig. 5). It is not clear how much the observed difference in chemical composition played a role in explaining the differences in mineralization between the POM and DOM. Clearly, such differences in composition and the very high solubility of the studied DOM in water with sizes of less than 0.7 µm contribute to their overall larger mineralization rates compared to the point-source POM in addition to spatial distribution alone. These differences in composition and solubility may play an important role when considering, for example, the point-source input of root exudates in the rhizosphere in comparison to particulate inputs from root turnover[19], or DOM leachates from the litter layer[4] in comparison to litter debris[7].

In the topsoil, we did neither find an effect of the spatial distribution of DOM on mineralization (Fig. 1d) nor an effect of point-source POM vs DOM on organo-mineral stabilization as shown by the similar recovery in the heavy fraction (Fig. 1c), as we observed in the subsoil (Fig. 1a, 1b). This demonstrates that the spatial distribution played a more important role in the mineral-rich subsoil, than in the C-rich topsoil. Since the differences between the point source POM and the microbially-derived DOM were also more pronounced in the subsoil, the evaluation of spatial distribution

and plant vs microbial inputs may be of greater importance for belowground inputs such as root system, rather than aboveground inputs as plant litter.

Aggregate occlusion as a mechanism for OM protection

The more than 80% of the total topsoil C recovered as what is traditionally interpreted as occluded particulate organic matter [20] (Supplementary Fig. 1), would suggest aggregate occlusion as a major mechanism for C stabilization. This is supported by the with up to 55% of added OM recovered in the topsoil light fraction, even with addition of DOM (Fig. 1a, 1c). However, a 3-dimensional assessment of the C distribution using EDX with successive sectioning of a topsoil microaggregate (~20µm) using cryogenic focused ion beam (cryo-FIB) revealed only small concentrations of occluded C in the interior of the aggregate compared to the external surface (Fig. 3). Because of the low abundance of directly observed particles inside the aggregate, we cannot confirm that the light fraction is mainly composed of occluded particulate organic matter and thereby protected by aggregation. Therefore, interactions of DOM with organic matter via metal bridging or intercalation of organic matter with SROs across a continuum of sizes may explain the large amounts of SOC in the studied topsoils.

The high C concentration of the light fraction (higher than 400 mg g^{-1} - Supplementary Fig. 1) indicates low presence of minerals[21], and SEM observations of this fraction revealed the predominance of amorphous organic matter, fungal hyphae and plant structures, likely derived from the decay of plant detritus (Supplementary Fig. 6). Although these light fractions in soils are considered as an important pathway for C stabilization, mainly due to their role as a source of microorganisms[22], their turnover time is short compared to the mineral associated fraction[21]. Therefore, the added DOM and POM recovered in the light fraction of the topsoil would likely be transformed into a form that may be stabilized by minerals and

therefore recovered in the heavy fraction in a longer term, or mineralized and released to the atmosphere as CO_2.

Fine-scale spatial analysis in the interior of cross-sectioned macroaggregates using Nano-SIMS revealed that the added distributed DOM was less occluded than the point source DOM and POM, observed by the ^{15}N enrichment (Fig. 4). This indicates that aggregate occlusion may be a less relevant stabilization mechanism for distributed sources of OM but more important for point source inputs. Our results suggest that the distributed arrangement would favor an immediate mineral adsorption in the external surface of soil particles rather than being occluded inside aggregates (Mechanism 2, Fig. 2). On the other hand, the point source spatial arrangement would facilitate the diffusion of the DOM through the soil pore system, facilitating aggregate occlusion (Mechanism 1, Fig. 2).

In summary, here we demonstrated that micro-scale spatial distribution of microbially-derived DOM plays a fundamental role in SOC mineralization and sequestration rates. This yet unrecognized influence could be of great importance for SOC models especially regarding belowground inputs.

References

1. Vermeulen S, Bossio D, Lehmann J, Luu P, Paustian K, Webb C*, et al.* A global agenda for collective action on soil carbon. *Nature Sustainability* 2019, **2**(1)**:** 2.

2. Lehmann J, Kleber M. The contentious nature of soil organic matter. *Nature* 2015, **528**(7580)**:** 60-68.

3. Liang C, Amelung W, Lehmann J, Kästner M. Quantitative assessment of microbial necromass contribution to soil organic matter. *Global change biology* 2019.

4. Marin-Spiotta E, Chadwick OA, Kramer M, Carbone MS. Carbon delivery to deep mineral horizons in Hawaiian rain forest soils. *Journal of Geophysical Research: Biogeosciences* 2011, **116**(G3).

5. Baumert VL, Vasilyeva N, Vladimirov A, Meier IC, Kögel-Knabner I, Mueller CW. Root exudates induce soil macroaggregation facilitated by fungi in subsoil. *Frontiers in Environmental Science* 2018, **6:** 140.

6. Castellano MJ, Mueller KE, Olk DC, Sawyer JE, Six J. Integrating plant litter quality, soil organic matter stabilization, and the carbon saturation concept. *Global change biology* 2015, **21**(9)**:** 3200-3209.

7. Mitchell E, Scheer C, Rowlings D, Conant RT, Cotrufo MF, Grace P. Amount and incorporation of plant residue inputs modify residue stabilisation dynamics in soil organic matter fractions. *Agriculture, ecosystems & environment* 2018, **256:** 82-91.

8. Cotrufo MF, Soong JL, Horton AJ, Campbell EE, Haddix ML, Wall DH*, et al.* Formation of soil organic matter via biochemical and physical pathways of litter mass loss. *Nature Geoscience* 2015, **8**(10)**:** ngeo2520.

9. Buettner SW, Kramer MG, Chadwick OA, Thompson A. Mobilization of colloidal carbon during iron reduction in basaltic soils. *Geoderma* 2014, **221:** 139-145.

10. Lehmann J, Solomon D, Kinyangi J, Dathe L, Wirick S, Jacobsen C. Spatial complexity of soil organic matter forms at nanometre scales. *Nature Geoscience* 2008, **1**(4)**:** 238-242.

11. Steffens M, Rogge DM, Mueller CW, Hoschen C, Lugmeier J, Kolbl A*, et al.* Identification of Distinct Functional Microstructural Domains Controlling C Storage in Soil. *Environ Sci Technol* 2017, **51**(21)**:** 12182-12189.

12. Blagodatsky S, Richter O. Microbial growth in soil and nitrogen turnover: a theoretical model considering the activity state of microorganisms. *Soil Biology and Biochemistry* 1998, **30**(13)**:** 1743-1755.

13. Van Haastert PJ, Bosgraaf L. Food searching strategy of amoeboid cells by starvation induced run length extension. *PloS one* 2009, **4**(8)**:** e6814.

14. Reynolds AM, Dutta TK, Curtis RH, Powers SJ, Gaur HS, Kerry BR. Chemotaxis can take plant-parasitic nematodes to the source of a chemo-attractant via the shortest possible routes. *Journal of the Royal Society Interface* 2010, **8**(57)**:** 568-577.

15. Dungait JA, Hopkins DW, Gregory AS, Whitmore AP. Soil organic matter turnover is governed by accessibility not recalcitrance. *Global Change Biology* 2012, **18**(6)**:** 1781-1796.

16. Dechesne A, Pallud C, Grundmann GL. Spatial distribution of bacteria at the microscale in soil. *the Spatial Distribution of Microbes in the Environment* 2007**:** 87-107.

17. Six J, Conant RT, Paul EA, Paustian K. Stabilization mechanisms of soil organic matter: Implications for C-saturation of soils. *Plant and Soil* 2002, **241**(2)**:** 155-176.

18. Kuzyakov Y, Ehrensberger H, Stahr K. Carbon partitioning and below-ground translocation by Lolium perenne. *Soil Biol Biochem* 2001, **33**(1)**:** 61-74.

19. Almeida LF, Hurtarte LC, Souza IF, Soares EM, Vergütz L, Silva IR. Soil organic matter formation as affected by eucalypt litter biochemistry—Evidence from an incubation study. *Geoderma* 2018, **312:** 121-129.

20. Golchin A, Oades J, Skjemstad J, Clarke P. Study of free and occluded particulate organic matter in soils by solid state 13C CP/MAS NMR spectroscopy and scanning electron microscopy. *Soil Research* 1994, **32**(2)**:** 285-309.

21. Wagai R, Mayer LM, Kitayama K. Nature of the "occluded" low-density fraction in soil organic matter studies: a critical review. *Soil Science and Plant Nutrition* 2009, **55**(1)**:** 13-25.

22. Angst G, Mueller CW, Prater I, Angst Š, Frouz J, Jílková V*, et al.* Earthworms act as biochemical reactors to convert labile plant compounds into stabilized soil microbial necromass. *Communications Biology* 2019, **2**.

23. DeCiucies S, Whitman T, Woolf D, Enders A, Lehmann J. Priming mechanisms with additions of pyrogenic organic matter to soil. *Geochimica et Cosmochimica Acta* 2018, **238:** 329-342.

24. Golchin A, Oades JM, Skjemstad JO, Clarke P. Soil-Structure and Carbon Cycling. *Aust J Soil Res* 1994, **32**(5)**:** 1043-1068.

25. Silva JHS, Deenik JL, Yost RS, Bruland GL, Crow SE. Improving clay content measurement in oxidic and volcanic ash soils of Hawaii by increasing dispersant concentration and ultrasonic energy levels. *Geoderma* 2015, **237:** 211-223.

26. Mehra O, Jackson M. Iron oxide removal from soils and clays by a dithionite-citrate system buffered with sodium bicarbonate. National conference on clays and clays minerals; 1958; 1958. p. 317-327.

27. Lavkulich L. Methods manual, pedology laboratory. *Vancouver, BC, CA: University of British Columbia, Department of Soil Science* 1981.

28. Knicker H, Lüdemann HD. N-15 and C-13 Cpmas and Solution Nmr-Studies of N-15 Enriched Plant-Material during 600 Days of Microbial-Degradation. *Organic Geochemistry* 1995, **23**(4)**:** 329-341.

29. Mueller CW, Weber PK, Kilburn MR, Hoeschen C, Kleber M, Pett-Ridge J. Advances in the Analysis of Biogeochemical Interfaces: NanoSIMS to Investigate Soil Microenvironments. *Adv Agron* 2013, **121**(1)**:** 1-46.

30. Abràmoff MD, Magalhães PJ, Ram SJ. Image processing with ImageJ. *Biophotonics international* 2004, **11**(7)**:** 36-42.

Material and methods

Soil samples and incubation design

We have used two Andosol samples from top (0 – 0.2 m) and subsoil (0.8 – 0.9) depths for this study. The samples were collected in a mixed fern vegetation (hapu'u - *Cybotium spp.*- and uluhe – *Dicronopteris linearis* Burm.) at the Kohala region – Hawaii (20°4'14.16"N, 155°43'21.94"E). The soil is characterized as volcanic Andosol derived from alkalic lavas of the 350 ka Pololu basalt that likely also received ash deposition from the younger (150 ka) Hawi basalt series (Wolfe and Morris, 1996). In order to maintain field-moist conditions, we kept the samples in boxes with ice bags while they were transported to the laboratory and stored in climate-controlled rooms at 4ºC.

The incubation experiment consisted in a completely randomized design with three replicates. We used soil samples from two depths: 0 – 0.2 m and 0.8 – 0.9 m. For each depth, we added ^{13}C and ^{15}N labelled amendments as follow: 1) control: incubated soil without amendment; 2) willow leaves (*Salix viminalis x S.miyabeana*); dissolved organic carbon (DOC) in two different forms: 3) point source (1 – 2 mm size pellets); and 4) distributed (colloidal particles filtered at 0.7 µm) (Supplementary Fig. 7, Supplementary Table 2).

The ^{13}C labelled DOC was extracted from shrub willow leaves enriched with $^{13}CO_2$ (the same used in the experiment as amendment). A detailed description of the plant cultivation can be found in DeCiucies, Whitman [23]. Briefly, the willow leaves were sieved with a 2 mm sieve and shaken in deionized water (leaves/water proportion of 1:10) during 72h at 32ºC with an orbital shaker at 100 rpm. After the shaking period, the suspension was filtered with a Whatman glass microfiber filter of 0.7 µm. The solution that passed through the filter was then freeze-dried.

For producing the point source DOC form, we have pressed the freeze-dried DOC using a hydraulic press to form solid pieces. Then, we have cracked the compressed material into 1 – 2 mm pieces and used them for the incubation. For the dissolved form, we simply dissolved the freeze-dried DOC into deionized water and used them as amendments for the incubation. We have also incubated the willow leaves used for producing the DOC as a reference. The ^{13}C enrichment levels of the amendments were 1.82, 1.77 and 1.77 atom percentage for the treatments leaves, point source DOC and distributed DOC, respectively. The ^{15}N enrichment levels were 8.07, 7.59 and 7.62 atom percentage for the leaves, point source DOC and distributed DOC, respectively.

For the incubation, we standardized the amendments inputs to 10 mg C g soil^{-1}. All the soil + amendment samples were maintained at 50% of water hold capacity. The samples were added to 60 ml Qorpak bottles with 3 g of soil + amendment mixture. The Qorpak bottle was placed in a 1 L Mason jar containing 30 ml of water to maintain 100% humidity. All the samples were incubated during 50 days. We have used a Picarro CO_2 stable isotope analyzer (G2201-I, Santa Clara, CA, USA) to monitor continuously the incubation. The headspace gas of each jar was sampled for 6 min during each sampling period, and in sequence purged with CO_2-free air. We collected the data at a rate of two measurements per second over the sampling time, and during the sample purge to record the baseline values before each cycle's respiration measurement.

The soils were incubated and the emitted CO_2 was measured during 50 days. After the incubation period, the soils were air-dried and submitted to soil organic matter fractionation.

Samples characterizations and soil organic matter fractionation

Top and subsoil samples characterization

Before working with the incubated samples, we performed soil organic matter fractionation of control samples from top and subsoil layers used as the base of this experiment. The procedure was adapted from the method of Golchin, Oades [24]. Briefly, the soil was mixed in a proportion of 1 : 2.5 (soil/solution) with a dense solution of sodium politungstate 1.8 g cm^{-3}. After an overnight standing, we separated the floating free particulate organic matter (fPOM) using an electrical pump.

The soil suspension was then sonicated with an energy input of 1500 J ml^{-1} using an ultrasonic disperser (SonopulsHD2200, Bandelin, Berlin – Germany). The chosen energy level is considered sufficient for providing dispersion of the highly stable Andosol microaggregates without causing damage to the primary mineral structure [25]. After the sonication, the soil suspension was centrifuged (8,500 g, 40 min) and the floating occluded particulate organic matter (oPOM) was separated using an electrical pump.

The mineral soil at the bottom of the centrifuge tube was then sieved using a 20 µm mesh size sieve so separate sand and coarse silt fraction. The soil that passes through the sieve was then subjected to sedimentation and divided into two size fractions of 20 - 2 µm and < 2 µm. All the fractions were rinsed until the electrical conductivity dropped 10 µS cm^{-1} and freeze-dried. The C and N contents were measured by dry combustion using a CN elemental analyzer (CHNSO Elemental Analyzer, Hekatech, Wegberg – Germany).

The fractionation revealed that topsoil samples were composed by approximately 80% of particulate organic matter (fPOM and oPOM), while the subsoil were composed by approximately 95% of mineral soil (20 – 2 and < 2 µm). The sand and coarse silt fraction was present in a low amount (less than 1% of total C) in both depths (Supplementary Fig. 1).

We have also performed Fe and Al extractions using dithionite citrate bicarbonate (DCB) and ammonium oxalate (OX) in parallel samples using the

methods described by and Mehra and Jackson [26], respectively. We measured soil pH on 0.01 M $CaCl_2$ using a pH meter (Orion Star A111, ThermoFisher Scientific, Waltham – MA, USA) and exchangeable Ca, Mg, and K using the NH_4OAc method at pH 7[27]. All the extracted elements were measured by inductively coupled plasma optical emission spectroscopy (ICP-OES) (Vista-Pro CCD simultaneous, Varian, Darmstadt - Germany). The soil properties of the top and subsoil samples used in the experiment are described on Supplementary Table 3.

Soil organic matter fractionation of the incubated samples

Because the previous fractionation procedure revealed a clear separation between particulate organic matter (mainly composed by oPOM) and mineral soil (mainly composed by < 2 µm clay), we separated the incubated samples into only two fractions, here denominated “light” (i.e., fPOM + oPOM) and “heavy” (20 – 2 + < 2 µm) fractions. The samples were fractionated using the same procedure described previously. However, the fPOM and oPOM fractions were merged and the mineral fraction was not submitted to sedimentation to be separated into 20-2 and < 2 µm fractions.

Soil organic matter characterization by ^{13}C CP/MAS NMR spectroscopy

The light and heavy fraction of control top and subsoil samples used for the incubation experiment as well as the leaves and the DOM amendments were analyzed by ^{13}C CP/MAS NMR spectroscopy (Biospin DSX 200 NMR spectrometer, Bruker, Rheinstetten, Germany) for organic matter characterization. We have used a contact time of 0.001 sec with a pulse delay of 0.4 sec for the heavy fraction and 1 sec for the light fraction. At least 100,000 accumulated scans were performed to obtain a well-resolved spectrum. The spectra were integrated using four major chemical shift regions: 0 to 45 ppm (alkyl-C), 45 to 110 ppm (O/N-alkyl-C), 110 to 160

(aryl-C), and 160 to 220 ppm (carboxyl-C) [28]. Despite the elevated Fe content of the heavy fraction, it was not necessary to perform a pre-treatment with hydrofluoric acid to obtain a well-resolved spectrum.

Aggregate cross sectioning and NanoSIMS analysis

In order to evaluate the presence of input derived OM inside aggregates, we performed cross sectioning of soil macroaggregates according to the method described by Mueller, Weber [29]. Briefly, we have randomly selected macroaggregates of approximately 2 mm size, embedded them in epoxy resin, polished them down until approximately half and performed the nanoscale secondary ion mass spectrometry (NanoSIMS) analysis in their interior. We hypothesized that infiltration through the soil pore system would be the main pathway of organic matter entrance into the soil macroaggregates. Therefore, we have aimed at the interfaces of the pore system (i.e., the space through which the resin has infiltrated during the embedding) and the soil structure. We have made four measurement in two macroaggregates for each treatment in top and subsoil samples, looking for “hot-spots” of $^{12}C^{15}N$ enrichment (Fig. 4). By calculating the $^{12}C^{15}N$ / $^{12}C^{14}N$ ratio of the enriched areas, we were able to measure the presence of amendment derived N-rich organic matter in the soil pore system interfaces. Measurements were processed using the ImageJ software[30].

FIB-SEM analysis

Scanning electron microscopic (SEM) analyses with cryo-sectioning were performed using a Focused ion beam (FIB-SEM) model FEI Strata 400 STEM FIB (Thermo Fisher Scientific, Waltham, Massachusetts, U.S.). Images were made by a primary beam operated at a landing energy of 5 KeV. Microaggregates were separates by dry sieving with a 53 µm sieve. A microaggregate of ~20µm diameter was sectioned into

1 µm-thick cross-sections using a cryo-ultramicrotome equipped with a diamond blade (Leica EM UC7/FC7, Leica Microsystems, Inc., Buffalo Grove, IL). Cryo-ultramicrotome thinning was performed at -60°C using a step size of 1000 nm, and thin sections were transferred to an adhesive-coated copper (Cu) TEM grid (300 or 400-mesh) and stored in cryo-TEM grid boxes under liquid N_2. Milling was completed at an ion beam voltage of 30 kV with varying current (between approximately 5 pA and 500 pA).

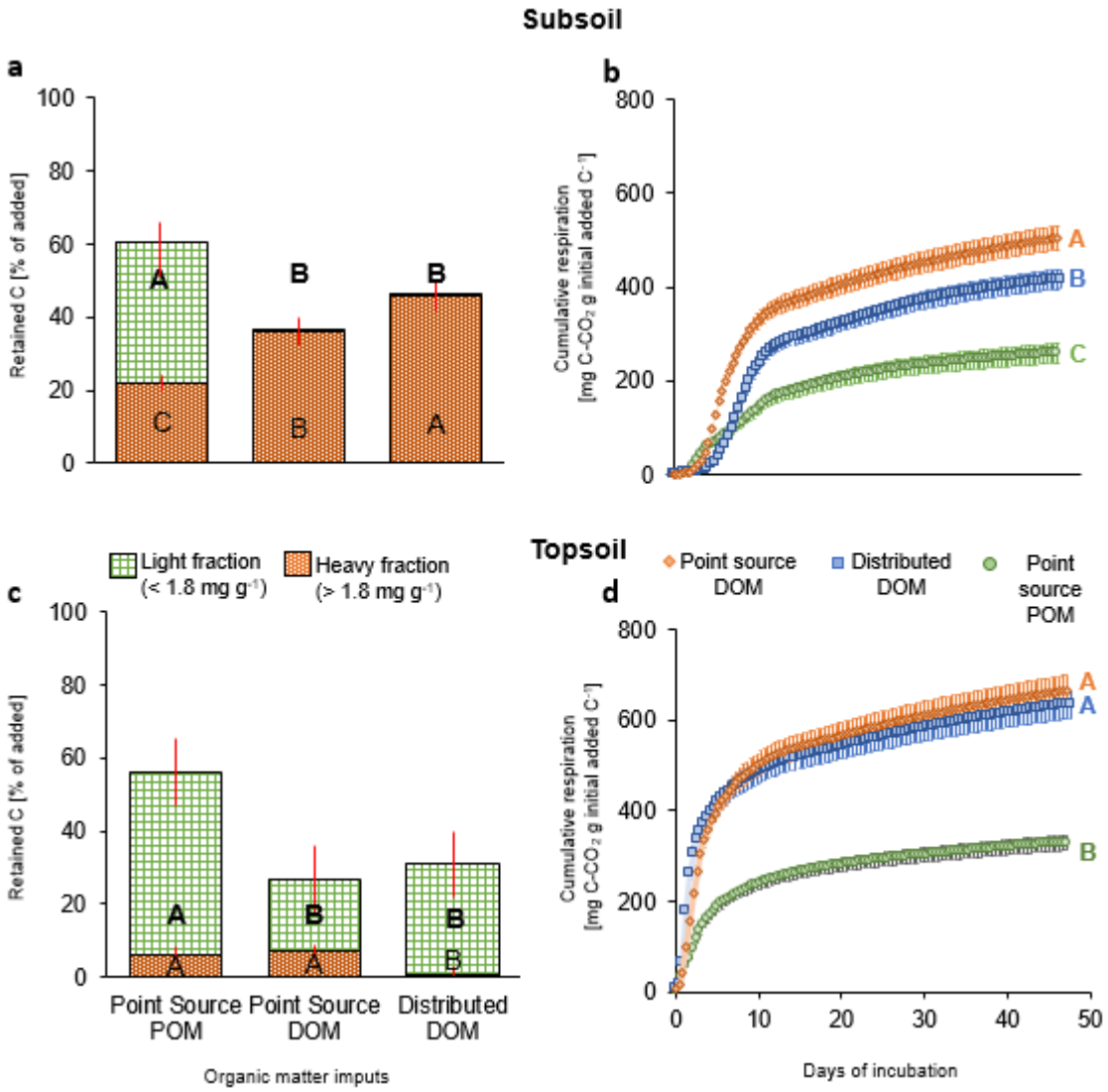

Fig. 1: **Soil organic carbon (SOC) stabilization and mineralization in top and subsoil. b, d:** cumulative respiration rates of the amendment derived C-CO_2 during the 50 days of incubation in topsoil (0 – 0.2 m) and subsoil (0.8 – 0.9 m) samples. For a given depth, cumulative respiration rates followed by the same letter do not differ among amendments at $p < 0.05$ (LSD test) **a, c:** Partitioning of the litter derived C among soil organic matter density fractions: heavy fraction (> 1.8 g cm^{-3}) and light fraction (< 1.8 g cm-3). For a given fraction, means followed by the same letter do not differ among amendments at $p < 0.05$ (LSD test).

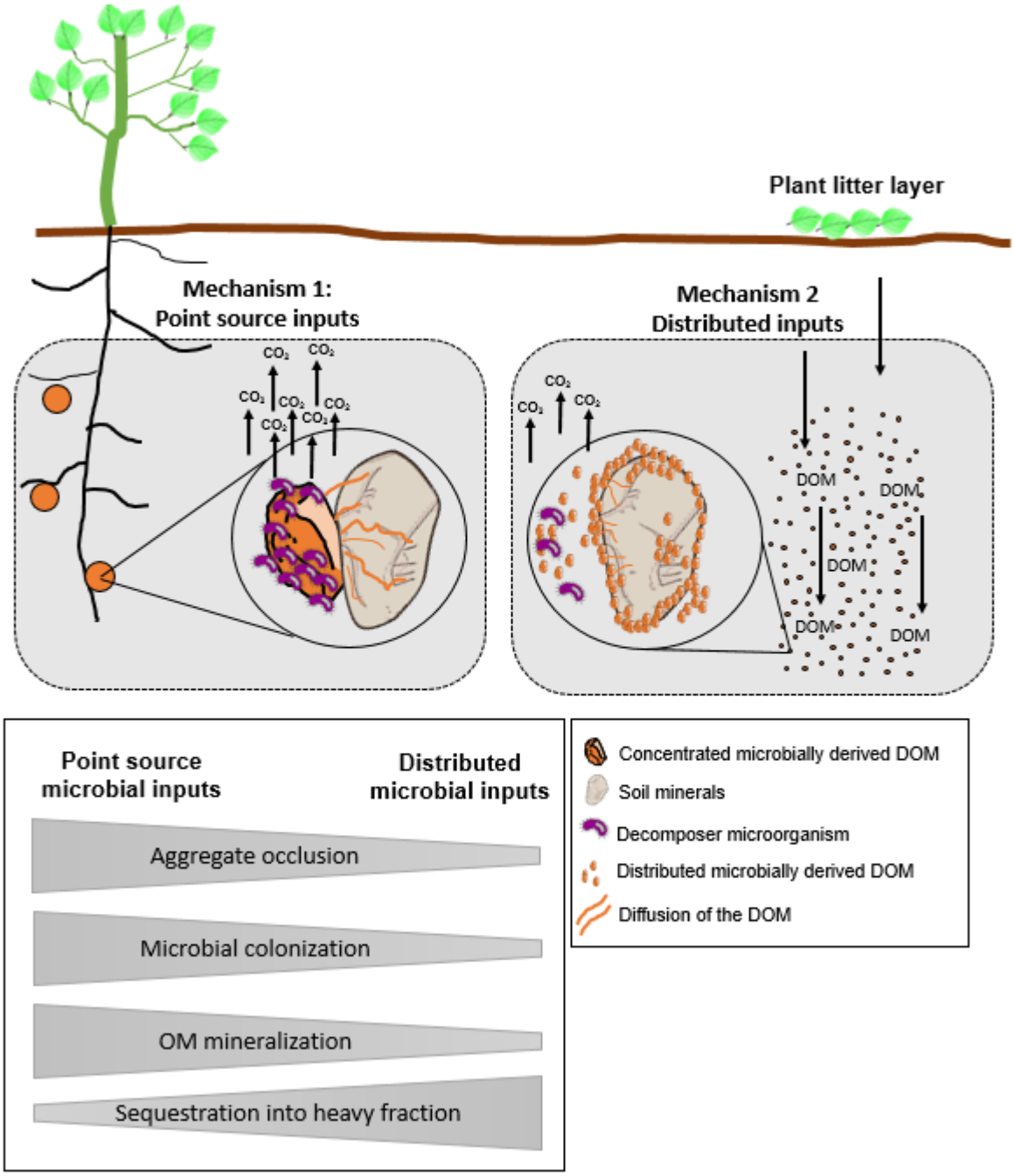

Fig. 2: **Proposed mechanisms for mineralization and stabilization of point source and distributed inputs of organic matter**. The Figure illustrates the colonization of the material by decomposing microorganisms, C sequestration through mineral interactions and the infiltration through the macroaggregates pore system.

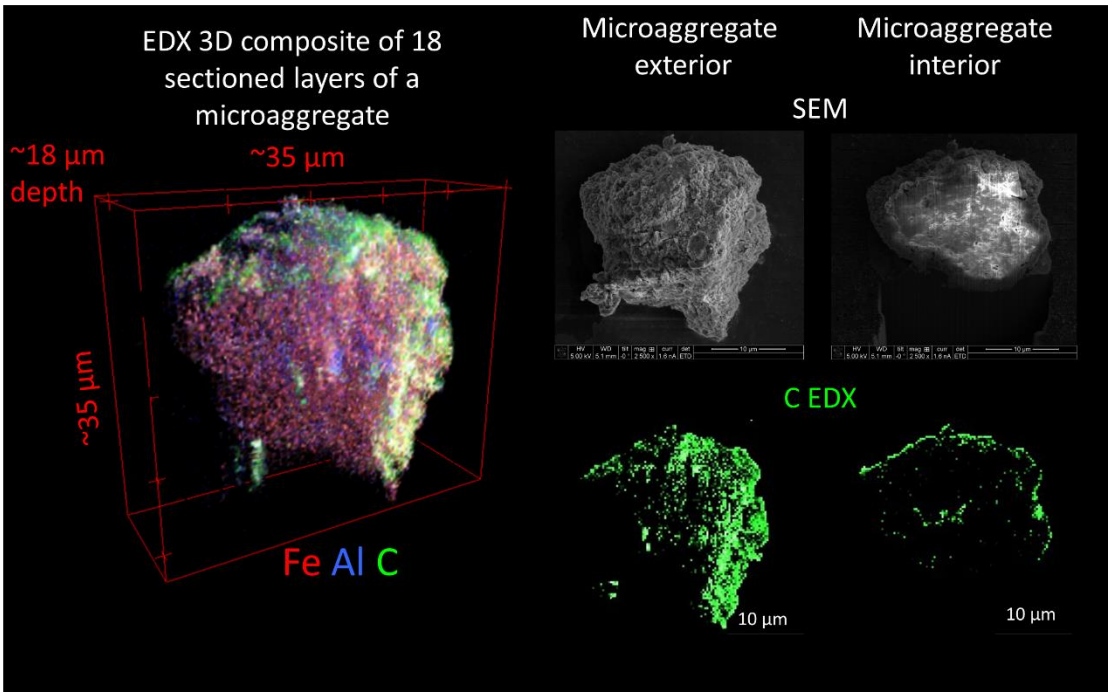

Fig. 3: **Observation of occluded particulate organic matter inside a topsoil microaggregate**. Composite 3D image showing the Fe, Al and C across a sectioned topsoil microaggregate; C contents measured by energy-dispersive X-ray spectroscopy (EDX) demonstrate that the majority of the C content was found in the exterior of the microaggregate rather than occluded in its interior. A fully animated version of the 3D image is available in supplementary materials.

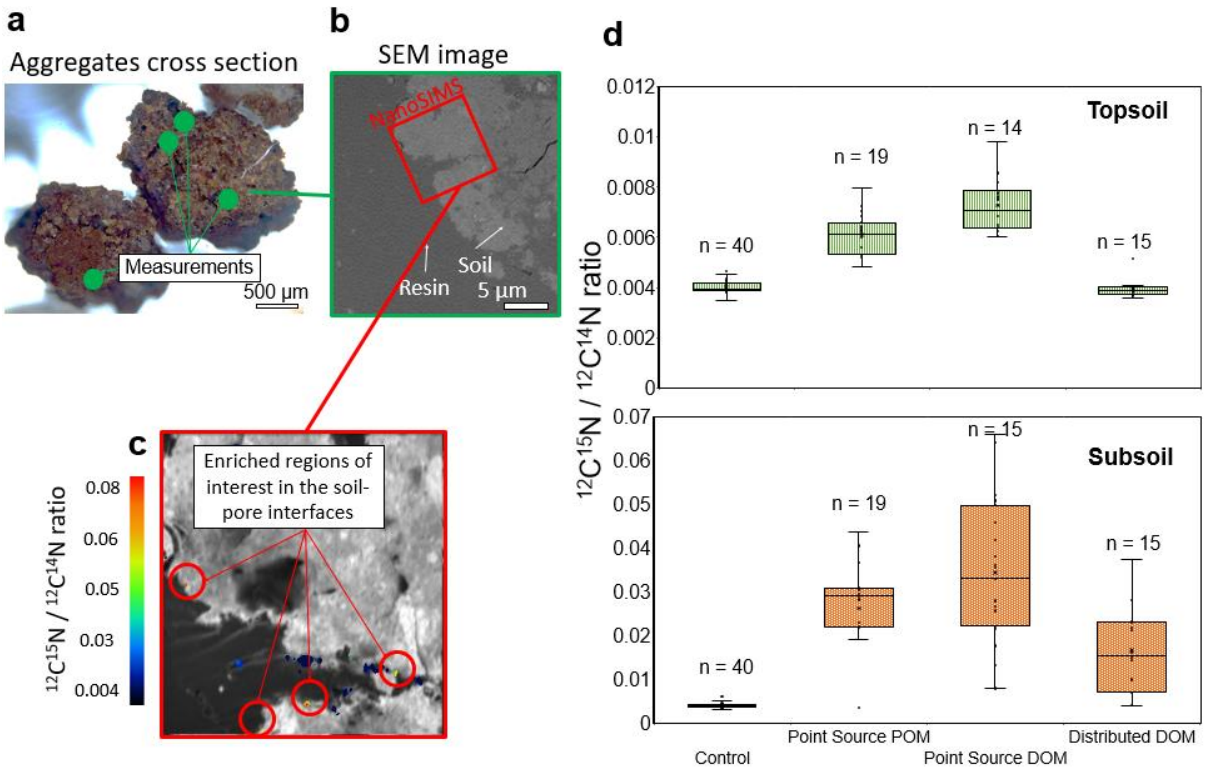

Fig. 4: **Aggregate occlusion of the added organic matter inputs in top and subsoil**. **a:** Reflected light microscopy image of aggregate cross sections from a subsoil. **b:** Scanning electron microscopy (SEM) images showing an overview of the soil pore system interfaces: the light gray colors show the soil structures whereas the darker gray colors show the space through which the resin has infiltrated during the embedding process. **c:** NanoSIMS measurements of the $^{12}C^{15}N$ /$^{12}C^{14}N$ ratios overlaying the $^{16}O^-$ secondary ion signal. The white colors shows the mineral particles and the dark gray the pore system (resin). The color bars on the right shows the $^{12}C^{15}N$ enrichment level, in which 0.004 is the natural abundance. **d:** Box plots of the $^{12}C^{15}N$ / $^{12}C^{14}N$ ratio obtained from NanoSIMS measurements by analyzing the regions of interest (ROI). Control samples were incubated without labeled amendments. n represents the number of ROI's. Boxplots represent the third quartile, the median, the first quartile range of the data, and data outliers.

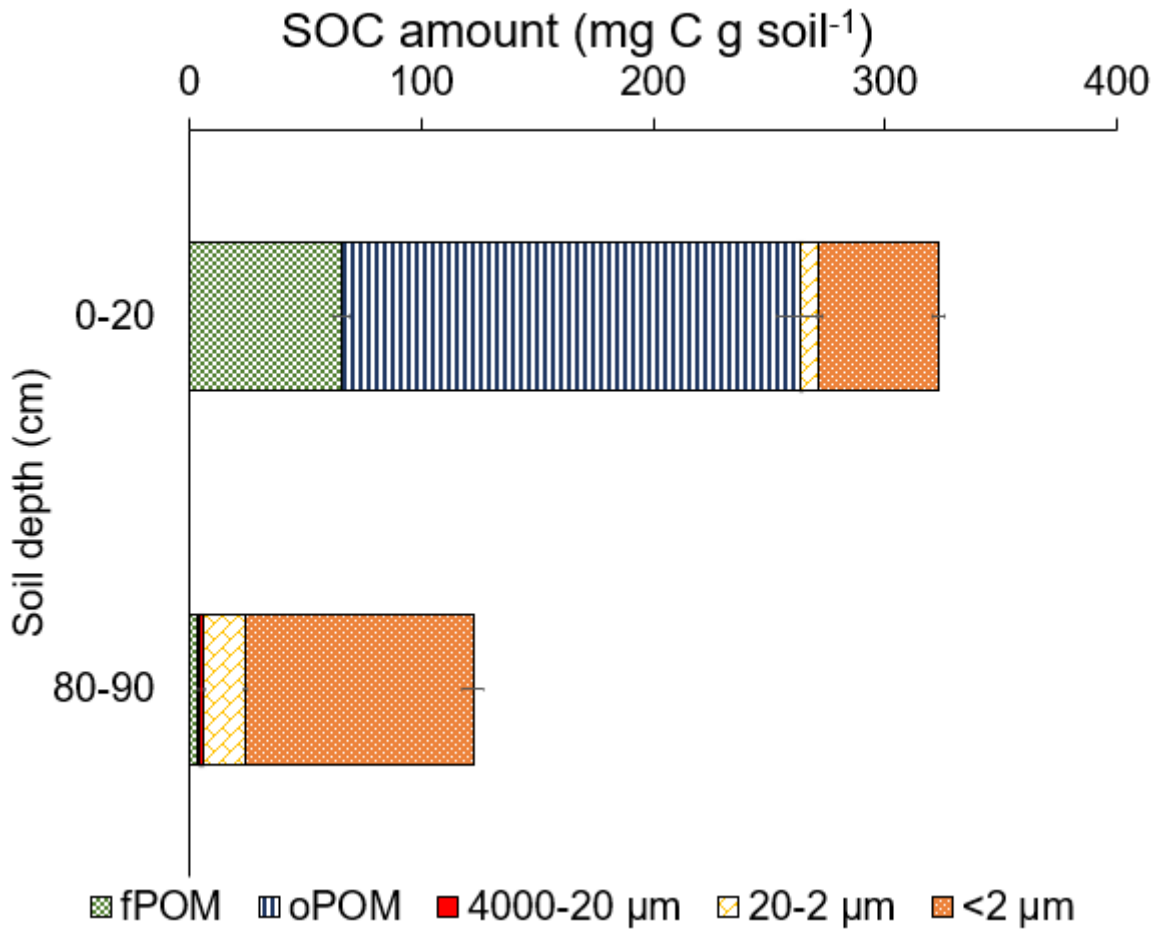

Supplementary Fig. 1: Soil organic matter fractions of the top and subsoil samples used in the experiment. fPOM = free particulate organic matter; oPOM = occluded particulate organic matter.

Supplementary Table 1: Soil organic carbon (SOC) and N concentrations, and CN ratio of each fraction displayed in Supplementary Fig 1 from top and subsoil samples used in the experiment.

SOC fraction	SOC concentration (g kg-1)	N concentration (g kg-1)	CN ratio
		Topsoil (0 - 20 cm)	
fPOM	395.57	11.52	34.34
oPOM	417.72	14.21	29.40
>20µm	72.35	2.83	25.57
20-2µm	71.34	3.9	18.29
<2µm	207.75	10.62	19.56
		Subsoil (80-90 cm)	
fPOM	345.20	12.95	26.66
oPOM	76.15	3.38	22.53
>20µm	73.27	2.14	34.24
20-2µm	71.27	2.18	32.69
<2µm	112.41	3.46	32.49

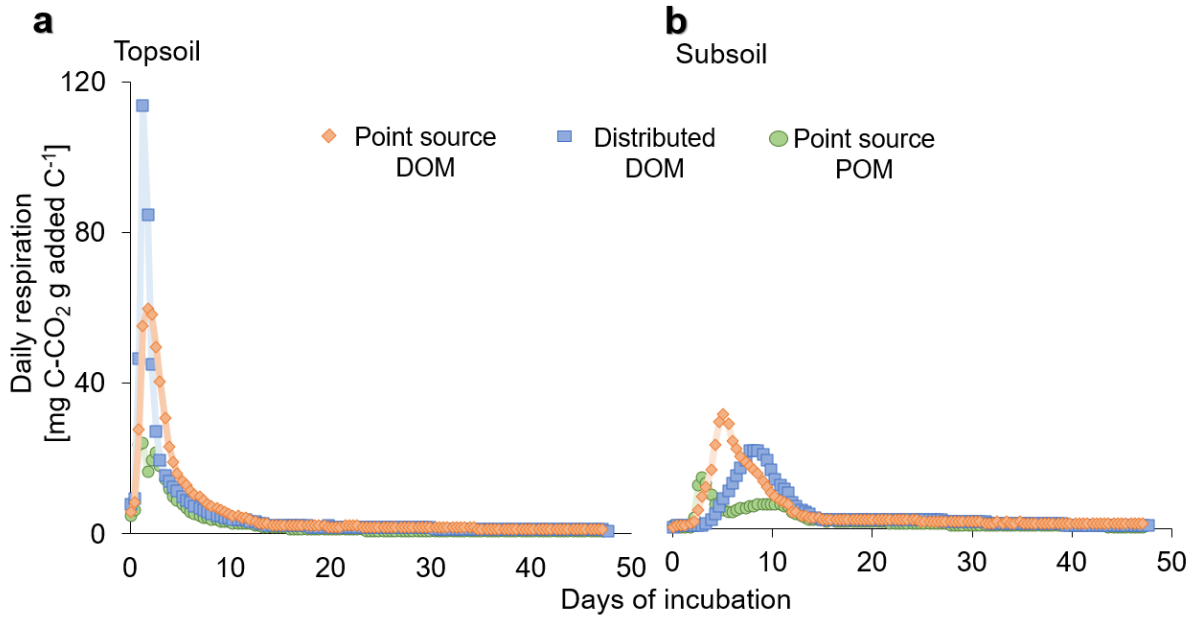

Supplementary Fig. 2: Daily respiration rates of the amendment derived C-CO_2 during the 50 days of incubation in topsoil (0 – 0.2 m) and subsoil (0.8 – 0.9 m) samples.

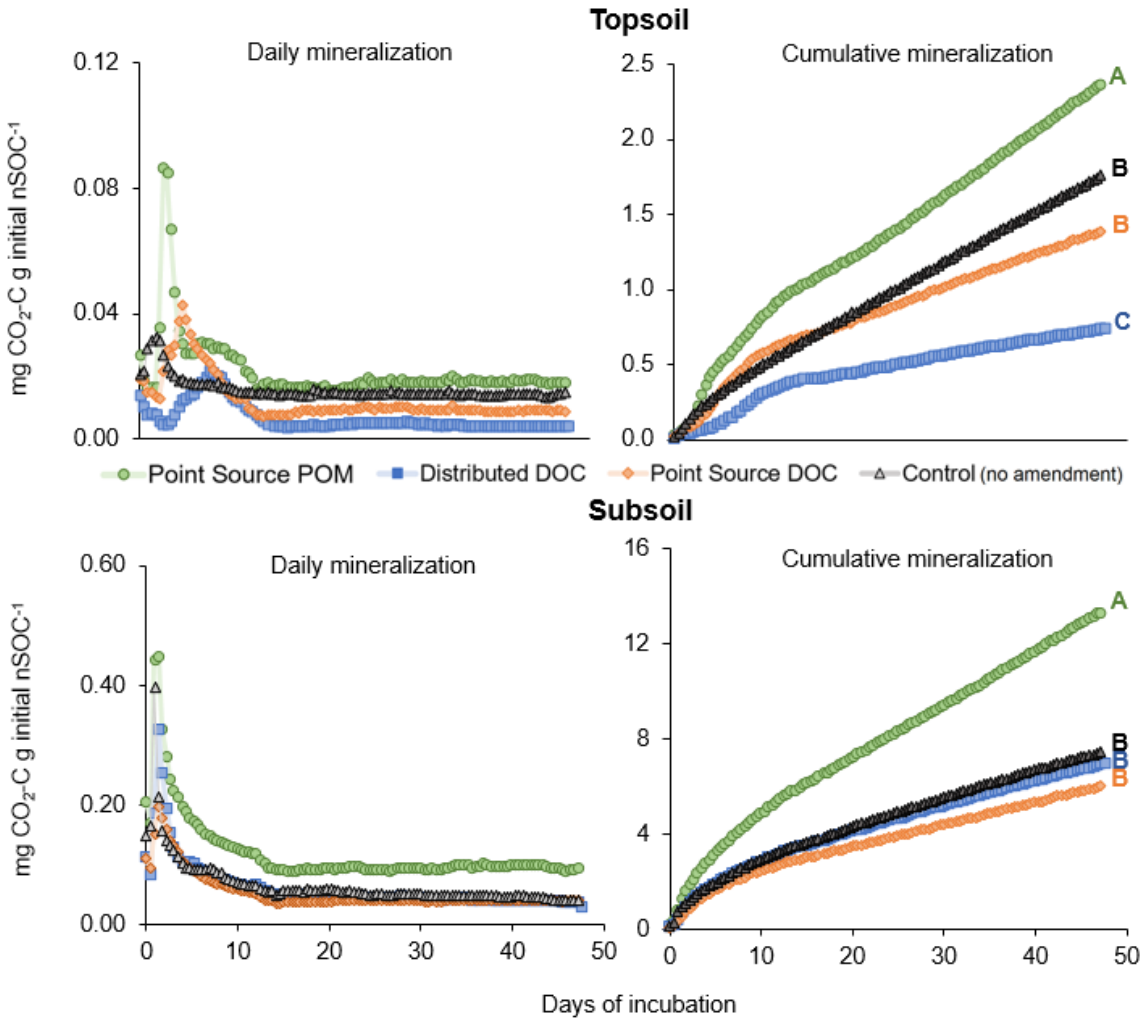

Supplementary Fig. 3: Daily and cumulative mineralization rates of the native soil organic carbon (nSOC) C-CO_2 during the 50 days of incubation in topsoil (0 – 0.2 m) and subsoil (0.8 – 0.9 m) samples.

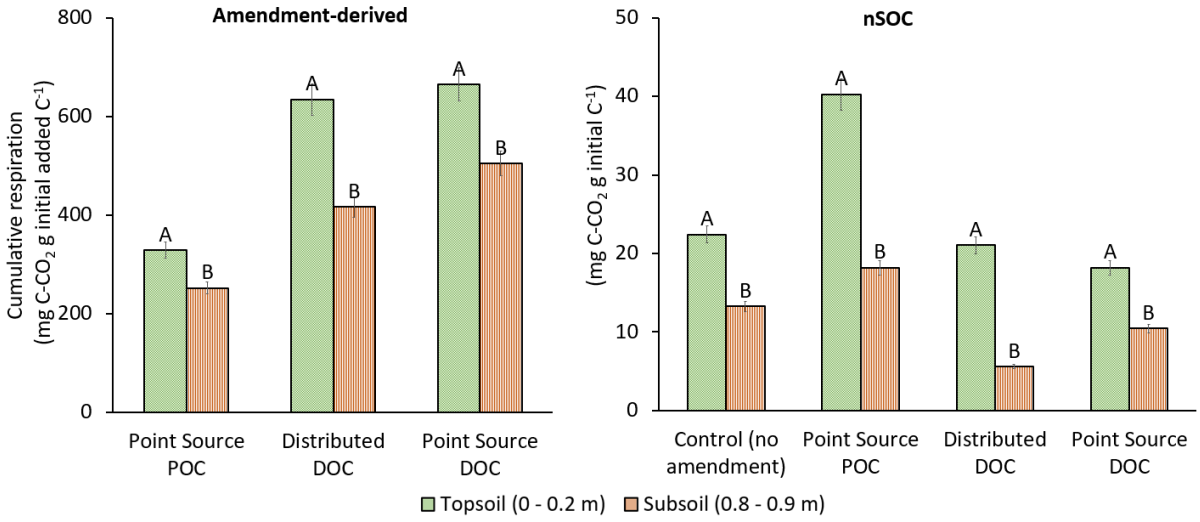

Supplementary Fig. 4: Cumulative amendment derived and native C-CO_2 respiration (nSOC) after 50 days of incubation in top and subsoil samples. For a given treatment, means followed by different letters differ between depths at $p < 0.05$ (LSD test).

Topsoil

Group	Topsoil (0-0.2 m)	
	Light fraction	Heavy fraction
Carboxylic-C	6.82	15.63
Aromatic-C	17.30	16.72
O/N Alkyl-C	46.94	32.91
Alkyl-C	38.45	34.73

Subsoil

Group	Subsoil (0.8-0.9 m)	
	Light fraction	Heavy fraction
Carboxylic-C	10.89	18.26
Aromatic-C	24.37	11.99
O/N Alkyl-C	32.89	22.74
Alkyl-C	31.85	18.24

Amendments

Group	Amendments	
	DOC	POM
Carboxylic-C	12.6	9.8
Aromatic-C	23.9	13.2
O/N Alkyl-C	51.2	48.0
Alkyl-C	12.2	28.0

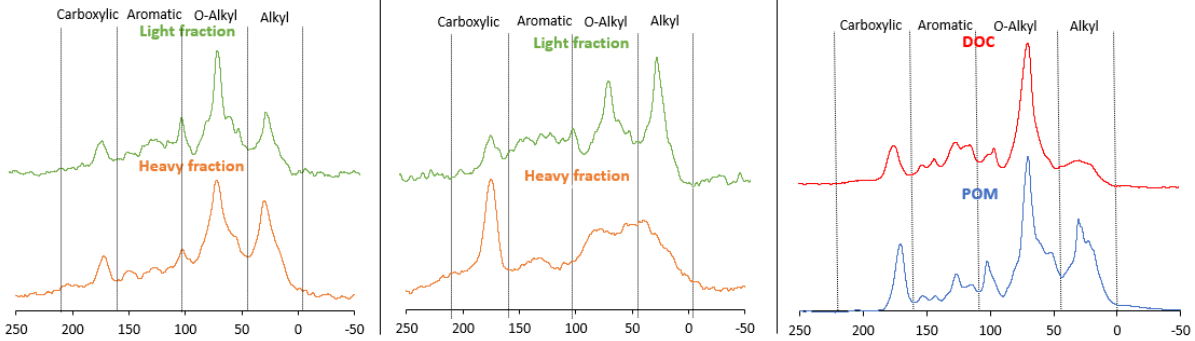

Supplementary Fig. 5: ^{13}C NMR spectra and integrals of the light and heavy fraction of control samples from top (0 – 0.2 m) and subsoil (0.8 – 0.9 m) used in the incubation experiment; the particulate organic matter (POM) i.e., *Salix spp.* and the microbially derived dissolved organic matter (DOM) used in the experiment as amendments.

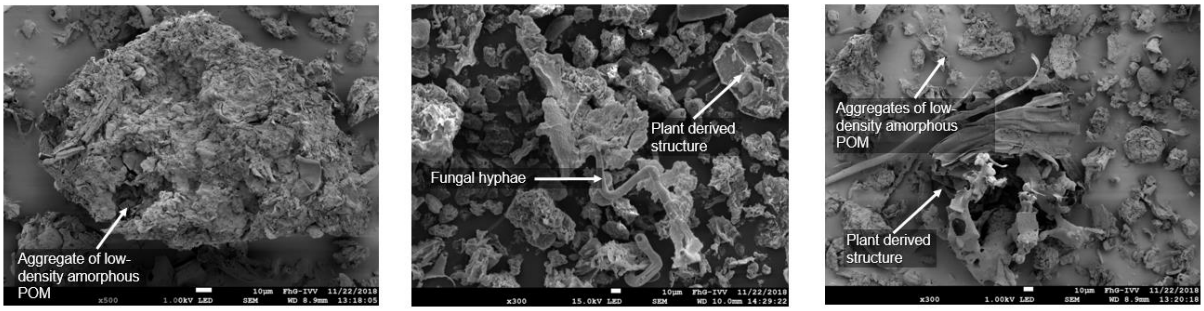

Supplementary Fig. 6: Scanning electron microscopy (SEM) images of the light fraction of incubated topsoil samples after the fractionation procedure.

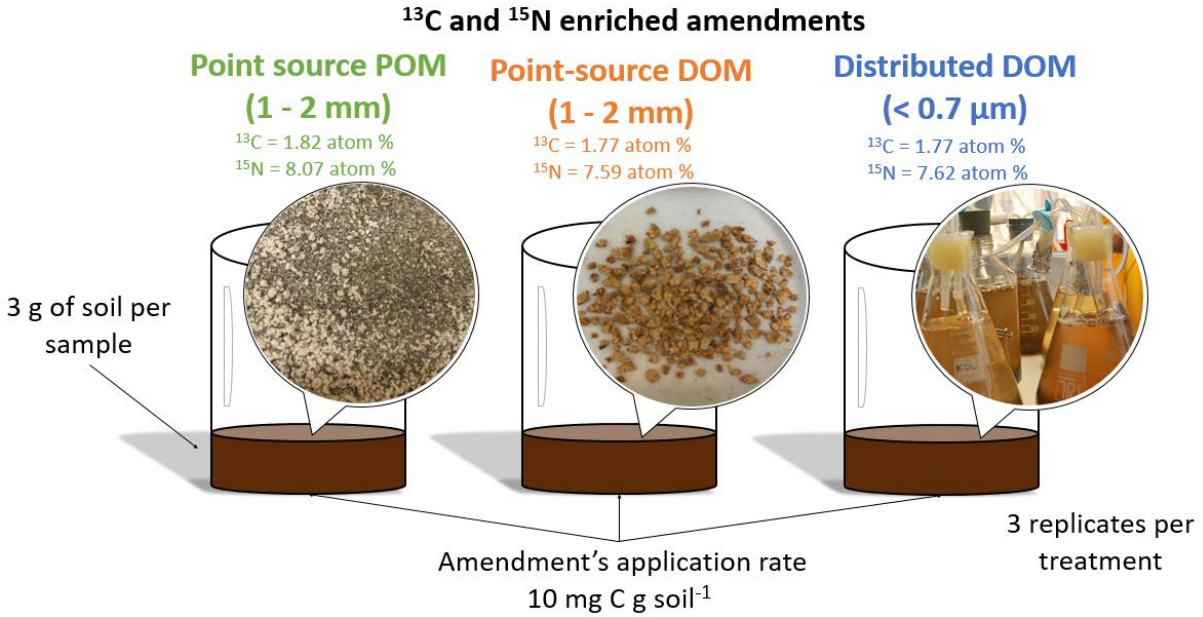

Supplementary Fig. 7: Summary Figure of the incubation experiment. The three units represent the C inputs used in the incubation as follow: 1 – Point source particulate organic matter (POM); 2 – Point source microbially derived dissolved organic matter (DOM); and 3 – Distributed DOM. The DOM was extracted from the POM material by shaking it in water during 72h at 32^{o}C. After this period, the material was filtered with a 0.7 µm filter and freeze-dried. The point source DOM treatment was pelleted in 1-2 mm size pellets and the distributed DOM treatment was re-dissolved in water.

Supplementary Table 2: CN contents, CN ratio, pH and ^{13}C and ^{15}N enrichment level of the point source particulate organic matter (POM) and microbially derived dissolved organic matter (DOM) used in the experiment.

Property	Point Source POM	Point source DOM	Distributed DOM
C (mg g^{-1})	427	300	299
N (mg g^{-1})	15	11.9	12
CN ratio	28.47	25.21	24.92
pH ($CaCl_2$)	5.5	4.6	4.5
^{13}C (atom %)	1.82	1.87	1.77
^{15}N (atom %)	8.07	7.59	7.62

Supplementary Table 3: Characterization of the topsoil and subsoil bulk samples used in the incubation experiment.

Analysis	Soil depth (m)	
	0 - 0.2	0.8 - 0.9
SOC content (mg g^{-1})	332.15	132.45
N content (mg g^{-1})	1.15	0.36
pH ($CaCl_2$)	3.4	4.4
Fe OX (mg g^{-1})	12.54	79.93
Al OX (mg g^{-1})	2.02	107.71
Fe DCB (mg g^{-1})	42.02	118.66
Al DBC (mg g^{-1})	4	52.95
Ca (mmol g^{-1})	0.44	0.00
Mg (mmol g^{-1})	0.21	0.02
K (mmol g^{-1})	0.05	0.02
SSA (m^2 g^{-1})	3.435	53.35

OX: ammonium oxalate extracted; DCB: dithionite citrate bicarbonate extracted; SSA: specific surface area.

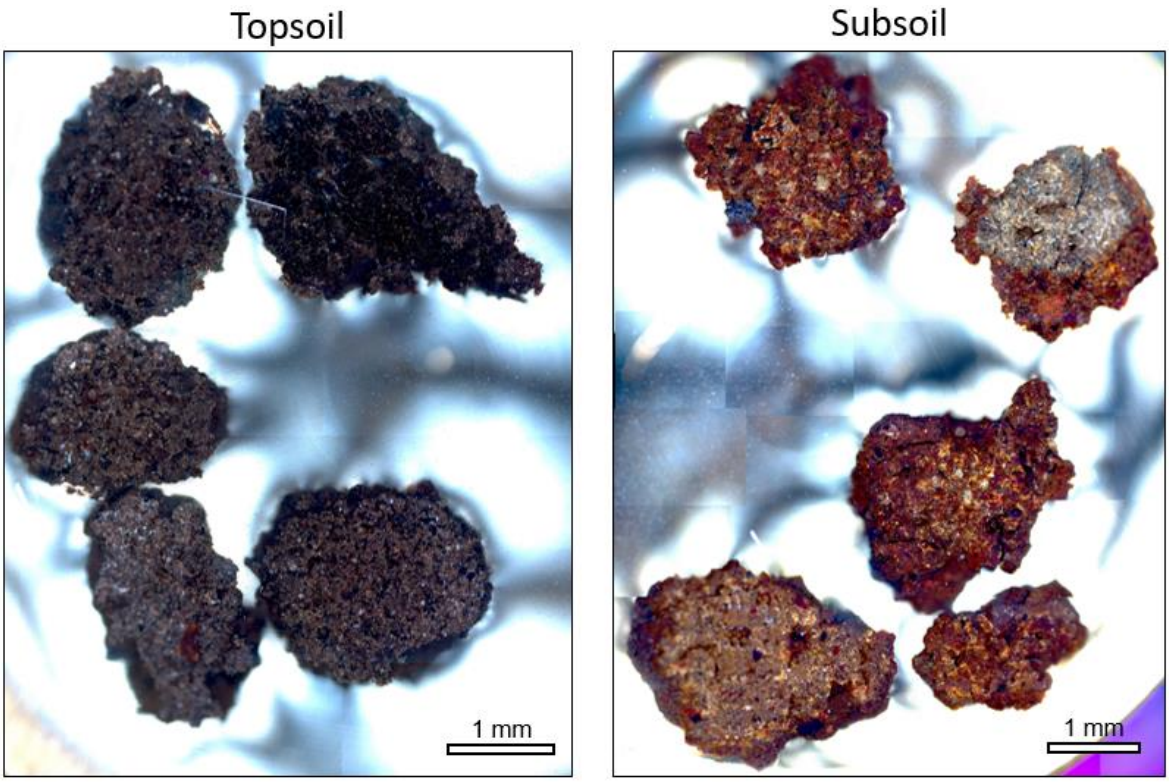

Supplementary Fig. 8: Reflected light microscopy images of sectioned topsoil and subsoil macroaggregates. The samples were collected from the bulk soil samples after the incubation period by sieving them between 4 and 2 mm. Five macroaggregates from each treatment were randomly selected, embedded them in resin and polished down until approximately their half.